DEVELOPMENT OF A NEW ELASTIC PATH CONTROLLER FOR THE COLLABORATIVE WHEELCHAIR ASSISTANT

ZHOU LONGJIANG

(M. Eng)

A THESIS SUBMITTED

FOR THE DEGREE OF DOCTOR OF PHILOSOPHY

DEPARTMENT OF MECHANICAL ENGINEERING

NATIONAL UNIVERSITY OF SINGAPORE

2010

Statement of Originality

I hereby certify that the content of this thesis is the result of work done by me and has not been submitted for a higher degree to any other University or Institution.

.....	.....
Date	ZHOU LONGJIANG

Acknowledgments

I would like to express my sincere appreciation to my supervisor, Assoc. Prof. Teo Chee Leong, for his invaluable guidance, insightful comments, strong encouragements and continuous personal concerns both academically and otherwise throughout the research project. I benefit a lot from his comments and critiques. I would also like to thank my Co-supervisor, Dr. Etienne Burdet, who have given me constructive directions and incisive comments to my research work.

I also show my gratitude to my colleagues, Mr Zeng Qiang, Mr Brice Rebsamen, Mr Boy Eng Seng and Mr Long Bo for their enthusiastic assistance and collaboration in the project. I gratefully acknowledge the financial support and research equipments provided by the National University of Singapore, which have enabled the realization of this research and academic work.

My thanks are also given to the staff and friends in Mechatronics and Control Lab for their support and encouragement. They have provided me with useful comments and a warm community during my PhD candidature.

Finally, I owe my deepest thanks to my wife, Cao Shoufeng, for her endless love, comfort and continual support to my work and care to my life, my lovely son, Zhou Peixin for his understanding that I cannot often accompany him for my studies, and my parents for their unconditional loves and encouragements.

Table of Contents

Acknowledgments **i**

Summary **vii**

List of Tables **ix**

List of Figures **xiii**

Acronyms **xiv**

List of Symbols **xvi**

1 Introduction **1**

1.1 Background 1

1.1.1 Collaborative Wheelchair Assistant (CWA) 2

1.1.2 Elastic Path Controller (EPC) 3

1.2 Research Problems 4

1.3 Research Objectives 6

1.4 Contributions of Thesis 6

1.5 Organization of Thesis 7

2 Literature Review **9**

2.1 Path planning approaches 9

2.1.1 Deliberative approach 10

2.1.2 Reactive approach 11

2.1.3 Hybrid approach 12

2.2 Path control approaches for robotic wheelchairs 13

2.3 Path controllers with elasticity 15

2.4 Concluding remarks of the literature review 16

3 Development of a new EPC for the CWA **18**

3.1 Introduction 18

3.2 Hardware 18

3.2.1 CWA 18

3.2.2 Input devices 20

3.2.3 Human-machine Interface (HMI) 20

3.3 Modes of motion control in CWA 21

3.3.1 Free Mode (FM) 22

3.3.2 Constrained Mode (CM) 24

3.3.3 Elastic Mode (EM) 26

3.4 Path generation 27

3.5 Two path controllers implemented for the CWA 27

3.5.1 Samson's path controller 28

3.5.2 Brent's path planner 31

3.5.3 Comparison of the two controllers 36
3.6 Development of a New EPC 37
3.6.1 Modification to the Brent's path planner 37
3.6.2 Principle and basic implementation of the EPC 37
3.6.3 Elastic coefficient 44
3.6.4 Stability analysis 48
3.6.5 Singularity analysis and handling method 51
3.7 Simulation Experiments 52
3.7.1 Devices and software used in the simulations 53
3.7.2 Simulation for fundamental functions of the EPC 55
3.7.3 Comparison of the new EPC with the old one 57
3.8 Real-time Experiments 58
3.8.1 Objectives 58
3.8.2 Subjects 58
3.8.3 Experimental environments 59
3.8.4 Training and instructions 59
3.8.5 Data analysis methods 60
3.8.6 Results 61
3.8.7 Discussions 62
3.9 Conclusion 64

4 Improvements of the EPC 66

4.1 Introduction 66

4.2 Parameter optimization of the EPC 66

4.3 The nonlinear form of EPC 70

4.3.1 Drawback of the linear EPC 71

4.3.2 Nonlinear EPC 72

4.3.3 Algorithm to search for the nearest point on the guide path . . . 75

4.3.4 Simulation for the nonlinear EPC 76

4.4 Summary of the chapter 78

5 CWA with force feedback joystick 80

5.1 Introduction 80

5.2 Application of FFJ 81

5.3 Hardware 82

5.3.1 Overall system configuration 82

5.3.2 FFJ used in the CWA 83

5.3.3 Server-client communication system in the CWA 84

5.4 Dynamic model of EPC 89

5.4.1 Obstacle force algorithm 90

5.5 Experiments 97

5.5.1 Training and instruction 98

5.5.2 Perpendicular motion toward a wall 99

5.5.3 Avoidance of an obstacle 105

5.5.4 Questionnaire 111

5.6 Conclusion 112

6 Conclusions and recommendations for future work 113

6.1 Contributions 113

6.2 Future work 115

Bibliography 117

Appendices 131

Appendix A. Research progress of robotic wheelchairs 132

Appendix B. Questionnaire about the Assistive Obstacle Avoidance of the CWA 139

Publications 141

Summary

Robotic wheelchairs are important transportation tools for assisting the mobility of disabled users. One such system is the Collaborative Wheelchair Assistant (CWA) developed at the National University of Singapore.

The CWA collaborates with the user by allowing him to use his cognitive skills while assisting him in the difficult task of maneuvering by guiding the wheelchair along virtual paths. The user decides where to go and controls the speed while the path controller of the system constrains the wheelchair along predefined guide paths. For practical purposes, the path controller should allow the user to deviate from the guide path should s/he encounters any unexpected obstacles. To that end, an Elastic Path Controller (EPC) has been developed previously. For the functions of the CWA, a stable path controller is hence vitally important to the reliability, maneuverability and cost of the CWA.

The current EPC has some limitations and can be unstable. This study developed a new elastic path controller for the CWA that can resolve the instability. The drive for the control system was generated by the weighted sum of the internal restoring force and the external applied normal force, and a pure rotation strategy was executed to solve the instability problem in the singularity region. The parameters of the controller are optimized so as to minimize the influence of external perturbations and parameter uncertainties. The elastic path controller was successfully implemented for the CWA. Real-time experiments showed that the newly proposed elastic path controller can drive the wheelchair to fulfill mobility tasks such as following a guide path, handling the singularity issue, and so on. The driving performance of the wheelchair is significantly improved by providing a guide path and that the driving performance of the elastic mode

is comparable to that of the constrained mode.

The drawback of the proposed EPC is that it cannot handle very large obstacles, as the normal force that needs to be applied to the CWA in this case can get excessively large when the wheelchair is far away from the guide path. In such situations, a non-linear elastic path controller is proposed with inverse exponential function that will allow the user to avoid arbitrarily large obstacles without needing to apply a very large normal force. The performance of the nonlinear EPC was verified by simulation experiments.

To improve the performance of the CWA, a force feedback joystick was used to replace the traditional joysticks. This will enable users with severe vision impairment to feel the feedback force generated by environmental obstacles or deviation of the wheelchair from the guide path so the users can adjust the magnitude and direction of force input according to the different situations. Experimental results indicated that the force feedback joystick used in the wheelchair control greatly improves the approaching performance, and that the feedback force is an effective tool to assist in the obstacle avoidance especially when vision feedback is not available for the users.

List of Tables

3.1 Relationship between $|det(M^{-1})|$ and $\triangle\theta$ 51

5.1 Shortest distance between the wall and the CWA 103

5.2 Shortest distance between the obstacle and the CWA 109

5.3 Statistical number of oscillations for all subjects 111

5.4 TTEST2 results of the numbers of oscillations 111

5.5 Number of subjects selecting a particular choice 111

List of Figures

3.1 Prototype of a CWA 19

3.2 GUI in the real-time CWA experiments 22

3.3 Joystick axes decomposition 23

3.4 Kinematic description of the CWA system 25

3.5 Generation of a guide path by WTP 28

3.6 Kinematic description of a moving wheelchair using Samson's controller 29

3.7 Kinematics model of Brent's path planner 32

3.8 Orthogonal projection decomposition of the control input U 34

3.9 Block diagram of the wheelchair controller without elasticity 36

3.10 The desired tangent is chosen as the reference vector to the coordinate system 38

3.11 Illustration of an EPC 39

3.12 A force/torque sensor working as an HMI in the simulation 40

3.13 Simulation result of the angle difference between l and T_d, with nonzero external forces imposed on the wheelchair 41

3.14 Generation of normal force using the method of rotation matrix multiplication 42

3.15 Transformation of force from joystick coordinate system to Frenet Frame 43

3.16 Relationship between nominal input and actual output of F_y 44

3.17 Block diagram of the whole EPC control system 45

3.18 Relationship of λ with respect to F_y and l 47

3.19 Relationship between l_{ss} and F_y 47

3.20 Relationship between the initial angular error and actual path of the wheelchair 49

3.21 Relationship between the angular error and determinant of inverse control matrix 50

3.22 Solution to singularity problem of wheelchair motion 53

3.23 Devices used in the simulation experiments 54

3.24 Hardware installation of the FT sensor FT6142 54

3.25 Signal acquisition and processing of the FT sensor 55

3.26 Simulations of singularity handling and obstacle avoidance functionalities 56

3.27 Simulations of path following and backward motion functionalities . . . 57

3.28 Simulation of EPC when the reference vector changes 58

3.29 Experimental environment 59

3.30 Parallel joystick move 62

3.31 Normal joystick move 63

4.1 Block diagram of of an EPC with an equivalent disturbance w 67

4.2 Shortest path of a wheelchair to avoid obstacles of different sizes 72

4.3 Relationship between steady state restoring force and position error . . 74

4.4 The desired point is reset if the normal angle is smaller than the threshold 76

4.5 The nonlinear EPC can break far away from the guide path 77

4.6 The control algorithm can automatically search for the nearest point on the guide path as the current desired point when angular difference α is beyond the tolerable scope. 78

4.7 Simulation for comparison of the nonlinear EPC with linear EPC 79

5.1 Wheelchair mobility control using the FFJ 82

5.2 The overall CWA system for server-client communications 83

5.3 Overall system structure of the CWA control system 84

5.4 Flow chart of the CWA control mode with FFJ 85

5.5 Communications between Windows and Linux RTAI systems 85

5.6 The original GUI and coordinate system of the FFJ 87

5.7 Modified GUI and Coordinate system of the FFJ 89

5.8 Dynamic model of the EPC with FFJ 91

5.9 Distribution map of ultrasonic sensors around the wheelchair 92

5.10 Generation of an OF with an obstacle around the wheelchair 93

5.11 Relationship between $\|F_{ob}\|$ and d, expressed as a straight line 94

5.12 Relationship between the OF and the distance expressed as a hyperbola 95

5.13 Modification of the force-distance relationship using a hybrid curve . . 96

5.14 GUI for the psychophysical experiments in two typical cases 99

5.15 The wheelchair moves perpendicularly toward the wall 100

5.16 Experimental environment and GUI settings for Case 1 101

5.17 Results of all trials in Ty1 for Case 1 104

5.18 Normal probability distribution of the shortest distance between the wall and the CWA 105

5.19 The wheelchair detours from an circular obstacle 106

5.20 Experimental environment and GUI settings for Case 2 108

5.21 Results of all trial in Ty1 for Case 2 109

5.22 Shortest distance between the circular obstacle and the CWA 110

Acronyms

ACK	Acknowledgment
ARE	Algebraic Riccati Equation
CM	Constrained Mode
CVT	Continuously Variable Transmission
CWA	Collaborative Wheelchair Assistant
EM	Elastic Mode
EPC	Elastic Path Controller
FFJ	Force Feedback Joystick
FFW	Force Feedback Window
FM	Free Mode
GM	Guide Mode
GUI	Graphical User Interface
HMI	Human Machine Interface
ICR	Instantaneous Center of Rotation
ISN	Initial Sequence Number
OF	Obstacle Force

OS	Operating System
PSJ	Position Sensing Joystick
RTAI	Real Time Application Interface
SD	Standard Deviation
SYN	Synchronization
TCP / IP	Transmission Control Protocol and Internet Protocol
VCP	Vehicle Center Point
WMR	Wheeled Mobile Robot
WTP	Walking Through Programming

List of Symbols

$A_{\perp}$	normal vector to the reference
$\tilde{A}$	extended form of matrix A
A_d	variable or vector on the guide path
$A \succ 0$	symmetric positive definite matrix
$\|A\|_2$	H_2 norm of the vector
$det(M)$	determinant of matrix M
ds	differential increment of variable s
$f(x)$	function f with respect to variable x
NA	not available
I	identity matrix
$I_{n\times m}$	identity matrix of n row and m column
$0_{n\times m}$	zero matrix of n row and m column
R_D^O	rotation matrix from coordinate system O to D
$\dot{x}$	first derivative with respect to time
Θ	zero vector
$(.)'$	first derivative with respect to actual path length
$(.)''$	second derivative with respect to actual path length

$|.|$ absolute value of a variable

$\|.\|$ magnitude of the vector

Chapter 1

Introduction

This thesis is concerned with the development of the motion control for a Collaborative Wheelchair Assistant, a wheelchair that is mainly used in hospitals or rehabilitation environments. It focuses on the development of a new Elastic Path Controller with low cost and safety for the wheelchair, and incorporation of force feedback joystick so that users can feel the environmental information through the input devices.

This chapter will address the background of the collaborative wheelchair assistant project and its elastic path controller. The main research problems, research objectives, contributions and organizations of this thesis will also be presented in this chapter.

1.1 Background

Wheelchairs take an important role in the modern society as we are entering a world with rapidly aging population [1]. In many developed countries, 15 percent of the population is over 65. This great number of elderlies may need a lot of wheelchairs to assist in their mobility tasks. In the United States alone, there were more than 1.7 million wheelchair users in 1999, and the number is expected to reach 4.3 million in 2010 [2].

Though the majority of the wheelchairs developed are manual wheelchairs [3], robotic wheelchairs have attracted more and more interests of research and application. Apart from providing mobility aid and saving effort for users, robotic wheelchairs are also compact and can have more complex and intelligent functionalities. Some have vision functions for users with vision impairments [4], while others have a functionality for decision-making for those who have neurological disabilities [5]. With the continual development of such techniques, robotic wheelchairs will be able to perform more and more labor tasks or even cognitive activities of human beings.

One interesting concept for the robotic wheelchair is the Collaborative Wheelchair Assistant (CWA), an important robotic wheelchair which can assist disabled users in regaining their autonomy by providing a guidance to the mobility task and making use of the remaining control skills of the users [6].

For the CWA, the path controller is important for its functionality as the reliability, maneuverability and safety are vitally important to a human-carrying robotic wheelchair. Many path control approaches have been used in the development of the path controllers of the robotic wheelchairs, but they have not been satisfactory in actual applications. In the next chapter, different approaches to path control - sensor-based navigation, shared autonomy, and path following - will be reviewed in order to find the best method as the basis of the path controller used in this research project.

1.1.1 Collaborative Wheelchair Assistant (CWA)

In this thesis, a path controller will be designed for the CWA [6] [7] developed by the Control & Mechatronics Lab at the National University of Singapore (NUS) to improve the life quality of those users with mobility disabilities. The CWA which aims at relieving the mental and physical labors of the wheelchair operators by providing motion guidance is a novel type of wheelchair assistant that can help wheelchair users regain their autonomy and increase their self-confidence and self-esteem.

A CWA is able to provide the wheelchair user with a guide path, or desired path, which is pre-designed and stored in the computer software and allows the wheelchair users to adjust the level of autonomy according to their own ability levels. The principle of the CWA is to relieve the user of the difficult task of maneuvering the wheelchair while allowing the user to control the speed along software-defined guide paths, thereby making use of the different abilities of the human user. This approach is useful especially for disabled operators with cerebral palsy, who are unable to control their movements and orientation.

A CWA system has three control modes: The Free Mode (FM) allows the users to drive the wheelchair like an ordinary powered wheelchair; Constrained Mode (CM) controls the wheelchair to strictly follow the guide path by going forward or backward along the guide path; and Elastic Mode (EM) enables the users to deviate from the guide path when a nonzero normal force is imposed. The wheelchair returns to or follows the guide path when the normal force is withdrawn.

1.1.2 Elastic Path Controller (EPC)

In normal operation [7], the CWA can follow the guide path when the chair is on the path and asymptotically return to the guide path when an error occurs between the guide path and the actual path of the wheelchair. This correction is under the control of an algorithm based on the path-following technique. However, this corrective ability does not ensure that the wheelchair can deviate from the guide path when it is on the guide path. In practical applications, users usually expect that the wheelchair can make deviations to avoid some obstacles on the guide path or to go to other places that are not on the path, and therefore the previous path controller is substituted with a new version, the Elastic Path Controller (EPC) [8].

The EPC is able to automatically produce a restoring force F_γ, which creates a tendency for the wheelchair to return to the guide path when a position error between the actual path and the guide path occurs. The larger the distance is between the actual path and

the guide path, the larger is the restoring force produced. An external normal force $F_{\perp}$ is imposed on the wheelchair to drive the wheelchair to deviate from the guide path. $F_{\perp}$ must be large enough to overcome the restoring force so that the wheelchair will break away from the guide path; the wheelchair will come back to the guide path gradually after withdrawal of the external normal force or when the external normal force becomes smaller than the restoring force.

This action is similar to that of a spring: when the spring is compressed, it will automatically generate a restoring force which tends to make the spring get back to its original, natural status. The more the spring is compressed, the larger the restoring force that is generated. The spring will asymptotically return to its natural status after withdrawal of the external force or when the external force is not large enough to overcome the internal restoring force.

Earlier EPC used in the CWA could not work stably in the singularity areas. In this study, a new EPC was developed for the CWA based on Brent's path planner. The new EPC overcomes the earlier problems encountered in wheelchair applications and ensures that the wheelchair works more efficiently and stably.

1.2 Research Problems

The prototype of the CWA has been built on the Yamaha JW-I, a commercial electric-powered wheelchair [7]. The elastic path controller was developed based on the Samson's controller [9], which drives the CWA to follow the guide path by control of angular speed. Since it's time dependent and not safe for users to operate, it was transformed into path following, which is dependent of geometric property and time impendent. So it's safe for operation, but the transformation is complicated, and it causes some possible instability in the control input. Later we developed an EPC based on the Brent's path following planning approach [10], which was successfully used to control the mobility task of Scooter Cobot, a collaborative robot that was developed by the North Western

University. However, it still does not work stably when the external normal force is large or changes frequently.

The EPC previously developed in the CWA project [8] could not work well in the case of singularities. The CWA following a predefined guide path tends to break away from the guide path and cannot return to the path when the direction (tangent) of the CWA is perpendicular to the direction of the guide path. The singularity problem of the EPC has not been addressed and solved up to now, possibly because the singularity rarely occurs in the mobility task of the CWA. However, the singularity can sometimes happen at the beginning of the mobility task.

Another problem is that it is difficult with the original controller to avoid unexpected large obstacles as the restoring force becomes too large. The existing path controller can avoid obstacles only of limited sizes, although obstacles of very large sizes may exist in the real environment. A nonlinear EPC with function of inverse sinusoid was developed [11] to make the wheelchair deviate far away from the guide path, but this EPC caused a singularity problem at a particular distance from the guide path. This EPC was improved by substituting the nonlinear function with an inverse exponential function [12]. However, it is easy for the wheelchair to become unstable when the distance is in the vicinity of the rotation center.

One more problem is that the human machine interface (HMI) used in the CWA project was a position sensing joystick (PSJ), which does not give any feedback. The feedback information about the environment can only be obtained by the human users. It is very difficult to acquire complete and accurate environmental information if the vision system of the users are impaired. The incomplete or incorrect environmental information may seriously affect the users' control of the CWA.

1.3 Research Objectives

The primary objective of the present study was to develop a new Elastic Path Controller for the Collaborative Wheelchair Assistant, to handle the singularity issues, and to make users feel the environmental information through input devices. More specifically, the objectives of this research were to:

- Develop an EPC for the robotic wheelchair so that the users can control the wheelchair according to their own abilities
- Optimize the parameters so that the path controller can tolerate all the possible uncertainties and disturbances
- Develop a nonlinear EPC for the CWA so that it can avoid arbitrarily large obstacles on the guide path
- Incorporate the force feedback joystick (FFJ) as the HMI so users can adjust their motion control strategies by sensing the deviation of the wheelchairs from the guidance and repulsion forces resulting from the environmental obstacles.

1.4 Contributions of Thesis

- This research may create a deeper understanding of the working principle of the path following planning and allocation mechanism of control power between human users and the wheelchairs.
- An improved EPC has been developed that solves the instability and singularity issues.
- The parameters of the EPC have been optimized using the H2 control.
- This study should contribute to the development of path controllers for robotic wheelchairs with good performance and low cost.

- It is the first study to integrate the force feedback functionality into the EPC to assist with obstacle avoidance in the mobility tasks of the CWA.

1.5 Organization of Thesis

The thesis is organized as follows:

Chapter 1 introduces the background of CWA and the EPC. Three central problems are put forward related to the path controllers used in the control of CWA. The objectives of this thesis are listed and the significance of this thesis is also discussed.

Chapter 2 surveys previous studies related to path controllers of robotic wheelchairs focusing on functionalities that the path controllers can fulfill and challenges that they encounter when disabled operators used them to control robotic wheelchairs.

Chapter 3 develops the new EPC. First, the hardware of CWA is introduced. Next, two path controllers that have been used in the CWA control are described and compared. Next, a new EPC based on Brent's path planner is proposed that works more stably by correcting the drawbacks of the original path planner. Singularity problem is also analyzed and handled in this chapter. Finally, simulation and real-time experiments are conducted to test the performance of the EPC.

Chapter 4 proposes solutions to improve the performance of the developed EPC and extends the application scopes of the EPC. The controller parameters are optimized using the robust control technique. The nonlinear form of EPC based on Brent's path planner is also put forward to allow the wheelchair to avoid obstacles of all sizes.

Chapter 5 describes the CWA equipped with an FFJ so the user can adjust the control strategies of the mobility task by feeling the path error force, which reflects the amount of deviation of the CWA from the guide path, and the repulsion force coming from the environmental obstacles.

Real-time experiments are also conducted to evaluate the performance of the CWA with force feedback joystick. The hardware used the TCP/IP communications between two notebook computers. The server computer is linked to the CWA and the client computer is connected with the force feedback joystick. The obstacle avoidance algorithm is fulfilled and tested by the real-time experiments.

Chapter 6 summarizes the main contributions in this thesis and gives direction for future research.

Chapter 2

Literature Review

This chapter surveys previous studies on path controllers for robotic wheelchairs, focusing on: (1) path planning approaches, and (2) path control approaches for robotic wheelchairs.

2.1 Path planning approaches

Given the geometry information of the robot and environmental obstacles, the task of robot path planning is to find a continuous collision-free path between the initial and goal positions by capturing the connectivity of the free space. Approaches developed to solve the path planning problem fall broadly into 3 categories: deliberative (hierarchical), reactive (reflexive) and hybrid planning. In general, the deliberative approach aims at computing a complete motion path to the goal while the reactive approach determines the mobility task only for the next-step in the path to the goal.

2.1.1 Deliberative approach

The deliberative planning approach [13] works at a supervisory level of control and uses the roadmap information from a global sensor such as GPS to navigate the robot to move from the initial position to the goal. Most deliberative architectures adopt the Tweak operator to model the actions of the robot [14]. It works well if the environment is well known and several actions of the robot are not performed simultaneously. However, those cases where more than one action are executed simultaneously require a model that permits simultaneous asynchronous actions [15].

Many algorithms are used in the deliberative planning approach to find the shortest collision-free path. A roadmap [16] [17] is usually built to represent the connectivity of free space and connect the initial position and goal to search for an available path between the two positions. Cell decomposition [18] decomposes the free space into simple cells using parallel lines via all the vertices of the configuration obstacles. The free path is then determined by searching the free space for polygonal lines that start from initial position, end at the goal and bisect the related cells. Dijkstra's algorithm [19] searches for the shortest single-source path from the initial point to the goal in a directed graph without negative edge weights. The algorithm repeatedly examines the vertices to choose one that is of the lowest cost to the vertex set to be examined, starting from the beginning and ending at the goal. In this way, it can find the shortest path from the beginning to the goal. A* Algorithm [20] [21] searches a connected graph in a static environment for the shortest path from the start to the goal and uses the Dijkstra's graph search algorithm to find the optimal path; it yields better performance with minimal search steps by using heuristics to guide itself, but it is not satisfactory with global constraints or dynamic environments and it is not efficient when re-planning is needed.

One problem of the deliberative planning is that it requires a world model of the complete environmental information. This is complex to describe in dynamic environments. Another problem is that it has difficulty avoiding unmodelled or dynamic obstacles because of the lack of local sensory information.

2.1.2 Reactive approach

The reactive planning approach [22] works at a lower level of control hierarchy and can operate on line using sensory information as feedback to reflect the local environment.

Many strategies and architectures have been developed using reactive approaches. Subsumption architecture [23] [24] [25] proposes a "horizontal decomposition" of planning tasks into a series of simultaneous behaviors in response to respective sensory inputs. It not only can robustly navigate a mobile vehicle in a dynamic environment but also be extended and adapted to the real-time control of an embedded system [26]; this architecture is flexible, but it has little ability to incorporate the world knowledge.

Other typical reactive approaches may have new features and functionalities to cater for their individual needs. Payton's Reflexive behaviors [27] are a series of motor responses which reflect directly the sensory-information-generating emergent behaviors. Kadonoff's arbitration strategies [28] employ a competition mechanism that chooses one from multiple behaviors to control the vehicle in rapid response to sensory information. Akin's motor schema [29] consist of a collection of motor behaviors, each of which outputs a velocity vector for the robot to move in response to the environmental sensory information. The Reactive Action Package (RAP) [30] provides a situation-driven execution that is most appropriate to the requirement of the goal; an unsatisfied task is selected and a corresponding method based on the current world state is chosen to satisfy it as long as it is active. The PENGI system [31] is a typical reactive approach in the game industry in which several behaviors are active simultaneously to control the strategies used by the video game and its relationship with its surrounding objects.

In comparison with deliberative planning, the reactive approach is more flexible and robust, and it can be applied in unknown and dynamic environments. However, this kind of planning approach lacks information for global navigation, so the convergence to the goal position cannot be ensured and it is easy for the robot to get trapped in a local minima.

2.1.3 Hybrid approach

The deliberative and reactive approaches have complementary characteristics such that the merits of one approach can compensate for the drawbacks of the other. In order to bridge the gap between these two approaches, some researchers have proposed the hybrid planning approach [32] [33], which applies the deliberative planning to compute a complete global path from the initial point to the goal using a priori information, and the reactive approach to execute the local mobility task with the functionality of obstacle avoidance.

Many hybrid applications emphasize different parts of the integrated mechanisms: Some approaches design the hybrid architecture in a more reactive form [34], which incorporates a reactive part as well as a search-based part to fulfill the principle of reacting to the environment when it can, plans the path when it must and tries to augment its reactive element as much as possible; Other approaches make the reactive control mechanism more representational [35], bringing in a fully integrated reactive architecture that eliminates the distinction between a reactive control program and a representational map.

Until now, the more popular approaches have incorporated two independent architectures with an interface to connect them [36] [37] [38]. For example, AuRA (Autonomous Robot Architecture) is considered the earliest robotic architecture to use the hybrid path planning approach for navigation [39] [40][41]. AuRA integrated several techniques including the a priori world model, reactive control, and integration of vision. At the highest cognition level, hierarchical planning is integrated by employing the knowledge representation, including a priori world maps and landmarks, spatial occupancy maps, collection of motor behaviors and perceptual strategies. The subordinate navigator chooses a continuous path made up of several piecewise segments according to the specifications of the mission planner. At the reactive execution level, no representational knowledge is needed for the dynamically changing reactive schemas. If the goal is not attainable at this level, the deliberative planner is stimulated again to renew the path scheduling based on the current world models.

ATLANTIS (A Three-Layer Architecture for Navigation Through Intricate Situations), another typical hybrid architecture, is a heterogeneous and asynchronous architecture for maneuvering a mobile robot to perform multiple tasks in noisy and unpredictable environments [42]. ATLANTIS is comprised of three components: The reactive controller is used to control the primitive activities without decision-making functionalities; the deliberator is designed to perform computation tasks, such as path planning, on the basis of world models; and the sequencer is responsible for the sequences of controlling the reactive activities and deliberative planning computations. The deliberator can be removed and the remaining system is still able to control the robot, which indicates that the ATLANTIS can work gracefully even when the deliberative planning level fails [43].

With the hybrid planning approach, global convergence is guaranteed provided that motion connectivity can be maintained, and the sensory information acquired online can compensate for the incompleteness of the global model with a priori knowledge. However, the hybrid planning approach requires accurate sensory data to perceive the local environment, and it is also sensitive to noise. In addition, it is difficult to obtain a series of smooth, collision-free motion paths on the basis of limited environmental information, and so it is desirable to develop other types of path planning methods which can provide reliable and collision-free paths when the sensory information is not sufficient. Moreover, intervention of human operators should be incorporated to improve the safety and maneuverability of the mobile system.

2.2 Path control approaches for robotic wheelchairs

The review of existing robotic wheelchair projects (see details in Appendix A) shows that different projects focus on different aspects of the mobility tasks, e.g., selection of control modes, autonomy about obstacle avoidance, perception of environment, pattern recognition, and so on.

Although the different robotic wheelchairs implement features according to their objec-

tives, almost all the projects emphasize on two fundamental requirements: safe navigation and friendly Human Machine Interface (HMI). Since it is inevitable that wheelchairs will encounter some unexpected situations, especially when they work in unstructured environments, a failure during the mobility task should not compromise the users' safety. At the same time, the wheelchairs may be the disabled users' primary companions in their daily lives, and so the control systems of the wheelchairs should interact with the users in a friendly and effective way, adding comfort and ease to their lives. The key issue in the development of a robotic wheelchair is how to design a reliable and safe controller with high maneuverability and low cost.

The earliest stage of path controllers used the simple collision-detection and line-following control approach, which was developed in the CALL centre smart wheelchairs [44]. In the application of this controller, the followed line can have some junctions in the middle that lead to different terminals and the control box is mounted with buttons that correspond to the junctions(e.g., the user can select the "left" button when he/she wants to follow the left junction). This kind of controller is easy and safe to operate, but the path that can be followed is fixed and inflexible.

A sensor-based navigation and automatic obstacle avoidance system was developed in [45]. It can navigate for the wheelchairs and automatically avoid obstacles by using sensory information. This controller has attracted much interest because of its reliability and maneuverability and has been widely used in robotic wheelchairs such as MANUS [46] [47], OMNI [48], and SENARIO [49]. This controller is successful in assisting in daily life tasks and for mobile service robots, but the main disadvantage is that this kind of path controller does not take users' special intentions and needs into consideration. The control of human-carrying wheelchairs should be quite different from that of mobile service robots [50] as otherwise the human users will feel powerless and frustrated in dealing with the machine. Moreover, the "safe" passageway, as detected by the obstacle detection and avoidance system, may be dangerous or inconvenient to the wheelchair users, since they may be too narrow or have some movable heavy objects overhead [51].

In order to incorporate human intervention into the control loop, some researchers have

proposed the sensor-based systems with "shared autonomy" [52] [53] [54], but it is usually difficult to find a solution to meet a broad range of the user requirements, and so this approach is not suitable for general application in the daily lives of disabled users.

One control algorithm for the robotic wheelchairs is the Brent's path following algorithm used in the Cobot control [10]. The controller keeps the robot on the guide path if there is no input of force normal to the guide path. The path following controller was successfully used in the control framework of Cobot, which works collaboratively using direct physical interaction with the human operators within the shared workspace [55]. Cobot uses the computer to control the steering of the wheels by way of the Continuous Variable Transmission (CVT) mechanism [56] to allow the path controller to guide the mobility task smoothly. Cobots have been used in industry as Intelligent Assist Devices (IADs) for material handling and to help the workers execute difficult tasks more efficiently and with reduced risk of injury. Brent's path following planner provides a guide path for the mobile robot to follow, which enables users to relieve their work burden to work out the motion path for the robot. Moreover, it is time independent, so it's safe for users to operate. Boy et al. [6] used this path planning approach in the EPC of the CWA. It works well at low frequencies in the area near the guide path, but it tends to be unstable when the normal force is large or changes frequently.

2.3 Path controllers with elasticity

The path following planning approach can drive the robotic wheelchairs to approach asymptotically and follow the predesigned guide path. However, it cannot make the wheelchair deviate from the guide path. Consequently, it may be risky if some obstacles are found around the guide path in front of the wheelchair. So it is significant if elasticity is provided for the path controllers of robotic wheelchairs. Elastic Band may be a good solution to the obstacle avoidance issue for the path following planner [57]. Normally, the robotic wheelchair follows the guide path without deviation if no obstacles in the environment are found. Once the sensor detects that an obstacle is near and may disturb

the safety of wheelchair, the wheelchair will deviate from the guide path driven by a repulsion force imposed on it. At the same time, the controller will generate internally a contraction force, which is a monotonic decreasing function of distance between the wheelchair and obstacle and tends to make the wheelchair return to the guide path. Elastic strip [58] allows the fulfillment of real-time obstacle avoidance tasks and therefore fits for the dynamic environments. Elastic roadmap [59] is an extension of elastic band and elastic strip, which applies a hybrid system combing task-level controller with a navigation function, so it satisfies the motion constraints and corresponding feedback requirements in the unstructured and dynamic environments.

The above elastic concepts were mainly developed for the automatic path planning situations, which is not the case about human-carrying wheelchairs. The newly developed EPC in this thesis will replace the contraction force with the restoring force that is a PD control function of the position error, and replace the repulsion force with a normal force which is generated by human users through joysticks and perpendicular to the guide path.

2.4 Concluding remarks of the literature review

Research in the field of robotic wheelchairs has increased during the last two decades and has improved the quality of people's lives by providing more reliable and safer mobility aids that can be operated more independently by people with a wider variety of abilities.

Many path control strategies and algorithms for the robotic wheelchairs have been developed and used safely to reduce human effort. The simple collision-detection and line following is easy to operate but is inflexible. Sensor-based navigation and obstacle avoidance is unfit for human-carrying wheelchairs because it may mislead the user to a path that endangers his/her safety. Sensor-based shared autonomy is not suitable for common users because it is dependent on complex techniques. Path planning ap-

proaches may find the best path from initial to goal positions with information about the wheelchair and the environmental obstacles, but they have difficulty presenting a series of collision-free paths for the wheelchair, and human intervention is not incorporated in the control loop.

The Brent's path following algorithm is a good solution to our application because it provides a pre-defined guide path that ensures the global convergence of the motion, and it also guarantees the stability of the wheelchair when the normal force of the controller does not change frequently.

Chapter 3

Development of a new EPC for the CWA

3.1 Introduction

In this chapter, an EPC for the CWA system is introduced. The main contribution of the author was the development of the new EPC based on the Brent's path follower. Experiments were conducted to verify the performance of the new EPC.

3.2 Hardware

3.2.1 CWA

Figure 3.1 shows a prototype of the CWA. It is based on a commercial wheelchair Yamaha JW-I (2). A joystick (3) works as a human-machine interface by which users control the wheelchair's following or deviation from the guide path. A barcode reader (5) is used to acquire position information from the environment, and the PC (4) processes the information and delivers commands to the controller. The manual frame (1)

is used for helpers to manipulate the wheelchair.

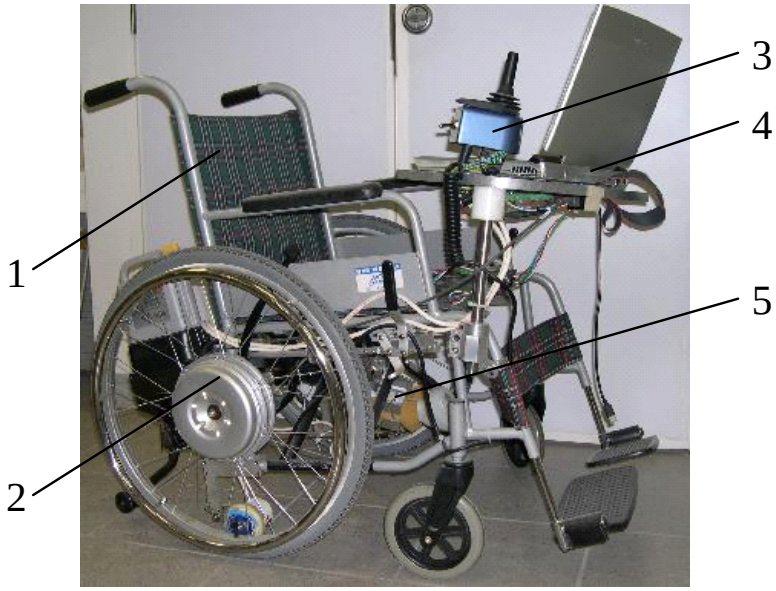

Figure 3.1: Prototype of a CWA

The guide motion path of the CWA is generated by a software that predefines the guide path using specific algorithms [6] [8]. By using EPC as its path controller, the wheelchair can deviate from a pre-designed guide path with a normal applied force and return to the path when the force is withdrawn. Two types of EPCs have been implemented for the CWA control. Samson's controller uses the trajectory tracking approach and transfers it into path following approach [8] [9], which follows a predefined path and ensures asymptotical convergence, but the control algorithm is complex and cannot handle the singularity when the wheelchair is at the center of rotation of the guide path (see equation (3.3)). Brent's controller uses the path following planning approach, which is decided by the geometric properties of the curves independent of time. Section 3.5 gives a comparison of these two controllers.

3.2.2 Input devices

A PSJ is used as an input device through which the human users exert force to control the motion task of the CWA.

The motion control strategy in the CWA is different from that of a common powered wheelchair. In an ordinary powered wheelchair, the two orthogonal elements of the joystick output directly generate the translation and rotation velocities simultaneously. The parallel output controls the translation of the CWA, and the perpendicular output controls the rotation of the wheelchair. However, the joystick used in CWA can only directly generate the translation velocity using the parallel output F_x . The perpendicular output F_y is used to generate a normal force, which is applied to control the deviation of the wheelchair from the guide path. The magnitude of the normal force is proportional to the perpendicular value of the joystick output. The rotation velocity ω in the CWA is generated through the path following control algorithm, from which the translation velocity v decides the differential variable of path length ds, so the input-output relationship is $\omega = f(v, F_y)$.

The PSJ only provides the force input to control the CWA, but the feedback information from the environmental obstacles is not presented to the users. An FFJ will be proposed in Chapter 5 as an input device so that the users can feel the environmental obstacles as well as how far the CWA deviates from the guide path and adjust driving strategies accordingly.

3.2.3 Human-machine Interface (HMI)

The programming platform for the CWA motion control system is based on the Linux Real Time Application Interface (RTAI) Abuntu 2.6.15. Besides being free, the main advantages of Linux RTAI Operation System (OS) are its real-time data acquisition and process and its rich resources and tutorials. The programming language for this project is C.

The HMI in the CWA architecture consists of the joystick and the Graphic User Interface (GUI). The joystick is an HMI through which the human operator exerts force to influence the behaviors of the mechanism. In comparison, GUI is another kind of HMI through which the machine presents the human operator with its characteristics, working conditions and status.

Figure 3.2 is the GUI that is used in the real-time CWA experiments. The GUI consists of 5 zones: the central part is the "display" zone, where the guide path and the current position and orientation of the wheelchair are displayed. The lower part is the "initialization" zone, where the initial status of the wheelchair, such as position, orientation and translation velocity, can be set. The upper right part is the "control mode" zone, where control modes such as "FreeMode", "GuideMode" and "AutoMode" can be chosen. The CM and EM are incorporated into the "GuideMode". In practical experiments, EM is in effect when the adjustment coefficient β of the normal force is not equal to zero. Otherwise, the CWA works in CM, and so the CM is a special case of EM. In "AutoMode", the CWA can move automatically, starting from the initial position at the predesigned constant speed. The upper left part is the "motionguidance" zone, from where different guide paths that are pre-defined and stored in the computer can be selected. The last part, the lower right part, is the "edit" zone, where the paths can be drawn, modified and stored into a specific folder in the hard disk.

3.3 Modes of motion control in CWA

There are three primary modes of motion control with which a CWA can match different abilities: the Free Mode, the Constrained Mode and the Elastic Mode [6]. Each of these three modes can be chosen with a switch or selective buttons.

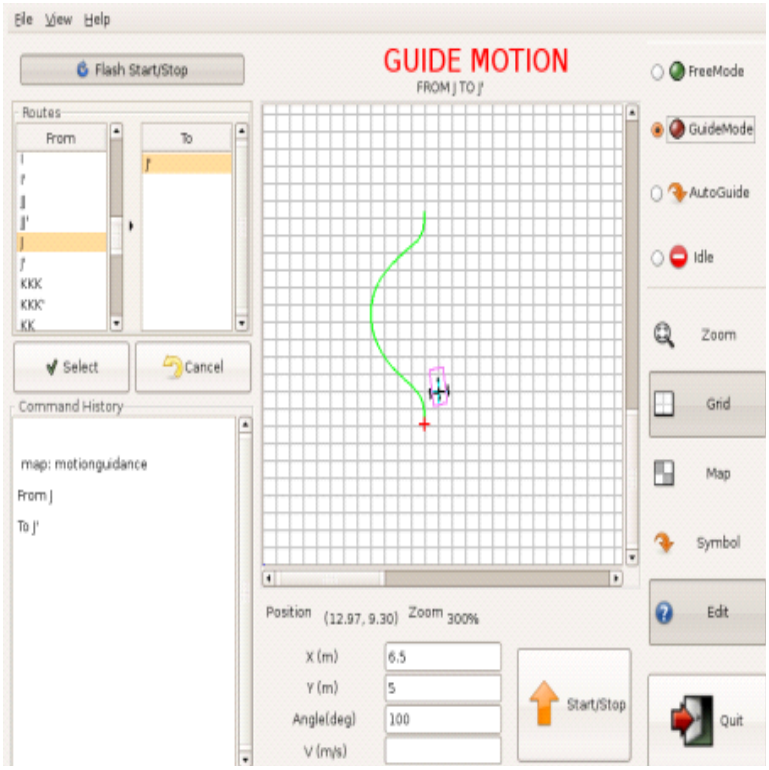

Figure 3.2: GUI in the real-time CWA experiments

3.3.1 Free Mode (FM)

FM allows the user to control the CWA just like an ordinary commercial powered wheelchair. In FM, the user is able to control the wheelchair's velocity and direction via a joystick. Thus, the wheelchair can go to the target without any constraints or limitations.

As in a common powered wheelchair, the joystick used in the CWA has two axes: speed axis x and steering axis y, as shown in Figure 3.3. The joystick coordinate system is different from the world coordinate system, however, in that the x axis and the y axis in the joystick coordinate system are in the direction of y and the opposite direction of x axis in the world coordinate system, respectively.

The joystick input F can be decomposed along the two axes. The parallel force F_x, which is along the speed axis x, generates a translation velocity of the wheelchair v, which is

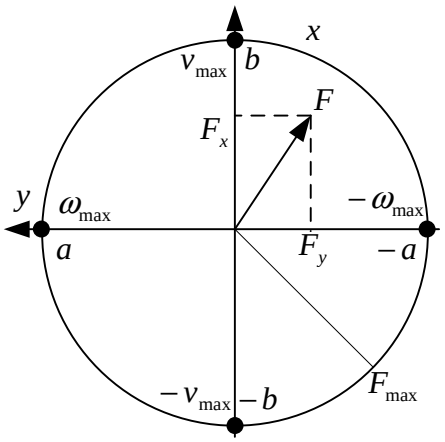

Figure 3.3: Joystick axes decomposition

a monotonic increasing function of F_x. The upward input is the positive direction of the axis x, and the perpendicular force F_y, which is along the steering axis y, provides the wheelchair with a rotation velocity ω, which is a monotonic increasing function of F_y.

The wheelchair makes a pure translation movement when F is on the x axis; the translation velocity reaches v_{max}(maximal velocity of forward motion) and $-v_{max}$ (maximal velocity of backward motion) when F is at point b and $-b$, accordingly. Similarly, the wheelchair makes a pure rotation movement when F is on the y axis; the translation velocity reaches ω_{max} (maximal angular velocity of counterclockwise rotation) and $-\omega_{max}$ (maximal angular velocity of clockwise rotation) respectively when F is at point a and $-a$, accordingly.

FM mode is useful when the user intends to generate a guide path via a Walk-through Programming (WTP) technique [6]. Another useful application is when the user wants to control and make decisions regarding the wheelchair motion completely on his or her own. Therefore, FM is beneficial to those users who want to gain the autonomy to control the wheelchair, assuming they have the necessary control ability.

3.3.2 Constrained Mode (CM)

The CM mode provides a pre-defined path for users who would not like to maneuver the wheelchair themselves. In CM, the wheelchair moves strictly along the pre-defined guide path presented by the computer when the controller gets the command to move forward or backward; the wheelchair cannot deviate from the guide path even if the perpendicular component of force input signal from the joystick is not equal to zero.

The key to implementing the CM is to control K, the velocity ratio of the two rear wheels. As depicted in Figure 3.4, when α, the direction angle of the wheelchair Γ, is not equal to the tangential angle of the guide path θ, the wheelchair has to make a rotation as well as a translation to comply with the orientation of the guide path s. The Instantaneous Center of Rotation (ICR) of the wheelchair is the intersection of the extension line of the wheels' axes and the line perpendicular to the velocity of end effecter V, which is along the orientation of the guide path s [60].

Assuming that $O_1P_1 = l_{11}$, $O_1P_2 = l_{21}$, $O_1O = l_{22}$ and $OO_1 = l_{12}$, where P_1, P_2 present positions of two rear wheels, O and O_1 represent the center of the CWA and its projection on the rear wheel axes, then the geometry relationship in Figure 3.4 provides that

$$\begin{cases} \frac{1}{k} = \frac{l_{22}}{sin(\alpha-\theta)} \\ \frac{1}{k_1} = \frac{l_{22}}{tan(\alpha-\theta)} - l_{11} \\ \frac{1}{k_2} = \frac{l_{22}}{tan(\alpha-\theta)} - l_{21} \end{cases} \tag{3.1}$$

where $\frac{1}{k}$,$\frac{1}{k_1}$ and $\frac{1}{k_2}$ represent the rotation radius of O, P_1 and P_2.

According to the physical meaning of ICR, the whole wheelchair system can be considered to be rotating around the ICR. Thus, the angular velocities in different points of the wheelchair are the same. The relationship among the velocities V, v_1 and v_2 can then be

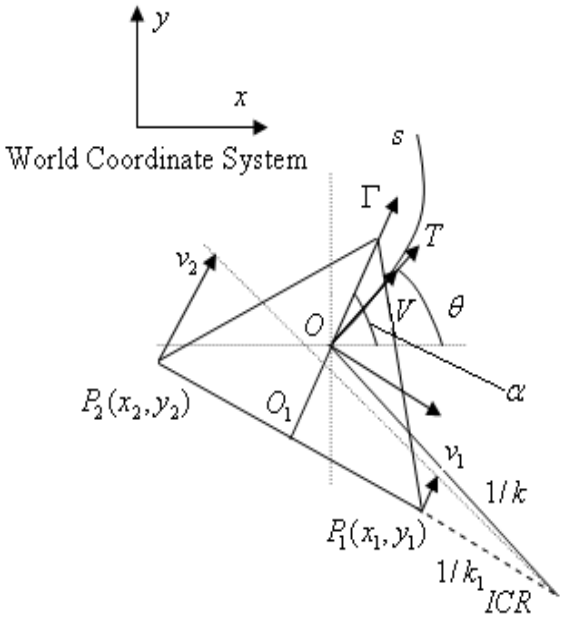

Figure 3.4: Kinematic description of the CWA system

calculated as

$$\begin{cases} v_i = \frac{k}{k_i}|V|, i = 1,2 \\ K = \frac{v_2}{v_1} = \frac{k_1}{k_2}, \end{cases} \tag{3.2}$$

where K is the velocity ratio of wheel P_2 to P_1.

CM cannot drive the CWA to break away from the guide path because the effective normal force is always zero. At the beginning of the mobility task, the CWA asymptotically returns to the guide path with the dragging effect of the restoring force if it is not on the guide path. The CWA cannot leave the guide path once it falls into the guide path. CM is an ideal solution when the motion path of the wheelchair is fixed and it is certain that there will be no obstacles or hazardous environments along the path. CM is especially suitable for the routine and fixed assistive tasks, such as those regular domestic activities and fixed-course human transportation.

3.3.3 Elastic Mode (EM)

When the wheelchair works in a changing and uncertain environment, it may need to deviate from the guide path by application of an external force when some obstacle or something unexpected that may endanger the safety of the user lies in the pre-designed path. In this case, the wheelchair will work in the EM. After the wheelchair passes the obstacle or hazardous environment, it should be able to return gradually to the original guide path by withdrawal of the external force. EM is useful so that users have the flexibility and autonomy to control the wheelchair by imposing force on it and can also ensure their safety and comfort by following the guide path.

In the EM mode, the translation velocity and rotation velocity of the CWA are closely related. The translation velocity v is still solely determined by the parallel input F_x, i.e. $v = v(F_x)$. However, the rotation velocity ω is controlled by the translation velocity v, as well as by the perpendicular joystick input F_y, that is, $\omega = \omega(v, F_y)$. The curvature of the CWA is determined by the control input, which is partially controlled by the F_y. The tangential vector T, which represents the orientation of the CWA, is proportional to the curvature kN, as well as to the differential coefficient of path length ds, which is in turn proportional to v. Thus, the rotation velocity ω is jointly controlled by F_x and F_y. When the joystick is pushed to the left or right side while there is no parallel input, ω is zero because v is zero, and the CWA does not react at all.

The CM and EM can both be considered to be in one category of Guide Mode (GM), since both CM and EM are subject to the motion guidance by the pre-defined guide path. The only difference between the two modes is that the CWA can deviate from the guide path in EM while it cannot deviate from the guide path in CM. In other words, the CWA's behavior does not respond to the normal force in CM. To demonstrate this mobility control task, we set the adjustment coefficient of the normal force to $\beta = 0$ so that the contribution of the normal force to the overall control input is zero (see equation (3.21)). Thus, the normal force does not influence the mobility behaviors of the CWA in the CM.

3.4 Path generation

The guide path can be generated by the computer software using a series of control points in GUI or by WTP. GUI has been addressed in Section 3.2.3.

The WTP process in our CWA project is shown in Figure 3.5. In the first stage, the designer determines the planning of the best path by driving the wheelchair to move in FM from the initial position to the goal based on the designer's detection of and estimation about the world information. The concepts of FM and EM have been addressed in detail in Section 3.3. When the user moves the wheelchair, the encoders mounted on the two rear wheels record the positions of the wheelchair in the Cartesian coordinate system. Assume N sampling points are recorded along the tracing path and symbolized as A_1, A_2, ..., A_N, as shown in Figure 3.5(a). These sampling points are stored in the computer and used as control points to generate a smooth B-spline as the tentative guide path, as shown in Figure 3.5(b). s_t can be modified manually by dragging the related control points to make the B-spline more suitable - e.g., smoother or able to avoiding too large a curvature - for application later. When the environments change and some permanent obstacles come to be in the way of s_t, or when the user intends to pass some special points, such as a door or other interesting places, which are not in s_t, the user will drive the wheelchair to deviate from the original path in EM to avoid the obstacles (Figure 3.5(c)). A new B-spline is generated using the renewed control points B_1, B_2,...,A_M, as shown in Figure 3.5(d). The ultimate path s_d is stored as the guide path of the wheelchair.

3.5 Two path controllers implemented for the CWA

Two path controllers have been implemented for the CWA: Samson's path controller and Brent's path planner. This section will describe these two controllers and make comparison between them.

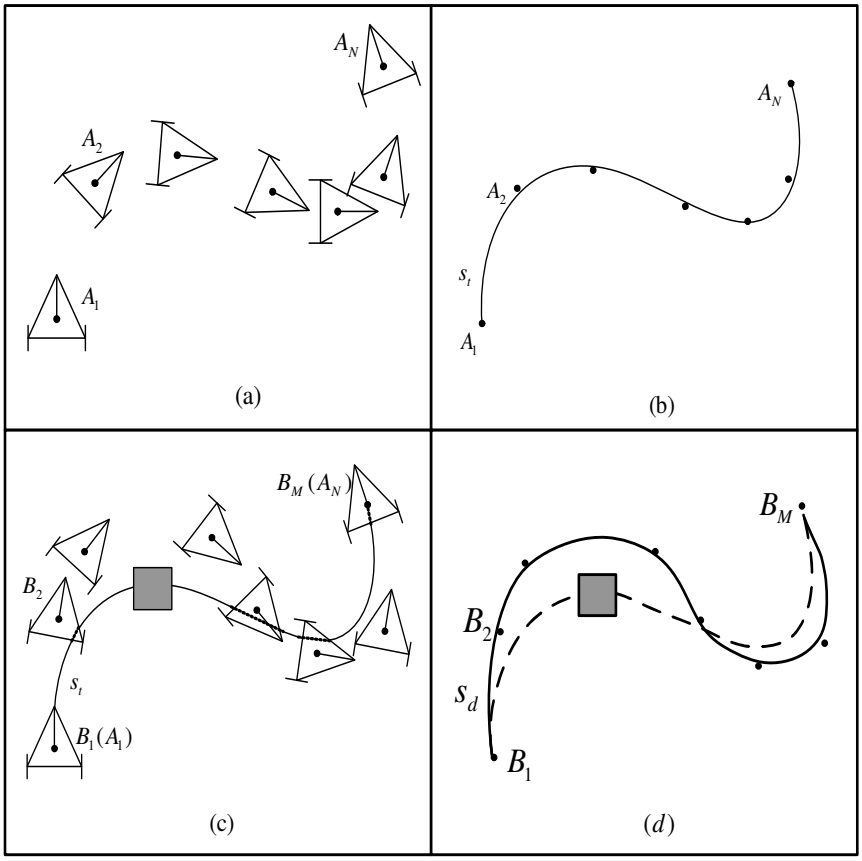

Figure 3.5: Generation of a guide path by WTP

3.5.1 Samson's path controller

Samson's path controller for mobile wheel-type robots was developed by Claude Samson et al. [9] in 1993. It initially developed the trajectory tracking approach, which is time-dependent, and then transferred into path following approach, which is time-independent. Samson's controller was used for the unicycle-type and two-steering-type wheeled mobile robots. In the wheelchair application, only the unicycle-type is used because the two steering wheels are parallel all the time during their motion periods and so may be regarded as one wheel from the kinematics point of view. A kinematic description of the wheelchair, taken as a moving point, is depicted in Figure 3.6.

Figure 3.6 shows two coordinate systems: world coordinate system $x-O-y$ and Frenet frame T_d-R_d-l. According to classical laws of mechanics, the kinematics equation

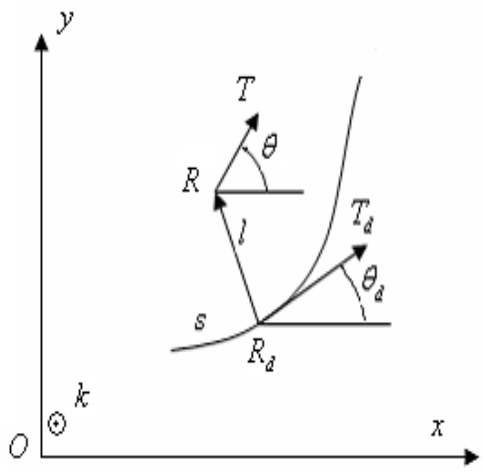

Figure 3.6: Kinematic description of a moving wheelchair using Samson's controller

set of the point R can be described as [9]:

$$\begin{cases} \dot{s} = v\cos(\theta - \theta_d)/(1 - c_c l) \\ \dot{l} = v\sin(\theta - \theta_d), \\ \dot{\theta} = \omega \end{cases} \tag{3.3}$$

where v and ω are the linear and angular velocities, respectively, of the moving point R; θ and θ_d are the actual direction angle and corresponding desired direction angle, respectively; and c_c is the curvature of the desired motion path s. For the sake of convenience, the angular error $(\theta - \theta_d)$ is replaced by the symbol $\triangle\theta$. The derivative with respect to path length is defined as $(.)' = d(.)/ds = \frac{d(.)}{dt}/\frac{d(.)}{ds}$. Equation (3.3) can be transformed into:

$$\begin{cases} s' = sign(v\frac{\cos(\triangle\theta)}{1-c_c l}) \\ l' = \tan(\triangle\theta)(1 - c_c l)sign(v\frac{\cos(\triangle\theta)}{1-c_c l}) \\ (\triangle\theta)' = \frac{\omega}{|v|}|\frac{1-c_c l}{\cos(\triangle\theta)}| - c_c sign(v\frac{\cos(\triangle\theta)}{1-c_c l}) \end{cases} \tag{3.4}$$

The second derivative of l with respect to s is derived from equation (3.4) such that:

$$l'' = \frac{\omega}{vcos^3(\triangle\theta)}(1-c_c l)^2 - c_c(1-c_c l)\frac{1+sin^2(\triangle\theta)}{cos^2(\triangle\theta)} - g_c ltan(\triangle\theta), \tag{3.5}$$

where g_c is the curvature's derivative with respect to s and it can be calculated via

$$\dot{c_c} = g_c \dot{s} \tag{3.6}$$

The feedback linearization technique is used to introduce a control variable u, which needs to satisfy the relationship

$$l'' = u \tag{3.7}$$

The control input term u can be obtained by the traditional control methods such as a PD controller

$$u = -P_l l - D_l l', \tag{3.8}$$

where P_l and D_l are coefficients of the PD controller. Appropriate selection of values P_l and D_l may make the position error l asymptotically converge to zero.

Combining with equations (3.5), (3.6), (3.7) and (3.8), we can get the expression of the resulting control ω:

$$\begin{cases} \omega = \frac{vcos(\triangle\theta)}{1-c_c l}(\frac{lcos(\triangle\theta)}{1-c_c l}(g_c sin(\triangle\theta) - P_l cos(\triangle\theta)) \\ +sin(\triangle\theta)(c_c sin(\triangle\theta) - D_l cos(\triangle\theta) sign(\frac{vcos(\triangle\theta)}{1-c_c l}) + c_c) \end{cases} \tag{3.9}$$

3.5.2 Brent's path planner

Another CWA path controller is based on Brent's path planner. Brent's path controller was successfully used in the control of Scooter Cobot, a kind of robot that can work collaboratively with human operators within a shared space, which was developed by Peshkin and Colgate at Northwestern University [55].

"Virtual Surface" [10] and "Virtual Path" [61] have been put forward and utilized in the designing of the path planner [62] [63]. "Virtual Surface" is not a real physical structure, but it acts as a substantial restraint to a moving robot. Like a real physical fixture or barrier, it produces reaction forces when the robot touches it and tries to penetrate it. "Virtual Path" can exert strength on the robot using the software to make it return and follow the originally designed path when the robot deviates from it. The "Virtual Path" is generated in the computer software and the path following procedure is realized through Continuously Variable Transmissions (CVTs) [64], which generate a smooth pathway by presenting continuous variations of the speed ratios. CVTs are inherently passive so as to ensure the safety of the operators while increasing the freedom of maneuver [65].

Brent's path planner is based on the path following algorithm instead of the trajectory tracking one. Path following is time independent and is decided by geometric properties of the curves, that is, all the variables of the curves can be regarded as the functions of the path length. The drive of the wheelchair's movement is completely controlled by the signals from external input devices, such as joysticks, force/torque sensors, and human operators. Thus, the controller will not send motion commands to the wheelchair if no signals come out of the external devices. This is vitally useful in many special cases, such as when a disabled user is faced with a complex environment and he/she does not instantly have an idea how to deal with it for the next step. The safest choice for the user is just to cease the control commands to the input device so that the wheelchair does not move. Once the user has solved the problem and wants to move again, he/she simply sends the command to move to the device.

The path following approach can be considered a special type of hybrid path planning

approach. At the higher level of the hybrid architecture, deliberative planning designs a virtual path which is generated in GUI or by WTP. In the lower level of the hybrid architecture, the reactive behaviors of the robot in their mobility tasks are under the control of human operators, who determines whether they move or not, the motion speed, the motion direction, and so on. Thus, the path following approach can be regarded as a hybrid path planning approach with the intervention of human designers and operators.

The kinematics model of the original Brent's path planner is presented in Figure 3.7, where s and s_d denote the actual path length and corresponding desired path length of the wheelchair motion, respectively; R and T denote the current actual position and its tangent vector, respectively; R_d and T_d denote current desired position and desired tangent vector, which are both on the guide path; l is the position error between R and R_d. In the original model of Brent's path planner, l and the external normal force $F_\perp$ are perpendicular to T. This strategy of vector relationship easily leads to the instability problem in the mobility task, which will be discussed in detail in Section 3.6.1.

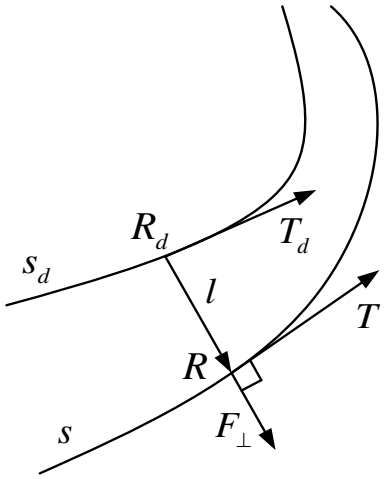

Figure 3.7: Kinematics model of Brent's path planner

The kinematics equation of the position error l is given by:

$$l = R - R_d \tag{3.10}$$

where the desired position R_d of the wheelchair is a function of desired path length s_d, and the actual position R of the wheelchair is a function of the actual path length s.

In the path following controller design, all the parameters can be taken as functions of the actual path length s. In particular, parameters on the guide path are indirect functions of s via the intermediate variable s_d. The first and second derivatives of l with respect to s, as deduced from equation (3.10), are given as:

$$l^{'} = T - s_d^{'} T_d \tag{3.11}$$

and

$$l^{''} = kN - s_d^{''} T_d - (s_d^{'})^2 k_d N_d, \tag{3.12}$$

where the symbol $(.)^{'}$ denotes the first derivative with respect to the path length s, kN denotes the current curvature vector of the actual path, and $k_d N_d$ denotes the corresponding curvature vector of the guide path.

The drive of the controller is provided by the control input U. In this application, we utilize the method of orthogonal projection decomposition of U, as shown in Figure 3.8. The second derivative of desired path length $s_d^{''}$, which is a scalar value, is given by projection of U onto the orientation of T, and the curvature vector kN is obtained from the projection of U onto the plane (Γ), which is perpendicular to vector T. From the inner product principle, $s_d^{''} = T^T U$, and $kN = U - s_d^{''} T$, so the expressions of these two variables are denoted as:

$$s_d^{''} = T^T U = U^T T \tag{3.13}$$

$$kN = (I - TT^T)U, \tag{3.14}$$

where the matrix $(I - TT^T)$ is a projection matrix which guarantees the perpendicular relationship $kN \perp T$.

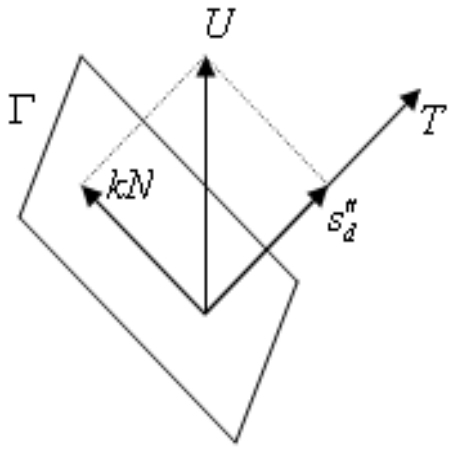

Figure 3.8: Orthogonal projection decomposition of the control input U

Substituting (3.13) and (3.14) into (3.12) gives

$$l'' = (I - TT^T - T_d T^T)U + (-(s_d')^2 k_d N_d) = MU + b, \tag{3.15}$$

where the square matrix $M = I - TT^T - T_d T^T$ is called the control matrix and $b = -(s_d')^2 k_d N_d$ is a bias because of nonzero values of s_d'' and $k_d N_d$. b is the zero vector when the motion direction of the wheelchair is perpendicular to the guide path, i.e., $T \perp T_d$ such that $s_d' = 0$, or when the guide path is a straight line, where $k_d N_d = \Theta$.

The control goal is realized by feedback linearization control method and the equivalent equation is given as

$$l'' = u \tag{3.16}$$

The combination of (3.15) and (3.16) gives

$$U = M^{-1}(u - b) \tag{3.17}$$

Thus, the complicated nonlinear system is now equivalent to a simple linear system and we just need to utilize a PD controller to implement the control task. The control law is given as

$$u = -(Pl + Dl^{'}) \tag{3.18}$$

Substituting (3.18) into (3.16) gives

$$l^{''} + Dl^{'} + Pl = 0, \tag{3.19}$$

where $P \succ 0$ and $D \succ 0$ are both positive definite matrices. Proper selection of P and D guarantees the asymptotic stability of the control system.

The block diagram of the wheelchair controller without elasticity is shown in Figure 3.9. The position error l and its first and second derivatives are calculated by the given variables kN and $s_d^{''}$, which are projections of control input U onto two perpendicular directions. Then the parameters T, R, $s_d^{'}$ and s_d are updated by integration of kN and $s_d^{''}$ respectively with respect to the differential element of ds. The position - related parameters in the guide path R_d, T_d and $k_d N_d$ are updated through both the shape of the path and the current first derivative $s_d^{'}$. The renewed parameters M and b can also be obtained with all the parameters given above worked out.

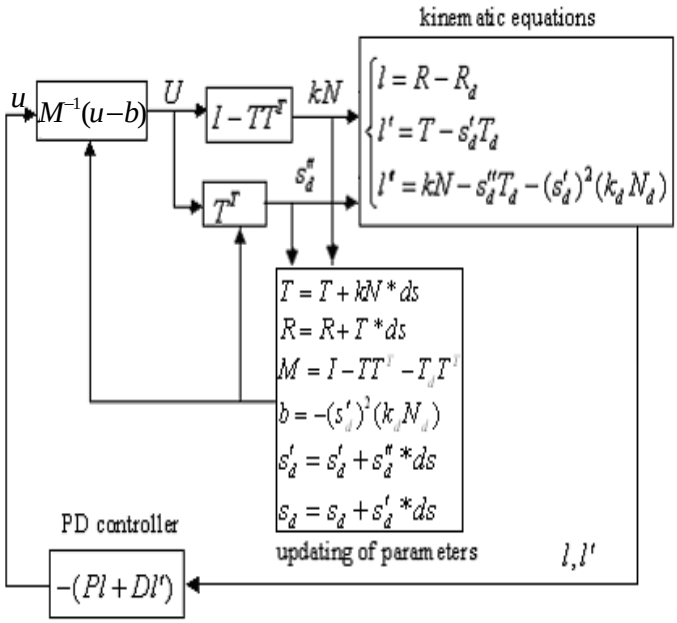

Figure 3.9: Block diagram of the wheelchair controller without elasticity

3.5.3 Comparison of the two controllers

The above analysis shows that Samson's controller utilizes two coordinate systems. The transformation calculation between these two coordinate systems is quite complicated, which may make Samson's controller generate larger cumulative error.

Furthermore, Samson's controller utilizes the trajectory tracking algorithm before transforming it into a path following algorithm. According to equation set (3.4), the first derivative $l^{'}$ is not continuous in the vicinity area $\frac{vcos(\triangle\theta)}{1-c_c l} = 0$, so $l^{''}$ does not exist in this area, which may cause the system to be unstable when $\frac{vcos(\triangle\theta)}{1-c_c l}$ is switched between 0^+ and 0^-.

In comparison, Brent's path planner sets up only one coordinate system, the Frenet Frame, on the motion path. It utilizes the path following approach directly, and its control algorithm is also much more concise than that of Samson. Therefore, Brent's path planner is likely to be safer and more stable than Samson's path controller.

However, one drawback of the Brent's path planner is that Brent's path planner origi-

nally selects the current actual tangent as its reference vector. This is not very stable when the external normal force is large or changes frequently. Moreover, Brent's path planner does not work properly and the wheelchair cannot return to guide path when its direction is perpendicular to the guide path, which is called the singularity problem. Therefore, it is necessary to design a new EPC based on Brent's path planner to solve these problems.

3.6 Development of a New EPC

3.6.1 Modification to the Brent's path planner

The original version of Brent's path planner is often unstable when the normal force is large or changes frequently because the chosen reference vector to the coordinate system is the current tangent in the actual path, which is a local vector with respect to the wheelchair. The normal force is always perpendicular to the actual tangent because it is from the joystick, which is fixed on the wheelchair. The normal force is always working as a centripetal force to the wheelchair, and so it is easy for the wheelchair to rotate frequently and the stability of wheelchair is not ensured.

The solution to this problem is to select the current tangent on the guide path instead of the one on the actual path as the reference vector of the coordinate system, as shown in Figure 3.10. The triangle symbol represents the wheelchair. Since the desired tangent is on the guide path, which is smoother than the actual path, it is easy to ensure the stability of the system.

3.6.2 Principle and basic implementation of the EPC

The Brent's path planner, without the effect of an external normal force, can satisfy the requirement of asymptotic stability of the CWA, which makes the CWA follows the

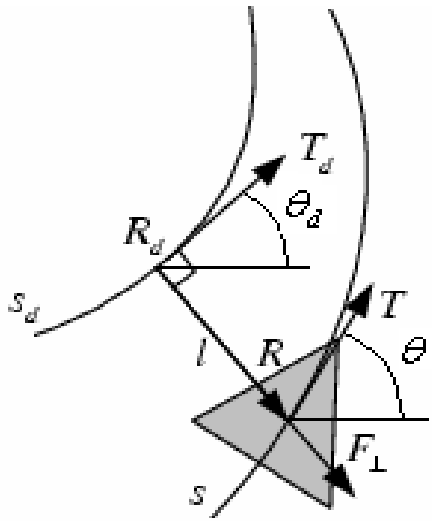

Figure 3.10: The desired tangent is chosen as the reference vector to the coordinate system

predefined guide path.

However, this kind of path planner is inflexible because it cannot perform some tasks users may need or solve some special events which often occur in practical application. In most cases, wheelchair users want the wheelchair to deviate from the guide path to avoid collision with obstacles or to go to the places beyond the guide path temporarily when required.

Figure 3.11 shows how the path controller is able to automatically produce a restoring force which brings the wheelchair a tendency to return to the guide path. The larger the distance between the actual path and the guide path, the larger the restoring force produced. At the same time, an external normal force is imposed on the controller. The normal force must be large enough to overcome that restoring force so as to make the wheelchair deviate from the guide path, and the wheelchair will come back to the guide path gradually after withdrawal of the normal force or when the normal force becomes smaller than the restoring force.

The steady state occurs when the normal force is equal to the restoring force, much like an elastic band. When the band is elongated, it will automatically generate a restoring

force which tends to make it spring back to its original status. The more the band is elongated, the larger the restoring force generated. The band will asymptotically return to its natural status after withdrawal of the external force or when the external force is no longer large enough to overcome the internal restoring force.

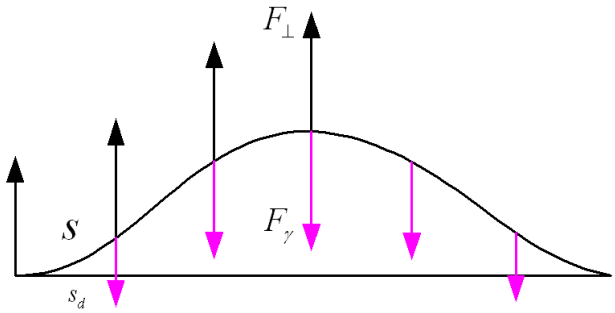

Figure 3.11: Illustration of an EPC

The control law of the EPC is expressed as

$$u = -(1-\lambda)F_\gamma + \lambda F_\perp \tag{3.20}$$

where $F_\gamma = Pl + Dl^{'}$ is called the restoring force and $F_\perp$ is the normal force because it is normal to the guide path; and λ is the elastic coefficient, which creates the balance between the two forces. The signs "-" and "+" before the restoring force and normal force are used to show the effect of opposite directions of these two forces. The restoring force is used to drag the wheelchair back to the guide path while the normal force is used to push the wheelchair to deviate from the guide path.

Wheelchair users can fulfill this task via some HMIs. A force/torque (FT) sensor was utilized in the simulation experiments. The application of FT sensor enables the operators to feel the magnitude and direction of their force imposed on the controlled subject. At the same time, they can build up a relationship between the velocity of the wheelchair and the force they impose, which will significantly contribute to the safety of the motion control of wheelchair. When the environment of the wheelchair is complex and the

users need enough time to identify the situation and decide how to deal with it, they can slow down the wheelchair by inputting a smaller force. In comparison, it is difficult for the users to control the wheelchair's velocity by only perception of the displacement of the handle of a common PSJ. Usually, the users are inclined to using the full capacity of their control to drive the wheelchair to its maximum velocity. An FT sensor is applied in the simulation experiments to prevent such risky operations in the complex or hazardous environments.

The FT sensor and its output decomposition are shown in Figure 3.12. Figure 3.12(a) shows the prototype of the sensor. A handle is fixed above the sensor with which users impose the force, which is measured by the sensor and sent out through the cable. As shown in Figure 3.12(b), the force vector coming from the sensor F can be decomposed into two perpendicular elements, horizontal element F_x and vertical element F_y, in the Cartesian coordinate system of the joystick. F_y can be taken as the source of the applied normal force, which tends to make the wheelchair deviate from the guide path. F_x works as a drive of the wheelchair, which provides the wheelchair with a value of translation velocity.

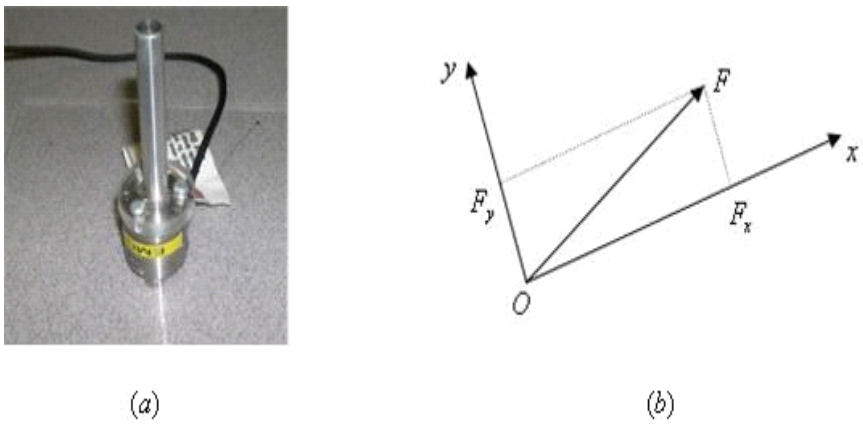

Figure 3.12: A force/torque sensor working as an HMI in the simulation

The orientation of the normal force on the wheelchair, generated through F_y, can be parallel to l with high accuracy after the motion program initializes the position error vector l by setting $l(0) \perp T_d(0)$. Figure 3.13 is the simulation result of the angular error

between l and T_d with nonzero applied forces imposed on the wheelchair. This indicates that the normal force is parallel to the position error because it is defined as being normal to the guide path.

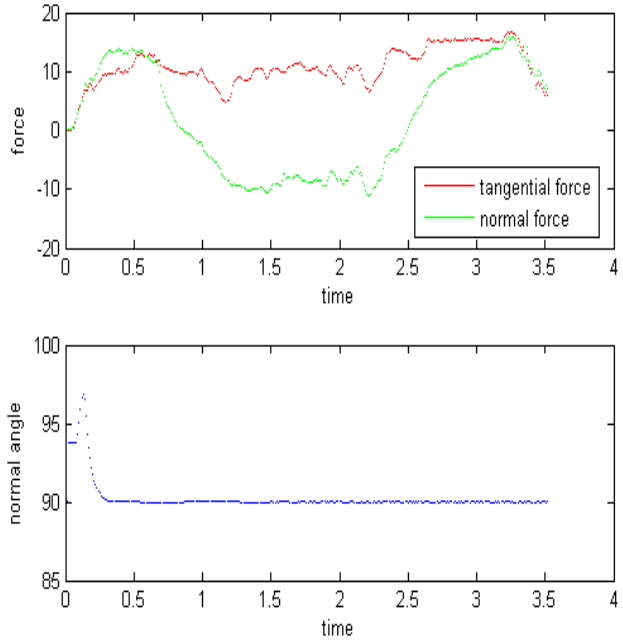

Figure 3.13: Simulation result of the angle difference between l and T_d, with nonzero external forces imposed on the wheelchair

At the beginning stage, the angular error can deviate substantially from 90°, possibly because the measurement error may be relatively large when the magnitude of l is small at the beginning. Another reason for the deviation occurs when the external force changes abruptly; however, the internal kinematics feature of this kind of controller will make the angular error asymptotically converge to 90°.

The generation of the normal force from the joystick input is an important part of this discussion. Normally, the normal vector is generated through left multiplication by a rotation matrix on the reference vector. For example, to generate a 2D vector that is perpendicular to the vector x, we can use $y = M_r x$, where the 2D matrix $M_r = \begin{bmatrix} 0 & -1 \\ 1 & 0 \end{bmatrix}$ is a rotation matrix, which leads to the relationship: $y \perp x$.

This method is available if the mobile base is always moving forward. Suppose F_x and F_y

are horizontal and vertical components of joystick input, respectively. If it is always true that $F_x > 0$, the normal force an be obtained by $F_\perp = \beta F_y M_r T_d$, where coefficient β is a multiplication factor to adjust the magnitude of the resultant normal force. This formula ensures that T_d rotates counterclockwise to form the direction of $F_\perp$ when $F_y > 0$, and that T_d rotates clockwise to form the direction of $F_\perp$ when $F_y < 0$ (Figure 3.14(a)). Thus, the direction of $F_\perp$ is determined by the direction of T_d and the sign of F_y.

The double movement case in our application will cause some problems. When $F_x < 0$, the direction of tangent T_d will be opposite to the heading direction of the wheelchair, as shown in Figure 3.14(b). According to the rule of rotation, the direction of $F_\perp$ is downward when $F_y > 0$, but the user sitting in the wheelchair expects the normal force $F_\perp$ to be upward since he/she inputs a positive value of F_y. This may cause confusion to the user.

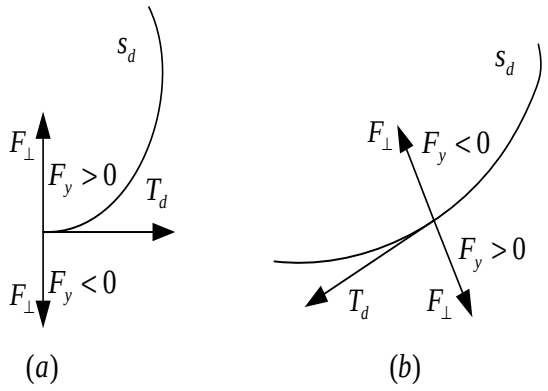

Figure 3.14: Generation of normal force using the method of rotation matrix multiplication

Thus, a new method of generation of normal force should be developed to eliminate the confusion to the wheelchair user. We propose two steps to fulfill this task. First, the force from the joystick input is transformed from the world coordinate system to the Frenet Frame built on the guide path. Next, the inner product is used to obtain the normal force from the transformed force.

As depicted in Figure 3.15, the coordinate system of the joystick mounted in the wheelchair can be transformed to the Frenet Frame on the guide path through multiplication by R_D^O,

a rotation matrix from coordinate system O to D. The newly transformed force $F^{'}$ is projected onto l to obtain intermediate normal force $F_{\perp}^{'}$, which can be easily transformed into required normal force by multiplying it by a scaling factor β. β is used here to adjust the contribution of joystick input to the control input. A larger value of β generates a larger normal force so it is easier for the wheelchair to deviate from the guide path. The ultimate normal force is expressed as

$$F_{\perp} = \beta(I - T_d T_d^T) R_D^O F \tag{3.21}$$

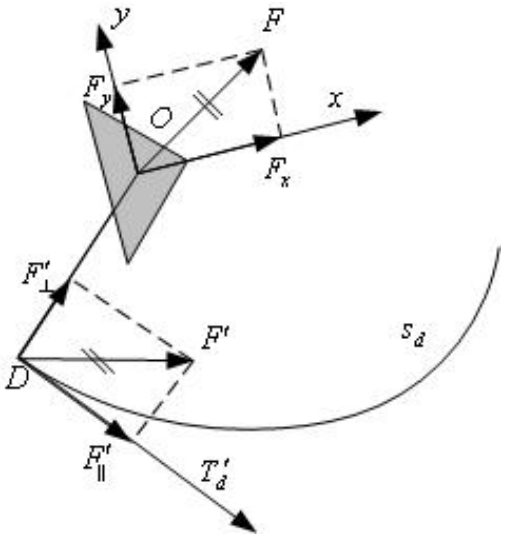

Figure 3.15: Transformation of force from joystick coordinate system to Frenet Frame

In most of the motion period, we expect the wheelchair to follow the guide path and for there to be no need for deviation. This requires the perpendicular force element F_y to remain at zero. However, users can not be certain that F_y is always zero when they push the handle of the joystick, since that pressure may cause the actual motion pathway to oscillate around the guide path. In order to eliminate this kind of unwanted oscillation, a threshold c_y is set for F_y. As shown in Figure 3.16, the actual value of F_y is set at 0 when the magnitude of F_y is smaller than c_y. This relationship between nominal input

and actual output of F_y is expressed as

$$\begin{cases} 0, |F_y| \leq c_y \\ F_y - c_y sign(F_y), |F_y| > c_y \end{cases} \tag{3.22}$$

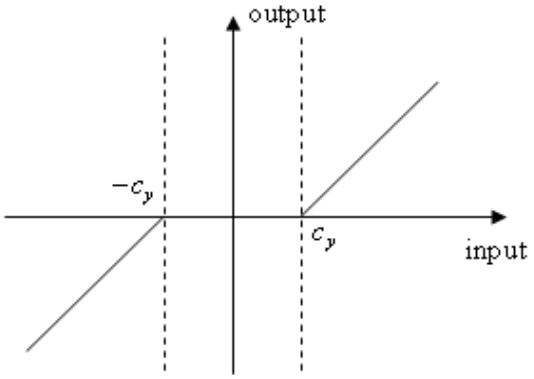

Figure 3.16: Relationship between nominal input and actual output of F_y

The block diagram of the whole EPC control system is given in Figure 3.17. The restoring force F_γ is worked out through the PD controller of which the input is the position error l. The normal force $F_\perp$ is calculated by equation (3.21). The elastic coefficient λ is decided by a function in equation (3.23). F_γ, $F_\perp$ and λ come together to determine the control variable u.

3.6.3 Elastic coefficient

In the control law of the EPC shown in equation (3.20), the symbol λ is called the elastic coefficient. λ acts as a weight which assigns different contributions of the two forces, the restoring force F_γ and the normal force $F_\perp$, to the overall control input u.

The selection rule of λ should satisfy the fundamental criteria of an EPC and it is a function of both F_y and l, that is, $\lambda = f(F_y, l)$ [66].

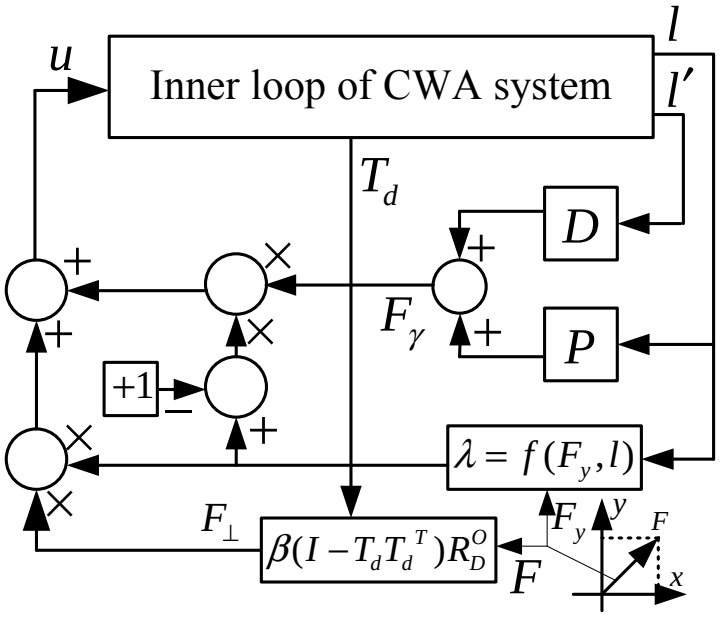

Figure 3.17: Block diagram of the whole EPC control system

Based on equation (3.20), five cases are related to the value of λ. When $\lambda = 1$, F_γ has no contribution to the feedback input, so the wheelchair is not to be dragged back to the guide path with the effect of the restoring force. When $\lambda = 0$, $F_\perp$ has no contribution to the feedback input, so the normal force cannot be applied to drive the wheelchair to deviate from the guide path. When $\lambda \in (0,1)$, F_γ and $F_\perp$ both have positive values, so their contributions to the feedback input are counter-effects and increase of λ increases the weight of $F_\perp$ while it decreases the weight of F_γ in the feedback input. When $\lambda \in (-\infty,0)$, $\lambda < 0$ and $(1-\lambda) > 0$, so both the restoring force and the normal force make negative contributions to the feedback input and keep the wheelchair from deviating from the guide path. Finally, when $\lambda \in (1,+\infty)$, $\lambda > 0$ and $(1-\lambda) < 0$, so both the restoring force and the normal force make positive contributions to the feedback input and impel the wheelchair to deviate from the guide path.

From this analysis, it is clear that, when $\lambda \notin (0,1)$, the restoring force and the normal force have the same directions of contributions to feedback input and cannot act as the counter effects to the wheelchair mobility task. In addition, the restoring force does not compel the wheelchair back to the guide path when $\lambda = 1$, and the normal force does not drive the wheelchair to deviate from the guide path when $\lambda = 0$. Therefore, the value of

λ should be in the range of $\lambda \in (0,1)$, but the value of λ is notably close to neither 0 or 1.

If we combine all of these factors, the expression of λ can be expressed as the following equation set:

$$\begin{cases} \lambda_1 = \frac{1}{2}\{(\frac{F_y}{F_{ymax}})^2 - (\frac{l}{l_{max}})^2 + 1\} \\ \lambda = \lambda_1, \lambda_1 \in [0.1, 0.9] \\ \lambda = 0.1, \lambda_1 < 0.1 \\ \lambda = 0.9, \lambda_1 > 0.9 \end{cases} \tag{3.23}$$

In equation (3.23), the upper limit value and lower limit value of λ are set as $\lambda_{max} = 0.9$ and $\lambda_{min} = 0.1$, respectively, to ensure that both forces make clear contributions to the wheelchair mobility task. (3.23) also guarantees the continuation requirement of the elastic coefficient.

Equation set (3.23) involves two parameters: F_{ymax} and l_{max}. F_{ymax} is easily decided by the maximal value of permitted perpendicular input of the joystick. However, the decision regarding l_{max} is more complex. It is evident that the minimum permitted value of l_{max} is the steady state value of l_{ss} when $F_y = F_{ymax}$, excluding the overshoot in the motion trajectory of the wheelchair. Therefore, $l_{ss} = l_{max}$ when $F_y = F_{ymax}$. The value of λ is 0.5 according to equation (3.23). In the steady stage, l does not change, so $l'' = l' = \Theta$. According to equation (3.20), the magnitude of l_{max} is given as

$$l_{max} = \frac{\lambda}{1-\lambda}\|P^{-1}\|\|F_{\perp max}\| = \beta\|P^{-1}\|\|F_{ymax}\| \tag{3.24}$$

Now we can plot the curve of relationship among λ, F_y and l. We set $P = 4I$, $\beta = 5$, and $F_{ymax} = 10$, and the magnitude of maximal position error is worked out as $l_{max} = 12.5$. The relationship curve is shown in Figure 3.18.

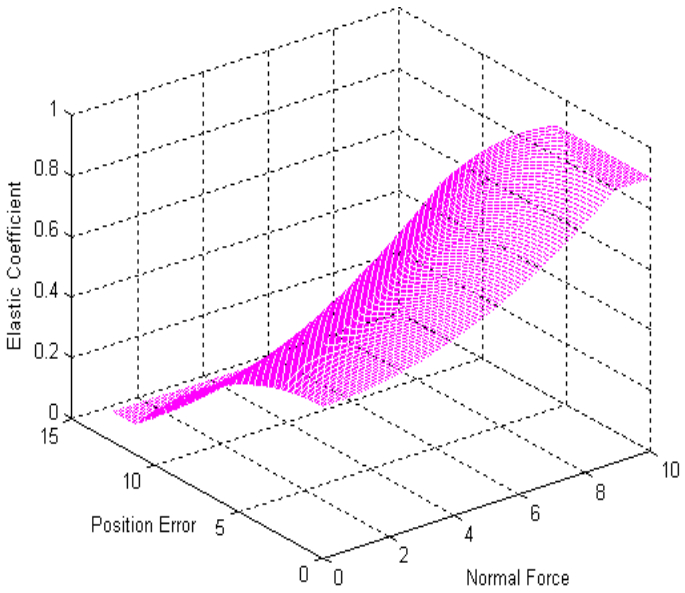

Figure 3.18: Relationship of λ with respect to F_y and l

The curve of the relationship between l_{ss} and F_y can be plotted, as shown in Figure 3.19. It is shown that the magnitude of steady state position error l_{ss} is proportional to that of the applied force F_y. This can be verified by calculation of l_{ss} with a given F_y.

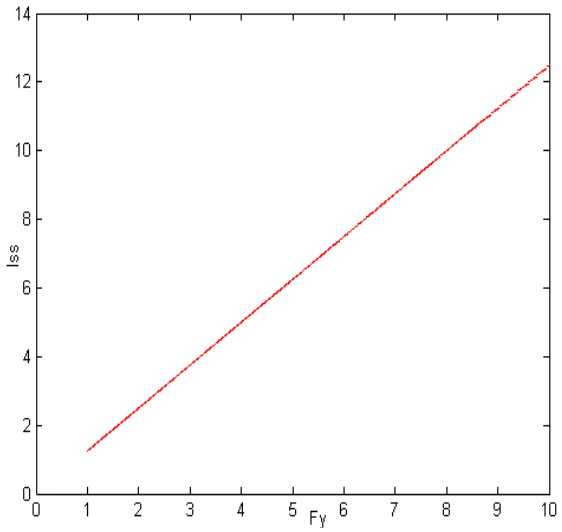

Figure 3.19: Relationship between l_{ss} and F_y

In the steady state, l does not vary, so $l^{'} = l^{''} = \Theta$. Since $F_{\perp}$ is a transformation form of

F_y multiplied by a scaling factor β, $\|F_\perp\| = \beta\|F_y\|$. Thus, from (3.20),

$$l_{ss} = \frac{\lambda\beta}{1-\lambda}\|P^{-1}\|\|F_y\| \tag{3.25}$$

All the related vectors in this paragraph represent their magnitudes. $\lambda = 0.5$ in the steady state based on the following proof: Assume that the position error reaches the steady state $l = l_{ss1}$, given the applied force $F_y = F_{y1}$. If the applied force is increased to some value $F_{y2} > F_{y1}$, and since l can not be changed immediately, λ will be larger than it was in the previous steady state, that is, $\lambda_2 > \lambda_1$. If the ultimate value of λ in the new steady state equals λ_2, the new steady state $l_{ss2} = \frac{\lambda_2\beta}{1-\lambda_2}\|P^{-1}\|F_{y2}$. Combining this equation with other two expressions, $l_{ss1} = \frac{\lambda_1\beta}{1-\lambda_1}\|P^{-1}\|F_{y1}$ and $\frac{\lambda_2}{1-\lambda_2} > \frac{\lambda_1}{1-\lambda_1}$, we obtain the inequality, $\frac{l_{ss2}}{F_{y2}} > \frac{l_{ss1}}{F_{y1}}$, meaning that l_{ss} increases faster than does F_y. On the other hand, a faster increase of l_{ss} causes a decrease in λ. The ultimate value of elastic coefficient in the steady state is $\lambda_2 = \lambda_1$, which denotes that $\frac{l_{ss2}}{F_{y2}} = \frac{l_{ss1}}{F_{y1}} = \frac{l_{max}}{F_{ymax}}$. Therefore, the elastic coefficient in any steady state with a fixed nonzero normal force is $\lambda = 0.5$. Substituting the value of λ into (3.25) gives

$$l_{ss} = \beta\|P^{-1}\|\|F_y\| \tag{3.26}$$

Equation (3.26) shows that the magnitude of l_{ss} is proportional to that of $\|F_y\|$, given a nonsingular matrix P^{-1}.

3.6.4 Stability analysis

The performance of the EPC is very much influenced by $\Delta\theta = \theta - \theta_d$, the angular error between the actual and desired tangent (Figure 3.10). Figure 3.20 shows the effect of the initial angular error on the actual path of the wheelchair that starts from an initial position not on the guide path. When the initial angular error $\Delta\theta$ increases, with all

other conditions fixed, the wheelchair takes a longer route to approach the guide path. Thus, the actual path has a tendency to deviate from the guide path as $\Delta\theta$ increases. Section 3.6.5 shows that the wheelchair will no longer return to the guide path if $\Delta\theta$ is near to 90°.

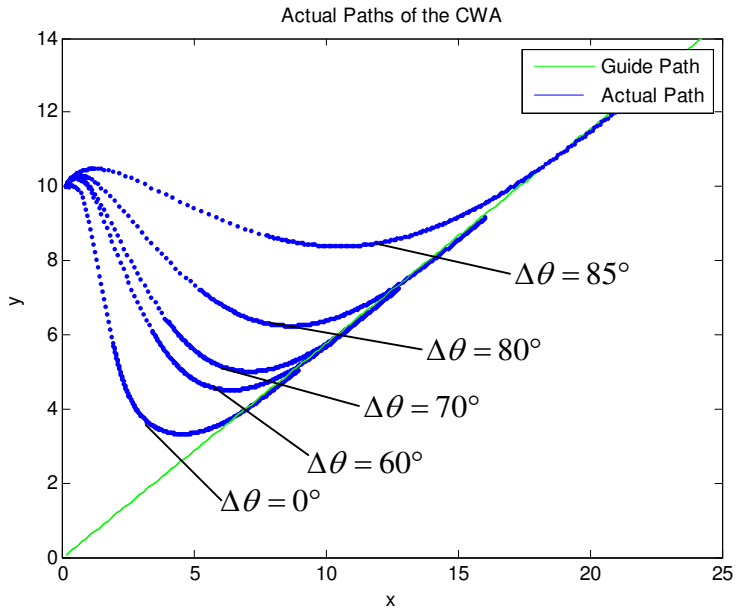

Figure 3.20: Relationship between the initial angular error and actual path of the wheelchair

From Figure 3.10, since θ and θ_d are the actual tangential angle and corresponding desired tangential angle, respectively, the tangential vectors can be expressed as

$$\begin{cases} T = \begin{bmatrix} cos(\theta) & sin(\theta) \end{bmatrix}^T \\ T_d = \begin{bmatrix} cos(\theta_d) & sin(\theta_d) \end{bmatrix}^T \end{cases} \tag{3.27}$$

We can calculate the control matrix M according to the definition of M. This gives

$$M = \begin{bmatrix} sin^2\theta - cos\theta cos\theta_d & -sin\theta(cos\theta + cos\theta_d) \\ -cos\theta(sin\theta + sin\theta_d) & cos^2\theta - sin\theta sin\theta_d \end{bmatrix} \tag{3.28}$$

After that, it is a simple matter to obtain the determinant of matrix M, as well as that of M^{-1}:

$$det(M) = -cos(\theta - \theta_d) = -cos(\triangle\theta) \tag{3.29}$$

$$det(M^{-1}) = \frac{1}{det(M)} = -\frac{1}{cos(\triangle\theta)}. \tag{3.30}$$

From (3.30), $|det(M^{-1})|$ is a monotonic increasing function of $\triangle\theta$ for $0 < \triangle\theta < 90°$, as shown in Figure 3.21. The relationship between $\triangle\theta$ and $|det(M^{-1})|$ for $90° < \triangle\theta < 180°$ is also drawn in Figure 3.21 based on the symmetry characteristics about the vertical axis of cosine function. The relationship curve is not drawn with the angular error $\triangle\theta \in [89°, 91°]$ because the value of $|det(M^{-1})|$ tends to explode and may affect the expression of other values beyond this region. $|det(M^{-1})|$ becomes larger when $\triangle\theta$ comes closer to 90°.

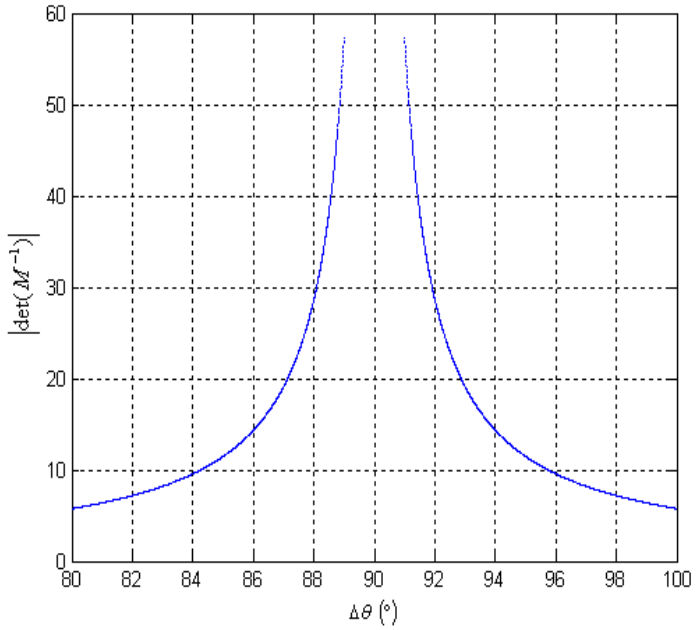

Figure 3.21: Relationship between the angular error and determinant of inverse control matrix

Table 3.1: Relationship between $|det(M^{-1})|$ and $\triangle\theta$

$\triangle\theta(^\circ)$	87	88	89	89.2	89.4	89.6	89.8	90
$\lvert det(M^{-1})\rvert$	19.1	28.7	57.3	71.6	95.5	143.2	286.5	∞

3.6.5 Singularity analysis and handling method

To illustrate in depth the relationship between $\triangle\theta$ and $|det(M^{-1})|$ when $\triangle\theta$ is very near to 90°, Table 3.1 shows the relationship with values $\triangle\theta \in [87^\circ, 90^\circ]$. Table 3.1 shows that the control input U goes to infinity when $\triangle\theta = 90^\circ$. Actually, U is so large that it is beyond the physical constraints in many industrial applications when $\triangle\theta(0) \geq 87^\circ$; that is to say, there is no bounded U that makes the position error l asymptotically converge to zero if the initial angular error $\triangle\theta(0)$ is in the vicinity of 90°.

To the best of our knowledge, no literature is available to handle the singularity problem of the EPC used in the robotic wheelchairs up to now. The kinematic singularities have been addressed for the control of manipulators. The basic idea is to use inverse kinematics to transform various control tasks into corresponding joint motions. Some tried to avoid going close to the singular configuration by maximizing the operation capacity of the end-effectors [67], but this is not feasible when the manipulator is not redundant. Others eliminated the degenerate motion components to avoid large joint velocity when the manipulator enters the vicinity of singularity [68]. Still others applied the singularity robust approach, which addresses the discontinuity problem with removal of degenerate components [69]. They might be effective in the control of robot manipulators, but robotic wheelchair has no complex kinematics configuration consisting of joints and end-effectors and no inverse kinematics is needed. So some simplified methods may be proposed in this thesis to solve the singularity issues in the EPC of the CWA.

To handle the singularity problem illustrated in Table 3.1, we need to define a singularity region when the angular error is within some range - say, $\triangle\theta \in [80^\circ, 100^\circ]$. Inside this singularity region, the controller will cause the wheelchair to make a pure rotation about its own axis so that it can jump out of the region. The direction of rotation is dependent

on the direction of the externally applied force and the orientation of the wheelchair relative to the guide path. The rule for the choice of the direction of rotation is to ensure that the wheelchair can follow the drive of the applied force after it jumps out of the singularity region. The application of this rule is shown in Figure 3.22, where the desired rotation of the wheelchair is classified into four cases.

Using case ① as an example, when the heading direction of the wheelchair Γ is within this singularity region and the applied force F_1 is forward, the controller will drive the wheelchair to rotate clockwise with angular speed ω_1. After the wheelchair jumps out of the singularity region, it can move according to the usual path control algorithm. Case ③ is similar to case ①, except that the wheelchair rotates in the counter-clockwise direction with angular speed ω_3 to get out of the singularity region. Cases ② and ④ are different from cases ① and ③, because cases ② and ④ stipulate that the orientation of force is backward while the orientation of the wheelchair always points to the forward direction of the guide paths. When the heading direction of the CWA Γ is upward and F_2 is to the left, as shown in case ②, the wheelchair will move backwards and rotate clockwise with an angular speed of ω_2 until the wheelchair is aligned to $-F_2$. Case ④ is similar to case ②, except that the wheelchair rotates counter-clockwise with angular velocity ω_4. The angular velocities, ω_i, $i = 1, 2, 3, 4$, are chosen so that $\omega_i \leq \omega_{max}$, where ω_{max} is the maximum value of the angular velocity that is permitted by the wheelchair controller.

3.7 Simulation Experiments

Simulation experiments were conducted mainly to test the control algorithm of the newly developed EPC before it is used in the CWA.

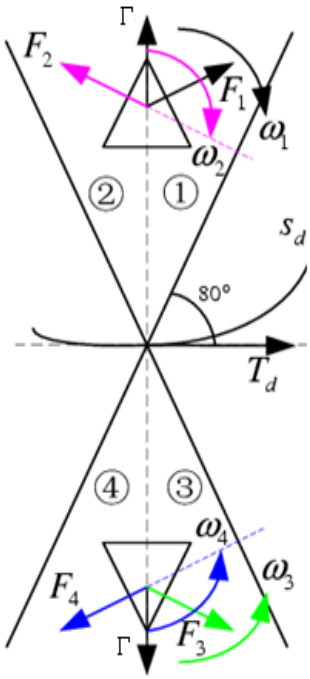

Figure 3.22: Solution to singularity problem of wheelchair motion

3.7.1 Devices and software used in the simulations

Devices used in the simulations includes a force/torque (FT) sensor, a PC and dedicated software, as seen in Figure 3.23.

The FT sensor is used as an HMI to simulate the force feedback function of the CWA. The FT sensor FT6142 was provided by ATI Industrial Automation Company. The multi-axis FT sensor system FT6142 can be used to measure the 6 dimension of information, 3D forces and 3D torques, in parallel. As depicted in Figure 3.24, the FT sensor consists mainly of 3 components - Transducer, Interface Electronics and DAQ Card - connected by dedicated cables. The semiconductor strain gauges in the transducer change their resistances according to the externally imposed forces/torques, which are detected and output in the form of low-level voltages. The Interface Electronics hardware receives the low-level voltages, creates signal processing, and outputs high-level voltages accordingly. The DAQ system converts the transducer signals from raw voltages to digital information that can be used by the computer. The DAQ Card is the PCI-

Figure 3.23: Devices used in the simulation experiments

6034E, supplied by the National Instrument Company. The DAQ Card driver installed in the PC receives the load information from the transducer, and the corresponding software converts the high-level voltages, which represent the change of resistances in the transducer, to force and torque components and display the change to the wheelchair users. The outline of the signal acquisition and processing of the FT sensor is shown in Figure 3.25.

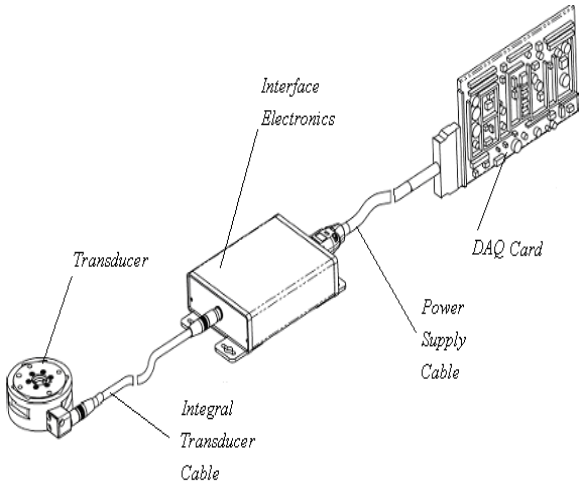

Figure 3.24: Hardware installation of the FT sensor FT6142

The PC was a DELL Pentium 4, with a main frequency of 3.00GHz and RAM of 512 MB. MATLAB7.0 was used as the programming software.

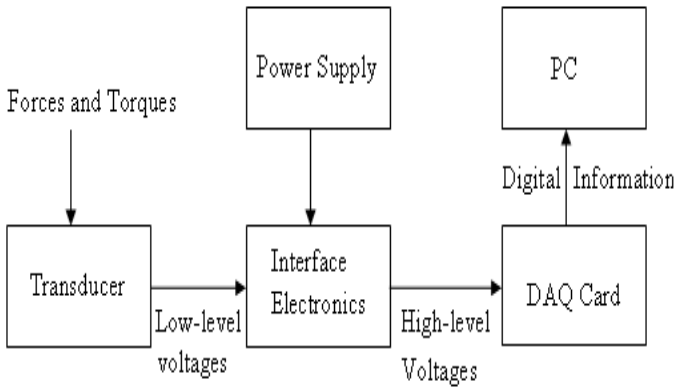

Figure 3.25: Signal acquisition and processing of the FT sensor

The pre-designed guide path is a B-Spline generated by the software in the computer. Since the two front caster wheels only take the role of support and have no contribution to the mobility task of the CWA, the symbol "△" is used to represent the moving wheelchair in the simulation experiments. Simulation experiments were conducted on the fundamental functions of EPC and nonlinear EPC.

3.7.2 Simulation for fundamental functions of the EPC

The EPC can fulfill fundamental functions, including the ordinary tasks of path following, obstacle avoidance, handling singularities and backward motion, as shown in Figure 3.26 and Figure 3.27. The thinner curve is the predesigned guide path, and the thicker curve denotes the segment of guide path that corresponds to the actual path of the CWA.

Figure 3.26 shows how the EPC drives the CWA to handle a singularity issue and avoid the obstacle. The CWA can move forward in the singularity region at the start point *A* (see Figure 3.26(a)) and asymptotically follow the guide path without externally applied normal force to reach the guide path at point *B*. The CWA will deviate from the guide path with normal force when the user finds the obstacle on the guide path and it arrives at point *C*. After that, the CWA returns to the guide path again with removal of normal force and ends at point *D*. In the simulation, the corresponding desired position of

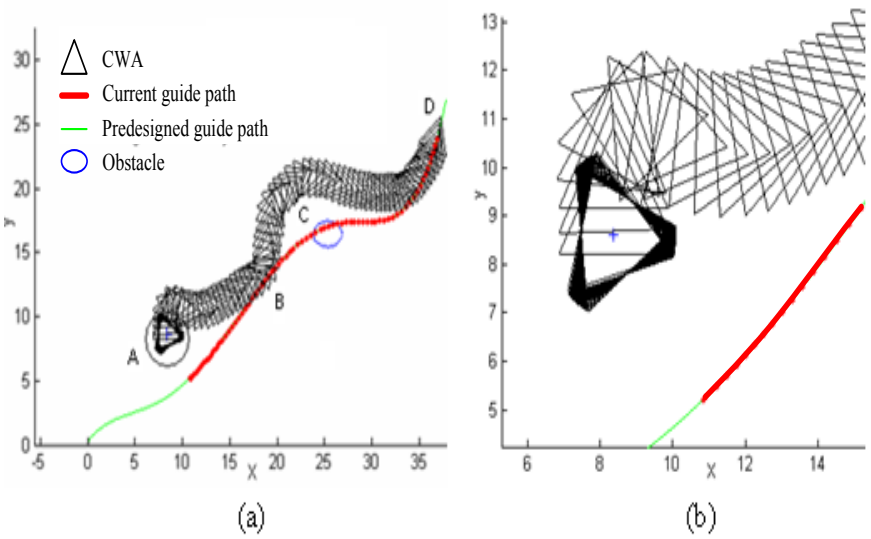

Figure 3.26: Simulations of singularity handling and obstacle avoidance functionalities

the CWA is always the perpendicular projection of the actual position on the guide path, meaning that the algorithm ensures the implementation of the Frenet Frame on the guide path. The singularity motion procedure at start point *A* is magnified and shown in Figure 3.26(b), from which it is clear that the CWA makes a pure rotation when it drops into the singularity region, and it moves as usual after it jumps out of the singularity region. The guide path is an arbitrary curve generated by the PC, so it can represent a general guide path that is utilized in the CWA applications. Simulation results show that the CWA can fulfill the mobility tasks under the control of the EPC proposed in this thesis.

Figure 3.27 simulates the path following and backward motion functionalities of the CWA. In this experiment, the wheelchair starts from *A* and follows the guide path (segment *B*). At point *C*, the wheelchair goes back toward the direction of start point *A* with its heading remaining in the same direction and not turned around. After it gets to *D*, the wheelchair goes forward and its direction follows the actual tangent again. The user then decides to go to point *E* and so he/she applies a normal force to the left to move the CWA from the guide path to point *E*.

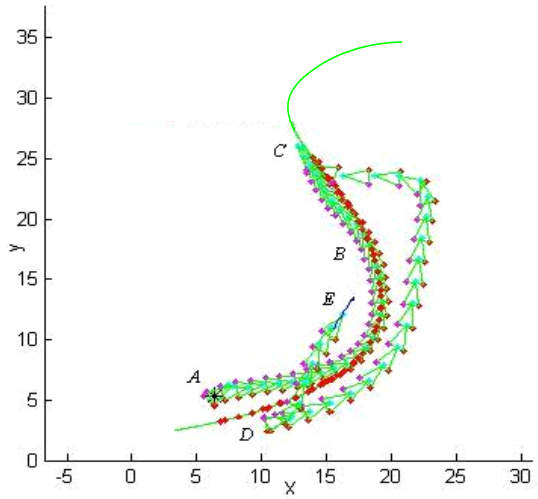

Figure 3.27: Simulations of path following and backward motion functionalities

3.7.3 Comparison of the new EPC with the old one

The new EPC selected the desired tangent T_d in stead of T as its reference vector. The new EPC was conducted simulation experiments in comparison with the old one, as shown in Figure 3.28. The solid curve in the lower subfigure represents the actual path of CWA under control of the new EPC, and the dashed curve represents the actual path of CWA controlled by the old EPC. It is seen that the actual path is oscillating at points A, B, and C when the perpendicular joystick input changes frequently between -5N and +5N for the CWA controlled by the old EPC. In comparison, the actual path of CWA controlled by the new EPC is always stable when the perpendicular joystick changes in the same pattern. Further increase of the input magnitude to 10N makes the actual path of old EPC controlled CWA explode, while the new EPC controlled CWA always moves stably.

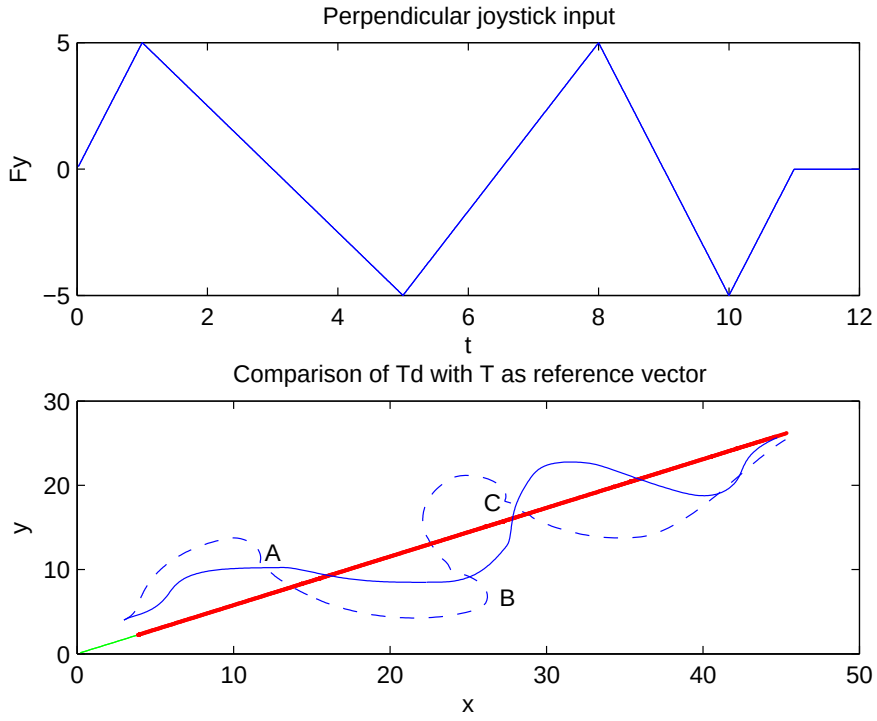

Figure 3.28: Simulation of EPC when the reference vector changes

3.8 Real-time Experiments

3.8.1 Objectives

Objectives of the experiments were to test if the CM and EM are easier to drive and less energy-consuming to users than FM, and if the EM is an effective assistive tool for the CWA users.

3.8.2 Subjects

5 able people, whose ages are between 24 and 33, with no body disabilities participated in the experiments. They all had no experience of driving wheelchairs.

3.8.3 Experimental environments

The experiments were designed in a laboratory environment with many tables, as shown in Figure 3.29. The subjects were asked to drive the CWA from the start point *A* to the end point *B*, passing through a narrow door of 0.8m in width in the middle of the travel.

The guide path for CM and EM to refer to was generated beforehand in software through the WTP and stored in the computer. In FM, the users would finish the motion task depending on their own mentalities and skills.

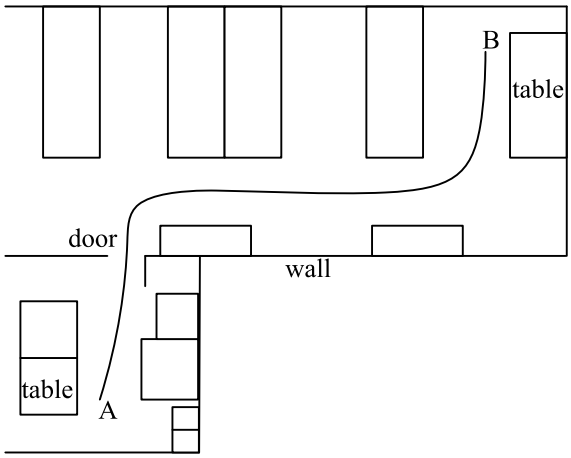

Figure 3.29: Experimental environment

3.8.4 Training and instructions

Each subject was seated on the CWA with motors turned off and he was told about the basic knowledge about the wheelchair and its components. Then the knowledge about the CWA, EPC and three control modes were described and the GUI was shown to him. He was instructed how to drive the CWA with FM, EM and CM comfortably.

After training and instructions, the subject was told about the task and objective of the experiments. He was instructed to drive the CWA from the start point *A* to the end point

B, and safely pass through the narrow door without collision. He was asked to minimize the movement of the joystick.

Each subject had to repeat the experiments in the order of FM, CM and EM for 5 times. The overall experiment time for one subject was about 55 minutes.

3.8.5 Data analysis methods

Three indices were investigated to evaluate the performance of EPC with different control modes: travel time, parallel joystick move and normal joystick move.

Travel time is used to estimate how fast the users can complete the motion task from the start point to the end point. Shorter travel time indicates that the users can finish the same motion task faster and so maneuver the CWA more efficiently.

Parallel joystick move is defined as sum of the parallel projection of the joystick move, which is the accumulated variation of the joystick position during the mobility task of the CWA. Parallel joystick move denotes the confidence of the users in control of the motion velocity of the CWA. Bigger parallel joystick move indicates that the user is more hesitant and intervenes more about the motion velocity of the CWA, and the velocity of the CWA also varies more frequently.

Normal joystick move is the normal project of the joystick move and is closely related to confidence of the user in steering control of the CWA. Bigger normal move indicates the user spends more mentality and intervenes more in the steering control of the CWA.

MATLAB' tool, TTEST2 (Two-sample t-test) was used to compare the performance between two control modes out of FM, CM and EM. The null hypothesis is "the means of given two samples are equal" and the significance level is $\alpha = 5\%$. The null hypothesis is rejected at the significance level when the p-value is $p < \alpha$.

3.8.6 Results

All the 5 subjects could fulfill the mobility tasks from the start point to the end with no collision with the environments. The driving performance of CWA using FM, CM and EM is evaluated as followings.

Travel time

The average travel time in FM, CM and EM is 33.7s, 27.2s and 27.6s respectively. The travel time was significantly longer in FM than in EM ($p < 0.0001$) and CM ($p < 0.0001$), while the travel time was not significantly different between CM and EM ($p > 0.7$).

Parallel joystick move

Figure 3.30 shows that the parallel joystick move was significantly larger in FM than in EM ($p < 0.0001$) and in CM. The parallel joystick move had no significant change between CM and EM ($p > 0.64$). Figure 3.30 also indicates that the parallel joystick move tends to be decreased with the increased number of trial in FM, CM and EM.

Normal joystick move

Figure 3.31 shows the normal joystick move was significantly larger in FM than in EM ($p < 0.0001$) and CM ($p < 0.0001$). The normal joystick move was not significantly different in CM from that in EM ($p > 0.069$). Figure 3.31 also shows that the normal joystick move tends to be decreased with the increased number of trial in FM, CM and EM.

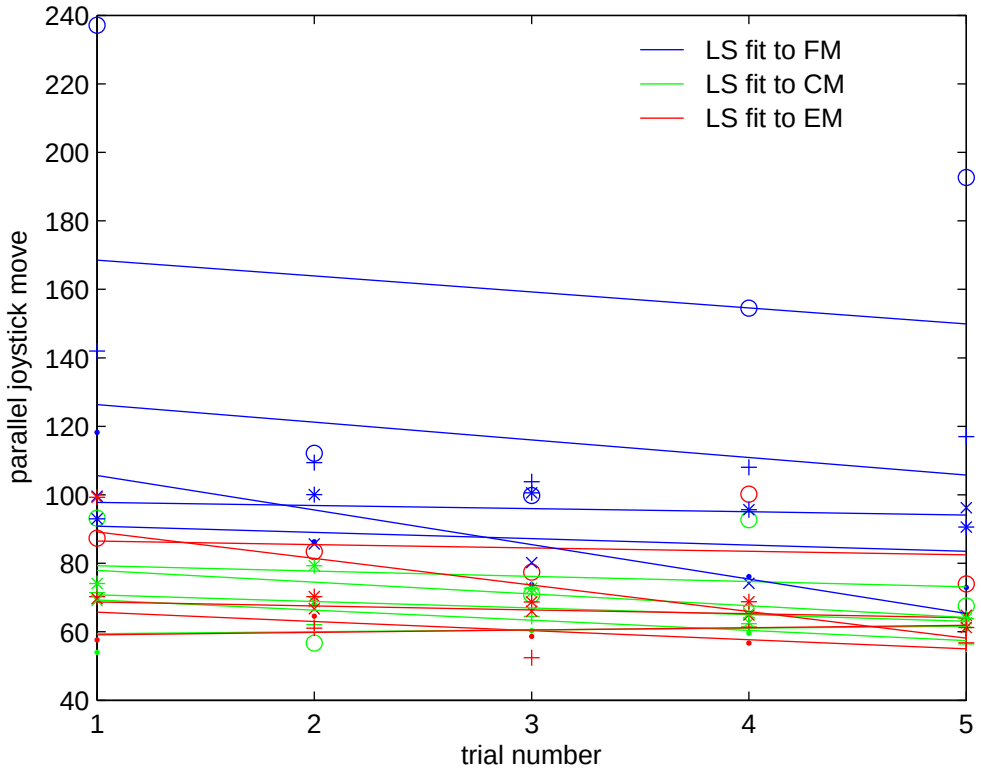

Figure 3.30: Parallel joystick move

3.8.7 Discussions

Driving efficiency

The travel time in CM and EM was significantly shorter than in FM for the same mobility task of the CWA, which shows that the driving efficiency of EM is higher than the one of FM. At the same time, the driving efficiency of EM is comparable to that of CM, because their travel time is not significantly different for the same mobility task of the CWA.

Intervention in the velocity control

The parallel joystick input is used to control the motion velocity of the CWA. The parallel joystick move reflects how much the user intervenes in the velocity control. Ac-

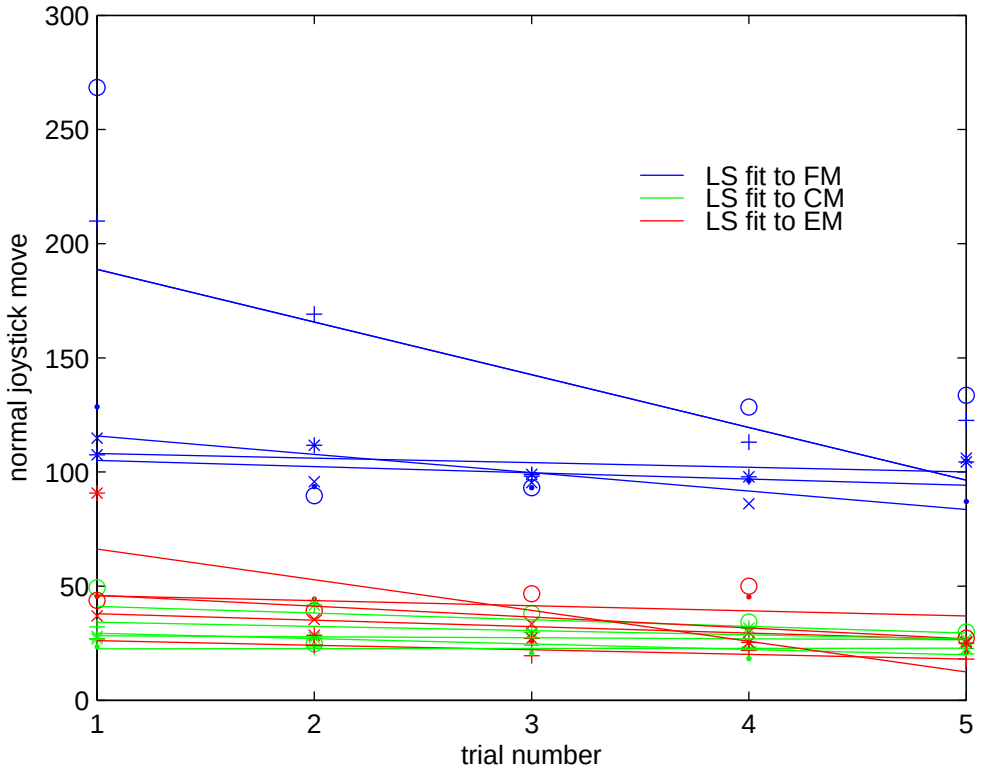

Figure 3.31: Normal joystick move

cording to Figure 3.30, the parallel move in FM was significantly larger than that in EM, which indicates that subjects intervene more in the velocity control in FM than in EM. The possible reason is that the subjects have no guide path to rely on when they drive the CWA in FM. So they hesitate to move forward to change the parallel joystick input frequently. In comparison, the subjects have guide path when they drive in EM, so they are more confident about the mobility task and need not vary the parallel joystick input so frequently as in FM. Subjects also have guide path to depend on in CM, which causes that the parallel move in CM is similar to that in EM.

The parallel move was decreased with the increase of trials, which confirms that training to drive the CWA improves the subjects' driving skills and make them more confident in the mobility task of the CWA.

Intervention in the steering control

The normal joystick input is used to control the steering of the CWA and the normal joystick move represents how much the user intervenes in the steering control. According to Figure 3.31, the normal move in FM was remarkably lager than that in EM. This may be because that the subjects have no guidance in FM and they have to vary the normal joystick input more to adapt to the environment. The subjects have guide path to rely on in CM and EM, so their normal move is similar and notably smaller in comparison with that in FM.

3.9 Conclusion

In this chapter, a new EPC was developed based on the Brent's path planner to suit for the application of CWA. The simulation experiments and real-time experiments were also conducted to evaluate the performance of the EPC. The results of these experiments show that the EPC can fulfill its fundamental functions and handle the singularity issues nicely.

The performance of three control modes was also compared based on real-time experiments by fulfilling the same mobility task. The results of the experiments showed that:

- The driving efficiency of the CWA is notably improved by providing the guide path.
- The user's intervention in the velocity control as well as in steering control is greatly decreased in comparison with that in FM.
- The user's intervention in the velocity and steering control is not significantly different between CM and EM.
- Training helps to improve the driving performance in FM, CM and EM.

The driving performance of EM is better than that of FM and is comparable to that of CM. At the same time, the CWA in EM can deviate from the guide path while it cannot deviate in CM. This indicates that users in EM have more autonomy to control the CWA. Such unique characteristics of EM make it an irreplaceable assistive tool for the disabled users in the daily driving tasks of the CWA.

Chapter 4

Improvements of the EPC

4.1 Introduction

This chapter mainly addresses how to further improve the performance of the newly developed EPC described in Chapter 3.

One aspect is how to optimize the controller parameters so as to minimize the influence of external perturbations and parameter uncertainties. Another issue is to make the controller drive the CWA to deviate no matter how far away from the guide path to avoid large size obstacles.

4.2 Parameter optimization of the EPC

The parameters P and D in equation (3.20) are two symmetric positive definite matrices such that $P = P^T \succ 0$ and $D = D^T \succ 0$. They determine the kinematic characteristics as well as the asymptotic stability of the closed-loop control system. Generally speaking, the larger the gain P, the faster the wheelchair goes back to the guide path. D represents the damping ratio of the control system. The system is over-damped when $D > 2\sqrt{P}$,

and under-damped when $D < 2\sqrt{P}$. It is known that faster response speed is obtained at the price of a larger degree of oscillation. Thus, we need to choose D as a compromise between smaller oscillation in the transient process and faster response to the command signals.

However, the parameters are not optimized when external perturbations and parameter uncertainties exist in the real environment. This chapter proposes the parameter optimization process using the H_2 robust control technique [70] [71] [72] when external perturbations and parameter uncertainties are taken into consideration in the real environment.

The EPC control system described in previous chapters is stable if the kinematic model is accurate and all parameters are determined exactly. In practice, however, the parameters cannot be known exactly. Parameters uncertainties, sensor noises, perturbations, disturbances, and other inputs will affect the stability and performance of the overall control system. Thus, the developed controller should be robust enough to tolerate all the possible uncertainties. In our case, we take the equivalent of all the uncertainty factors as disturbance w on the control vector u, as shown in Figure 4.1.

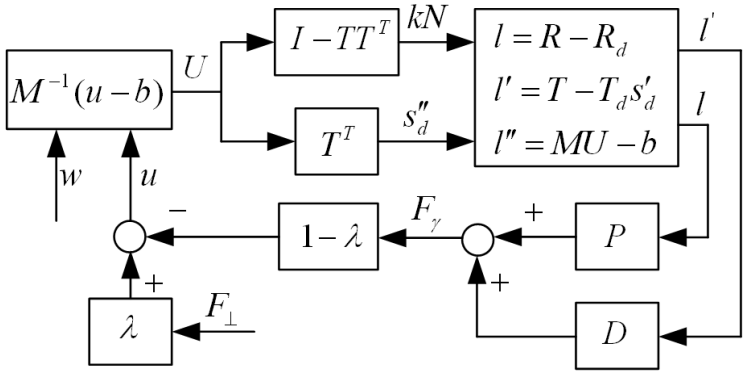

Figure 4.1: Block diagram of of an EPC with an equivalent disturbance w

The equivalent equation of the system after feedback linearization can be rewritten as

$$l'' = u + w, \tag{4.1}$$

where w is the equivalent disturbance to the system. We can define a new four-dimension vector as

$$x = \begin{bmatrix} l \\ l' \end{bmatrix}$$

And, taking $z = l$ as the controlled output, the state equation of the control system can be expressed as

$$\begin{cases} x' = \begin{bmatrix} l' \\ l'' \end{bmatrix} = Ax + Bu + Ew \\ z = \begin{bmatrix} I & 0 \end{bmatrix} x = C_2 x + D_2 u, \end{cases} \tag{4.2}$$

where the matrices are

$$A = \begin{bmatrix} 0_{2\times 2} & I_{2\times 2} \\ 0_{2\times 2} & 0_{2\times 2} \end{bmatrix}$$

$$B = E = \begin{bmatrix} 0_{2\times 2} \\ I_{2\times 2} \end{bmatrix}$$

$$C_2 = \begin{bmatrix} I_{2\times 2} & 0_{2\times 2} \end{bmatrix}$$

$$D_2 = 0_{2\times 2}$$

The goal of robust control is to make the influence of the disturbance w on the whole system as small as possible, that is, for a given $\|w\|$, the H_2 norm of T_{zw}, $\|T_{zw}\|_2$, is as small as possible. Since $D_2 = 0$, which is not an injective matrix, we can take this equation set as the singular case of the H_2 optimization problem [73] [74], which may be solved by a small perturbation approach. If we define an extended vector of controlled output:

$$\tilde{z} = \begin{bmatrix} z \\ \varepsilon x \\ \varepsilon u \end{bmatrix} = \begin{bmatrix} C_2 \\ \varepsilon I \\ 0 \end{bmatrix} x + \begin{bmatrix} D_2 \\ 0 \\ \varepsilon I \end{bmatrix} u,$$

where ε is a perturbation with small positive value, the control system (4.2) is trans-

formed into

$$\begin{cases} x^{'} = Ax + Bu + Ew \\ \tilde{z} = \tilde{C}_2 x + \tilde{D}_2 u, \end{cases} \tag{4.3}$$

where

$$\tilde{C}_2 = \begin{bmatrix} C_2 \\ \varepsilon I \\ 0 \end{bmatrix}$$

and

$$\tilde{D}_2 = \begin{bmatrix} D_2 \\ 0 \\ \varepsilon I \end{bmatrix}$$

Here, the symbol $\tilde{(.)}$ represents the extended form of the corresponding matrix $(.)$. Since now $\tilde{D}_2$ is of maximal column rank and it is an injective matrix for any $\varepsilon > 0$, we can take it as a regular H_2 optimization problem and find the control law by solving the Algebraic Riccati Equation (H_2 -ARE) [75].

$$A^T\tilde{P} + \tilde{P}A + \tilde{C}_2^T\tilde{C}_2 - (\tilde{P}B + \tilde{C}_2^T\tilde{D}_2)(\tilde{D}_2^T\tilde{D}_2)^{-1}(\tilde{D}_2^T\tilde{C}_2 + B^T\tilde{P}) = 0 \tag{4.4}$$

Equation (4.4) has a unique solution $\tilde{P} \geq 0$ that is a function of ε. The H_2 optimal state feedback law is then given as

$$u = \tilde{F}x = -(\tilde{D}_2^T\tilde{D}_2)^{-1}(\tilde{D}_2^T\tilde{C}_2 + B^T\tilde{P})x \tag{4.5}$$

A suitably small ε will ensure that T_{zw} has the property $\|T_{zw}\|_2 \longrightarrow \gamma_2^*$, as $\varepsilon \longrightarrow 0$, where γ_2^* is the infimum of $\|T_{zw}\|_2$ for all proper controllers.

The selection of ε should be arbitrary according to the needs of the different situations. A smaller ε will get performance closer to the optimal one. However, this will lead to a higher resulting gain. So a trade-off should be made between the performance and the gain of the control system. For the CWA project $\varepsilon = 0.01$ is enough to satisfy the needs of uncertainty tolerance. The positive matrix $\tilde{P}$ and the feedback control matrix $\tilde{F}$ can be worked out by a special MATLAB linear system toolkit [76].

$$\tilde{P} = \begin{bmatrix} 0.142 & 0 & 0.01 & 0 \\ 0 & 0.142 & 0 & 0.01 \\ 0.01 & 0 & 0.0014 & 0 \\ 0 & 0.01 & 0 & 0.0014 \end{bmatrix}$$

$$\tilde{F} = \begin{bmatrix} -100 & 0 & -14.2 & 0 \\ 0 & -100 & 0 & -14.2 \end{bmatrix}$$

In this way, we can obtain optimal parameters for $\tilde{F} = (-P, -D)$, where $P = 100I_{2\times 2}$ and $D = 14.2I_{2\times 2}$. This makes the influence of disturbances on the system as small as possible.

4.3 The nonlinear form of EPC

The EPC with feedback linearization control approach is effective in following arbitrary shapes of guide paths. However, the current EPC cannot deviate too far away from the guide path in avoiding obstacles of large sizes because the maximal magnitude of the deviation is proportional to the magnitude of normal force. Cao [11] proposed a nonlinear EPC with a polynomial function, and Ayoub [12] improved this EPC by introducing an exponential decay function. Both controllers are based on Samson's trajectory tracker [9], which can have stability problems when transforming from the trajectory tracking to the path following algorithm. The separation of controls about position and angle also increases the complexity of the controller so, to integrate the advantages of both Brent's path planner and the nonlinear EPC, we propose to incorporate the nonlinear function

into the developed EPC.

4.3.1 Drawback of the linear EPC

The general design criteria of the EPC for a CWA are [8]:

- The CWA can follow the pre-designed guide path when no external normal force is applied to it. However, the EPC should enable the CWA to deviate from the guide path when non-zero normal force is imposed through an HMI. The distance of deviation is a monotonic increasing function of the value of normal force.
- The EPC is activated only when the input given by the operator is above a certain threshold so as to avoid undesired deviation from the guide path.
- The ability to deviate from the guide path decreases with increase of the deviation distance so the user can feel the negative gradient of attraction from the guide path.
- The EPC is not specified with an upper limit of deviation so the CWA can deviate a large distance to avoid large obstacles.

The EPC described in Chapter 3 conforms to all the criteria except the last; it works well within limited distances but it cannot make the wheelchair move infinitely away from the guide path. The magnitude of F_γ in the steady state is proportional to that of l, while the magnitude of steady state l is also a monotonic increasing function of that of $F_\perp$ [66]. Thus, it is impossible for the human user to provide input force enough to avoid obstacles of unlimited large size on the guide path. In practical application, however, we hope to drive the wheelchair to deviate arbitrarily as far away from the guide path as might be necessary in any situation. Figure 4.2 provides an illustration. The CWA can deviate from the guide path s_d to avoid the rectangular obstacles. The shortest path to avoid obstacles A, B and C is s_A, s_B and s_C, respectively, and the length of the shortest path extends with increases in the size of obstacle. Thus, it is necessary to design an

EPC which can limit the magnitude of restoring force F_γ so that a normal force $F_\perp$ with limited magnitude may drive the wheelchair to get across any large obstacles.

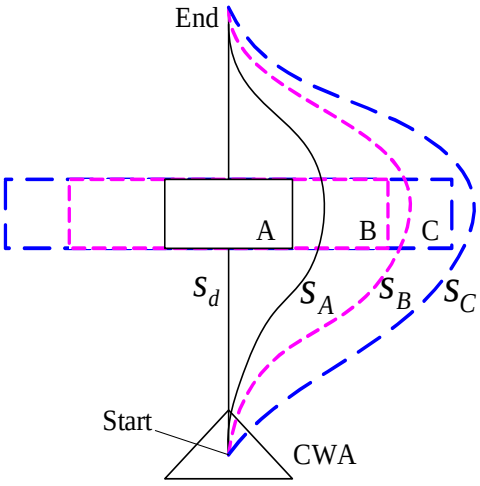

Figure 4.2: Shortest path of a wheelchair to avoid obstacles of different sizes

4.3.2 Nonlinear EPC

The basic idea of the nonlinear EPC is to make the restoring force be a monotonic function of distance while still restricting it within a limited value; the wheelchair will break away from the guide path easily if the applied normal force is larger than that value. The proposed 1-D nonlinear EPC may be of the form of control input [11] such that

$$u = -\frac{F_m y^2 + 3Ty_0^2}{y^2 + 3y_0^2} - k_{vy} y' + F_\perp, \tag{4.6}$$

where y is the distance between the current actual position of the wheelchair and the desired position. y_0 is the distance corresponding to the inflexion of the y curve. $F_\gamma = \frac{F_m y^2 + 3Ty_0^2}{y^2 + 3y_0^2} + k_{vy} y'$ is the restoring force, which is a nonlinear function of the position error y.

The controller takes advantage of the characteristics of nonlinear function that the slope of the function decreases when y is larger than the inflexion point, which decreases the restoring force so as to make the CWA deviate farther away from the guide path. The stability is also proved by the Lyapunov Function method, as seen in [11].

However, simulation experiments show that the controller has a singularity problem [12], so this kind of EPC is improved by substituting the nonlinear function with an exponential decay function, and the form of control input is given as

$$u = -(F_m - T)(1 - e^{-\delta y}) - T - k_{vy}y^{'} - F_{\perp}, \tag{4.7}$$

where F_m is the maximum value of the applied input force and T is the threshold of the applied input force below which the trajectory will not be deformed. Equation (4.7) is based on an exponential decay function. The restoring force is expressed as

$$F_{\gamma} = (F_m - T)(1 - e^{-\delta y}) + T + k_{vy}y^{'} \tag{4.8}$$

In the steady state, the first derivative of the distance is: $y^{'} = 0$, so the restoring force is reduced to $F_{\gamma} = (F_m - T)(1 - e^{-\delta y}) + T$. The curve of the restoring force is shown in Figure 4.3. The maximum value of the restoring force is set as $F_m = 10N$, and the threshold is $T = 1$. The value of F_{γ} is a monotonic increasing function with respect to y, and it asymptotically approaches F_m. In the steady state, the first derivative item is $y^{'} = 0$, so it can be deduced from equation (4.7) that $u \to (-F_m - F_{\perp})$ when $y \to \infty$. It is possible to let the wheelchair deviate from the guide path as far as we want if the direction of $F_{\perp}$ is opposite to that of F_m and $\|F_{\perp}\| > F_m$.

However, the control input of EPC is a function with respect to the scalar y, not the 2D vector l, so the control input should make some modifications so that the good geometric characteristics of the nonlinear function can be incorporated into the developed EPC. In

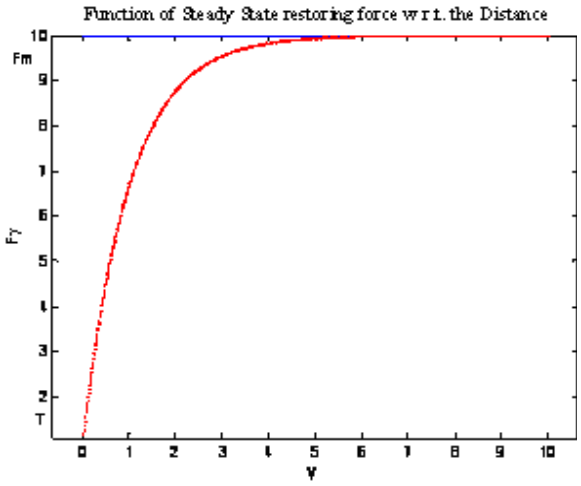

Figure 4.3: Relationship between steady state restoring force and position error

addition, previous works only took straight lines as the guide paths. This section will consider some curves as the guide paths.

The control law of the new nonlinear EPC is given as

$$u = -((F_m - T)(1 - e^{-\|l\|}) + T)\frac{l}{\|l\|} - Dl^{'} + F_{\perp}, \|l\| \neq 0 \tag{4.9}$$

$$u = -Dl^{'} + F_{\perp}, \|l\| = 0, \tag{4.10}$$

where the vector $\frac{l}{\|l\|}$ is a normalized form of the position error that represents the direction of l. The signs "-" and "+" are added before the restoring force and the normal force, respectively, so the effect of the two forces are in opposite directions. The control input u must remain continuous in the vicinity of 0 in equations (4.9) and (4.10), so the equation (4.9) can be modified as

$$u = -((F_m - T)(1 - e^{-\|l\|}) + T)\frac{l}{\|l\|} - Dl^{'} + F_{\perp}, \|l\| \geq ts \tag{4.11}$$

$$u = -((F_m - T)(1 - e^{-\|l\|}) + T)\frac{l}{ts} - Dl^{'} + F_{\perp}, 0 < \|l\| < ts, \tag{4.12}$$

where ts is a positive value of the threshold below which the magnitude of the direction item $\frac{l}{ts}$ is proportional to the value of $\|l\|$.

Equations (4.11) and (4.12) show that the direction of restoring force F_γ is always opposite to that of position error l in the steady state, which ensures that the restoring force can always counteract the deviation of the wheelchair from the guide path.

4.3.3 Algorithm to search for the nearest point on the guide path

For a linear EPC, the path following control algorithm can find the point in the guide path which is nearest to the corresponding position in the actual path because the algorithm can work out with high accuracy the point that will ensure that the position error l is perpendicular to T_d. For a nonlinear EPC, however, the situation becomes more complex. The current desired position that is calculated by the previous control algorithm may not be the perpendicular projection of the actual position in the guide path if the guide path varies its curvature sharply. The reason for this occurrence may be that the nonlinearity of the EPC makes it difficult for the desired point to follow the perpendicular projection of the actual point, and the discrepancy of these two points leads to the uncertainty in the trace of desired points.

Two remedies may solve this problem. In the first the algorithm sets the desired position to be perpendicular to the actual position for, for example, every 100 sampling points. In the second method illustrated in Figure 4.4, we can calculate the normal angle α, the angular difference between the position error and desired tangent. α is the normal angle because, ideally, it should be 90°. We set an angle value near to 90°, e.g., 80°, as the threshold of that normal angle and reset the desired position if the normal angle is smaller than that threshold (in which case the position error is not notably perpendicular to the guide path). Thus, the current desired point moves from R_d to R_{d1} in Figure 4.4.

This second approach is deemed to be better than the former one since the nearest point is checked for every sampling period in the latter.

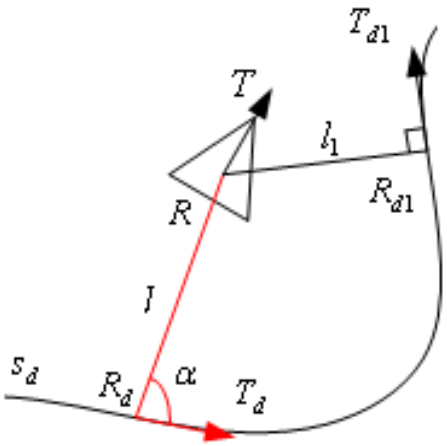

Figure 4.4: The desired point is reset if the normal angle is smaller than the threshold

4.3.4 Simulation for the nonlinear EPC

Simulation experiments were conducted to verify the performance of the newly developed nonlinear EPC. The maximum value and threshold of the restoring force are set as $8N$ and $1N$, respectively. The maximum value of the normal force that can be generated by the FT sensor is $10N$. Experiments include arbitrary deviation of the CWA from the guide path and automatic searching for the nearest desired point corresponding to the current actual position of the CWA. The nonlinear EPC is able to deviate far away from the guide path when required to avoid large obstacles. As shown in Figure 4.5, the wheelchair deviates farther away from the guide path when the normal force keeps increasing. The normal force can overcome the restraint of the restoring force and drive the wheelchair forward no matter how far away from the guide path when $\|F_\perp\| > F_m$.

When the position error is obviously not perpendicular to the desired tangent, the proposed control algorithm can automatically search for the point on the guide path that is nearest to the current actual point and take it as the new desired point. As shown in Figure 4.6, the algorithm is able to find the real-time shortest position error when the

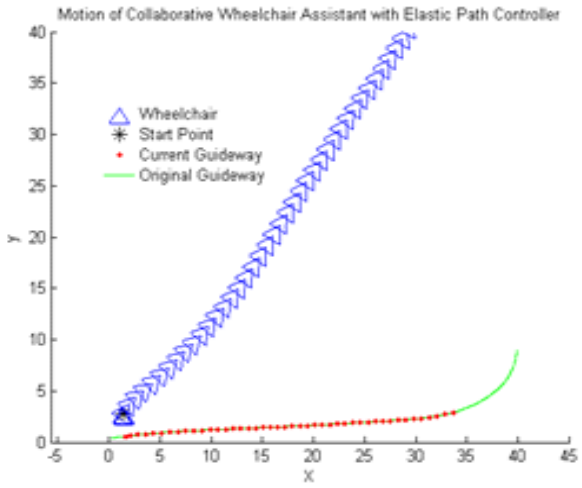

Figure 4.5: The nonlinear EPC can break far away from the guide path

wheelchair moves from starting point A to point B. Then the wheelchair deviates farther away from the guide path and α, the angular difference between position error l and desired tangent T_d, gradually deviates from 90°. $\alpha < 80°$ when the wheelchair reaches point R, so the algorithm begins to search the guide path for the nearest point to R. The old desired point R_d is substituted for by the new nearest point R_{d1}. Later, the angular difference α is always within the tolerable scope and the algorithm does not need to search for the nearest point any more. The CWA asymptotically approaches the guide path with decrease or withdrawal of the normal force until the wheelchair gets to the end point E.

The simulation experiment about comparison of nonlinear EPC with linear EPC is shown in Figure 4.7. In the lower subfigure, the solid curve represents the actual path of linear EPC, and the dashed curve represents the actual path of nonlinear EPC. The nonlinear EPC can drive the CWA to deviate no matter how away from the guide path if the perpendicular joystick input keeps at 10N. In comparison, linear EPC can only drive the CWA to deviate at most 12m from the guide path. However, Figure 4.7 also indicated that the linear EPC reacts faster to the perpendicular joystick input than the nonlinear EPC does.

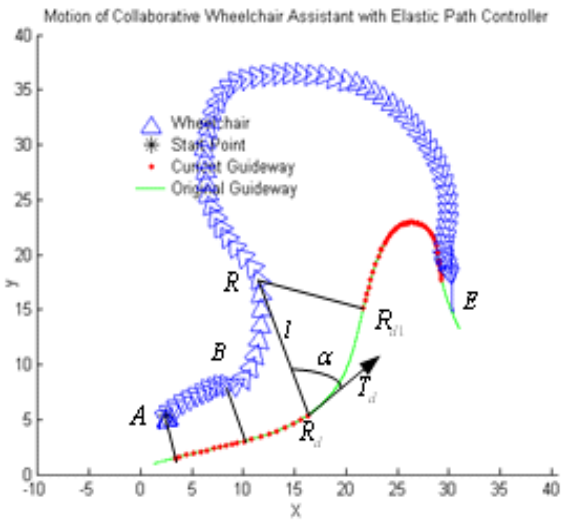

Figure 4.6: The control algorithm can automatically search for the nearest point on the guide path as the current desired point when angular difference α is beyond the tolerable scope.

4.4 Summary of the chapter

In this chapter, the control performance of the CWA is improved in two aspects: parameter optimization and nonlinear EPC.

The parameters of the controller are optimized using the robust control technique. It is shown that the optimized parameters can effectively restrain the influence of the equivalent disturbance on the CWA control system.

The nonlinear form of EPC is adopted to drive the CWA to avoid the environmental obstacles of any sizes. The nonlinear fulfills all the fundamental functions of linear EPC, such as path following, obstacle avoidance, singularity handling. Nonlinear EPC can drive the CWA to deviate no matter how far away from the guide path, while linear EPC can only deviate limited distance from the guide path.

To prevent that the calculated desired position deviates too much from the perpendicular projection of the actual position, a special algorithm is used to search for the nearest point on the guide path when the normal angle is beyond the tolerable scope. It is shown that the new algorithm can maintain the stability of the system with nonlinear EPC.

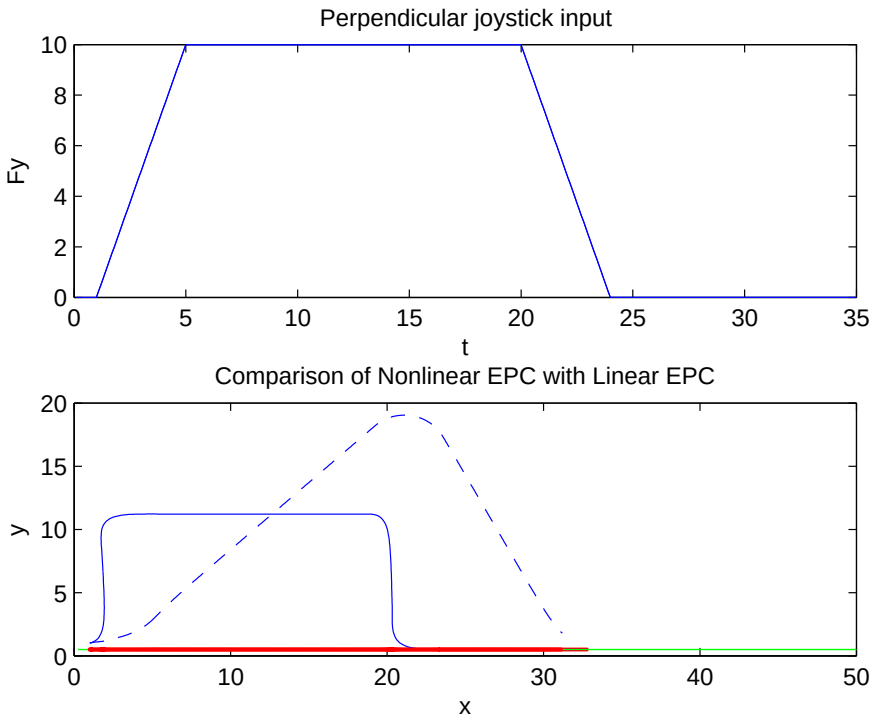

Figure 4.7: Simulation for comparison of the nonlinear EPC with linear EPC

Chapter 5

CWA with force feedback joystick

5.1 Introduction

Chapter 3 has proposed and conducted experiments using two kinds of command input devices as the HMIs for the CWA project.

The FT sensor enables the users to feel the magnitude of the applied force, but the feedback information about how far away the CWA deviates from the guide path and the position displacement of the sensor stick cannot be felt by the users. The PSJ obviously shows the users the position displacement of the sensor stick, but the feedback information about environmental obstacles and the deviation of the CWA from the guide path are still not felt by the users.

This chapter addresses this problem by introducing a force feedback joystick (FFJ) as the HMI, which can take on all the functionalities of FT sensor and PSJ and greatly assist the motion guidance of the CWA. The incorporation of FFJ can also provide the users with the feedback information about the environmental obstacles as well as deviation of the CWA from the guide path.

5.2 Application of FFJ

In chapter 3, the joystick employed in the real-time CWA experiments has been an ordinary PSJ used only for motion control of the wheelchair, but little attention has been paid thus far to the feedback information. The EPC depends fully on human operators to perceive the environmental information and make decisions about mobility tasks, such as how much the CWA must deviate from the guide path to avoid an obstacle. However, as the guide path is virtual, it is not easy to determine how far from the guide path the CWA is. It is thus useful to have a joystick that can provide feedback information about how much the CWA has deviated from the guide path. In addition, the feedback information about the environmental obstacles can also assist the users in identifying correctly the situation and drive the CWA to avoid obstacles effectively.

The control of CWA can be taken as a shared control, which fulfills the motion control task by combining the human operators with the controller [51]. The disadvantage of the traditional shared control is that the user cannot set the actual speed, position and direction of the wheelchair, which may disrupt the user. FFJs are expected to solve these problems in virtual [77], unstructured [78] or known environments [79] [80] [81] [82]. Besides working as a force input device, the FFJ enables the user to feel the repulsive force which reflects the obstacle information in the environment, as well as the deviation of the wheelchair from the guide path. Thus, it is especially important for people with vision impairment so they can perceive the world and feel at home interacting with it.

As shown in Figure 5.1, the FFJ not only fulfills the motion control task of the CWA as a common PSJ does, it also implements the force feedback functionality. On the motion control side, the user pushes the joystick, and the output signals control the mobility task of the CWA. On the force feedback side, the path controller of the wheelchair generates a feedback force, which reflects the current status of the wheelchair as well as the environmental information. This feedback force is sent back to the joystick so the user can feel the repulsion and push the joystick to control the wheelchair by following the repulsion of the feedback force.

The input-output signals in the FFJ are different from those of a common PSJ. For an ordinary PSJ, the input of the joystick is the position deviation of its handle to the central position of the pedestal, and the outputs are two voltages, which represent two orthogonal force elements: Parallel force F_x and Perpendicular force F_y. For an FFJ, however, the input is comprised of two kinds of signal sources. One is the position deviation of the handle and another is the feedback force consisting of two orthogonal elements: parallel element FF_x and perpendicular element FF_y. The output of the FFJ is the same as that of a PSJ.

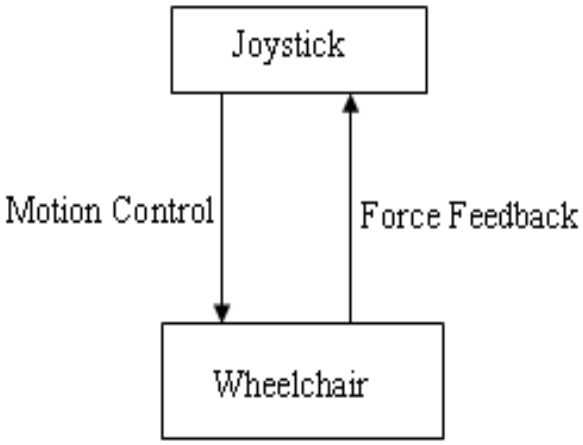

Figure 5.1: Wheelchair mobility control using the FFJ

5.3 Hardware

5.3.1 Overall system configuration

The CWA with an FFJ as its force input device is shown in Figure 5.2. The FFJ used in the CWA project is the Microsoft Sidewinder Force Feedback 2. The server-client computer communication system is linked to the original EPC controlled CWA. The server and client notebooks are connected by the linking cable, a data transmission line shown in blue. The server notebook is linked to the mobile base of the CWA, which is originally controlled by an ordinary PSJ. The client notebook is connected to the

FFJ, so the CWA may be controlled by two sources of joysticks: a common PSJ linked directly and an FFJ linked indirectly through the client-server communication network. When the FFJ is activated, the common PSJ should be disabled and replaced by the FFJ beforehand, which is realized by using the output of the FFJ to overwrite the data from the common PSJ as the control input of the CWA.

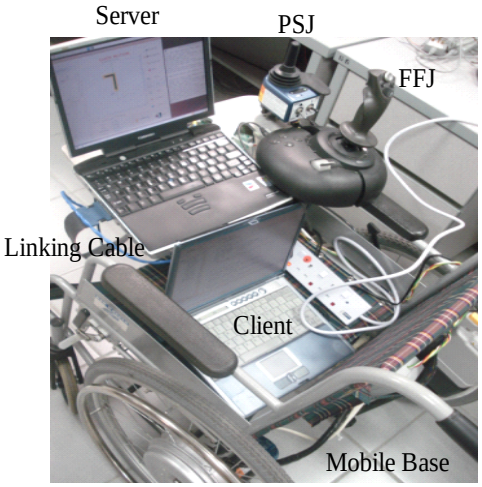

Figure 5.2: The overall CWA system for server-client communications

5.3.2 FFJ used in the CWA

The structure of the overall CWA system using the FFJ is shown in Figure 5.3. The position information of the wheelchair is read by the two encoders mounted on the axes of the rear wheels. The existence of obstacles is detected by the ultrasonic range sensors and transformed into Obstacle Force (OF) by the OF Algorithm. The 2D position signal of the FFJ pushed by the human operator is detected by the sensor installed inside the joystick base and transformed into force by software. All three channels of information are sent to the EPC to calculate the control force and the feedback force. The resultant control force is used to control the dynamic characteristics of the wheelchair and the feedback force is sent back to the joystick so the human user can feel the state of the environment and of the deviation of the CWA from the guide path.

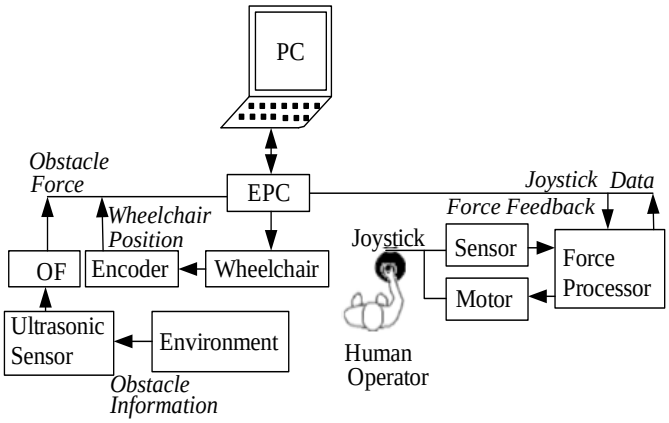

Figure 5.3: Overall system structure of the CWA control system

The flow chart of the CWA with FFJ is shown in Figure 5.4. After initialization of the CWA system, the encoders in the wheelchair read the data of the wheelchair position and calculate the restoring force. Next, the perpendicular element of the joystick input is transformed to the normal force. These two forces are added together to get the control input of the dynamic control system.

Then range sensors read the environmental data, and the OF algorithm calculates the OF if some obstacles are found in the security region of the wheelchair. The path error force and OF are added together to generate the feedback force that allows users to feel the repulsion which reflects the obstacles as well as deviation from the guide path. The mobility task is terminated if the CWA reaches the target.

5.3.3 Server-client communication system in the CWA

The ordinary PSJ in the CWA is driven by software running on the platform of Linux RTAI. However, the OS to run the FFJ program is Windows, and currently there is no driver available for the FFJ in the Linux RTAI. Thus, a way to realize the communications functionality between two PCs with the Windows and Linux RTAI systems is needed. As shown in Figure 5.5, the FFJ is attached to a notebook with Windows XP, which works as a client. The CWA is connected to a notebook installed with the Linux

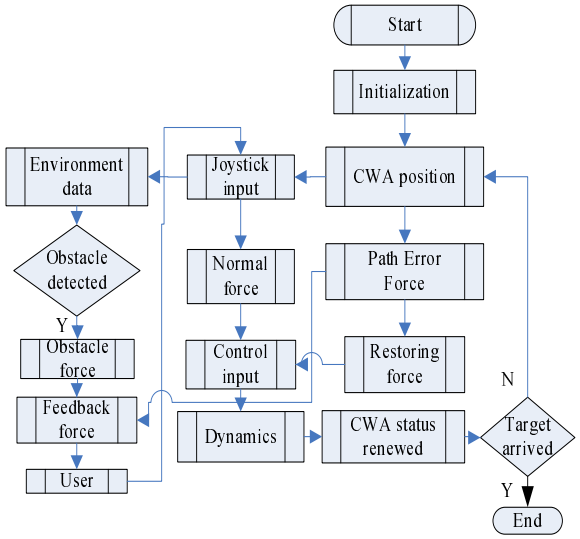

Figure 5.4: Flow chart of the CWA control mode with FFJ

RTAI system, which works as a server.

The server executes the low level motion control task of the CWA, including PD control of the position error, odometry of the position, display of the CWA's status, computing the feedback force, and so on. The client fulfills GUI and joystick control tasks, including reading the joystick positions and presenting users with feedback force in GUI.

The server-client communication works bi-directionally, with the server sending out the feedback force and receiving the joystick force, while the client sends the joystick force and receives the feedback force. The server and client must be synchronized so the data sent by one host can be received in time by the other, and vice versa.

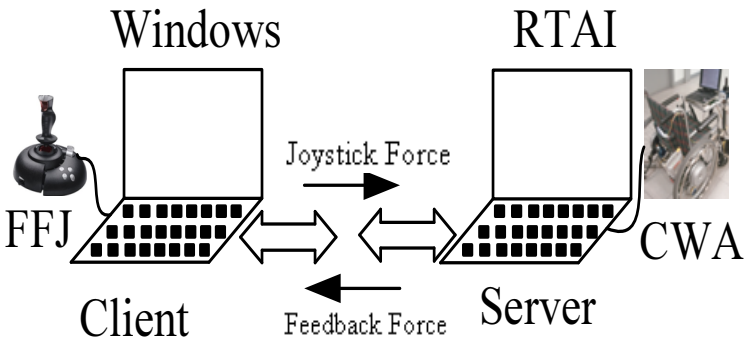

Figure 5.5: Communications between Windows and Linux RTAI systems

The server and client in the CWA control system implement their communications through the wired network by the TCP/IP protocol, which is a set of communications protocols that execute the protocol stack on which the Internet operates. TCP/IP is named after two of its most important protocols: Transmission Control Protocol (TCP) and Internet Protocol (IP) [83]. The TCP/IP suite can be thought of a set of layers, each solving a series of problems related to the transmission of data, providing support to the upper layer, and obtaining support from the lower layers. These days, the TCP/IP stack is included and installed in most commercial OS such as Linux and Windows, so ordinary users working in these systems don't need to look for the implementations of the communications protocols.

In this application of CWA, the main work to be done is to open a socket, connect it to the host, and read/write data. The programming steps for the server in Linux RTAI system are: ①. open a socket; ②. connect the socket to the host using the IP address and port number; ③. read joystick force from the joystick and write feedback force to the joystick. On the client side of the Windows system, data are read from and written to the joystick in a periodic loop. The main programming steps are: ①. open the socket; ②. connect the socket to the server; ③. read feedback force from/write joystick force to the socket.

A. Server side: Linux RTAI

The server computer with the Linux RTAI OS is responsible for the main part of the CWA's motion control task. The two odometers mounted on the axis of the rear wheels measure the displacements of the rear wheels' centers. The measured data are transformed to 2D actual position of the CWA, and the EPC algorithm finds the corresponding nearest point on the guide path as the current desired position. The restoring force is also calculated using the PD feedback control, and the normal force, which is obtained from the joystick in the client side, is also incorporated to calculate the control input. The actual curvature and second derivative of the desired path length are also worked out, and the status of the CWA is renewed by two steps of integration and then displayed on the GUI screen. When obstacles are found in the security region of the CWA, the OF

is also calculated and added to the path error force to get the feedback force, which is sent to the client side through the network. The parallel element of the joystick output is used to decide the translation velocity of the CWA.

B. Client side: Windows

The client computer with the Windows OS is mainly responsible for sending the joystick force to the server, receiving the feedback force coming from the server, and displaying force information on the GUI screen. The FFJ used in the CWA is the Microsoft Sidewinder Force Feedback 2, for which the original GUI and coordinate system are shown as Figure 5.6. The maximal digital values of joystick output in X and Y axes are $X_{max} = Y_{max} = 1000$, respectively, as shown in Figure 5.6 (a). The top position of the joystick handle is denoted as a dark dot in the square Force Feedback Window (FFW). The joystick output F corresponds to the dark dot, as shown in Figure 5.6 (b). The feedback force F_{FB} always counteracts the position deviation of the joystick with respect to its central position. F_{FB} originates from the dark dot, points to the center of the FFW, and has a magnitude proportional to the distance between the dark dot and the central position.

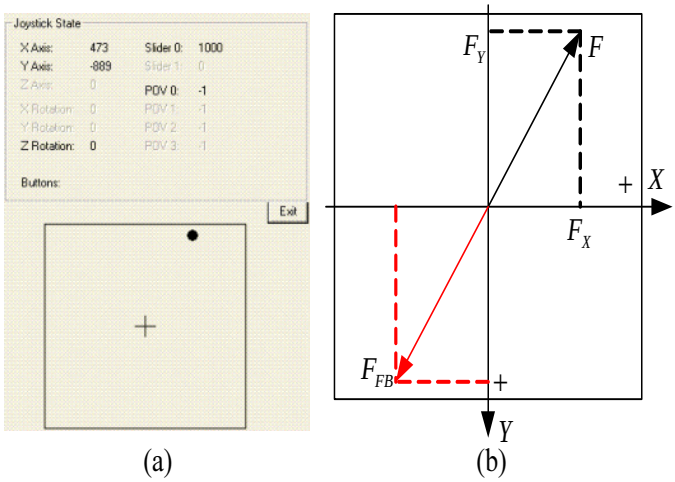

Figure 5.6: The original GUI and coordinate system of the FFJ

C. Communications between the server and client notebooks

The main issues in the server-client communications are the coordinate and scaling match and establishment of a connection.

The scaling match is needed to make the digital values of the joystick output match the analog values of voltages used to control the CWA. The joystick coordinates in GUI should also be transferred to the form that is compliant to the driving and viewing habits of the wheelchair users. Figure 5.6 (b) shows that the positive direction of the Y axis is downward, and the positive direction of the X axis is to the right, which is different from the directions of the PSJ joystick coordinate system in the CWA. To comply with the driving habits of wheelchairs users and to make the driving force compatible with the control force in EPC, the directions of the joystick output elements are changed and multiplied by factors before being sent out as the control force of the EPC. The parallel and perpendicular elements of control force of the EPC on the side of server are $F_x = -\frac{F_Y}{Y_{max}} F_{max}$ and $F_y = -\frac{F_X}{X_{max}} F_{max}$, where $F_{max} = 2.5$ is the maximal value of the normal force in the CWA motion control.

The analogous values for the feedback force transmitting from the server to the client should be transformed conversely into digital forms. The reversed transformation equations are $F_Y = -\frac{Y_{max}}{F_{max}} FF_x$ and $F_X = -\frac{X_{max}}{F_{max}} FF_y$. The feedback force $F_{FB} = (FF_x, FF_y)$ is displayed as the gray dot in the FFW of the GUI on the client side. Both the joystick output force and the feedback force are displayed in the FFW. The corresponding values are dynamically displayed in their right-hand sides accordingly. The maximum values of the force elements are all 2.5. In the real-time application, the joystick output is not necessarily used to counteract the effect of the feedback force. As shown in Figure 5.7, the dark dot is not in the same position as the gray dot.

Before the TCP/IP protocol is employed to transmit data between two hosts, a connection should be established reliably and stably between these devices [84]. This connection setup process accomplishes several tasks as it creates a connection appropriate to data exchange: Contact and Communication, Synchronization and Acknowledgment, Three-Way Handshake.

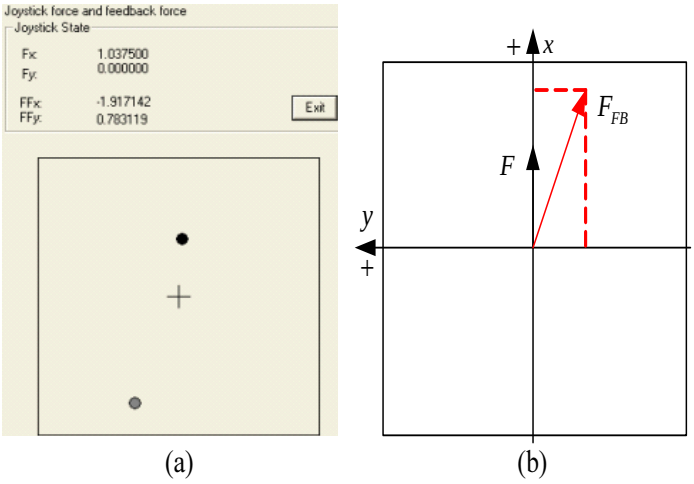

Figure 5.7: Modified GUI and Coordinate system of the FFJ

Then the client contacts and establishes the communications with the server and they exchange data continuously. After the test programs pass the check and run normally, transfer and integrate the server-client communication system into the wheelchair project. The client can send the FFJ output data to the server to control the CWA's mobility task, and the server transmits the feedback force data back to the client to show the users the environmental obstacle information and the deviation status of the CWA relative to the guide path.

5.4 Dynamic model of EPC

The dynamic model of the EPC with FFJ is shown in Figure 5.8. Like the common EPC, the path controller of the wheelchair is subjected to two forces: the restoring force F_γ and the normal force $F_\perp$, so the dynamic characteristics of the EPC are retained.

One input of the FFJ is the position deviation of the handle from the central position of its base. This position deviation is pushed by the user and generates two voltages that reflect the parallel and perpendicular elements of the position deviation, respectively. These two voltages are transformed to the force F with tangent element $F_{||}$ to control the translation speed of the wheelchair, and the normal element $F_\perp$ to control the deviation

of the wheelchair from the guide path.

Another input of the joystick is the feedback force F_{FB}, which is also composed of two forces. The first is the path error force, which is proportional to the position error: $F_{pe} = Pl$; since the positive definite diagonal matrix $P = pI$, vector F_{pe} is p times of l. The other force is the obstacle force F_{ob}, which is caused by the obstacle Γ, calculated by a specific algorithm (see Section 5.4.1). Thus, the feedback force can be expressed as $F_{FB} = F_{pe} + F_{ob}$.

The feedback force F_{FB} does not intervene directly with the mobility task of the wheelchair. The joystick output F is related only to the position of the handle relative to the central position of the joystick base and is not necessarily related to the feedback. However, F_{FB} makes the user feel the repulsion coming from the obstacles as well as the deviation of the wheelchair from the guide path. The user usually needs to adjust his or her joystick output to counteract the effect of the repulsion, but the user can overrule the effect of the repulsion and stick to the previous operation strategies, meaning that the mobility task of the wheelchair is still under the full control of the user. The only difference between the EPC with FFJ and the pure EPC is that, the user usually behaves in response to the repulsion of the feedback force so the wheelchair's behaviors may also change accordingly by using the FFJ.

5.4.1 Obstacle force algorithm

Obstacles in the environment can be detected by 24 ultrasonic range sensors $S_1 \tilde{} S_{24}$, which are evenly distributed around the wheelchair, as shown in Figure 5.9. The angle between any two neighboring sensors with respect to the Vehicle Center Point (VCP) is 15°. The range sensors are employed to assist the wheelchair in detecting and avoiding potentially dangerous obstacles in the environment.

The obstacle force (OF) comes from the obstacle and is imposed on the joystick as part of the feedback force. The OF is determined by the nearest distance between the obstacle

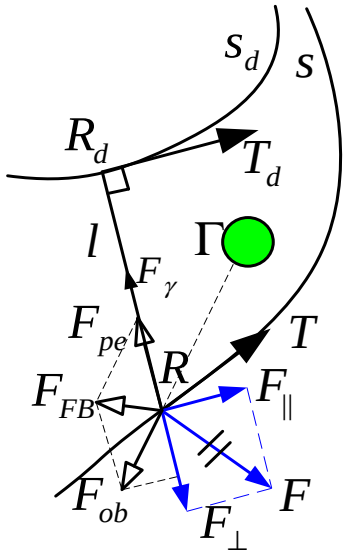

Figure 5.8: Dynamic model of the EPC with FFJ

and the centre of the wheelchair through a curve called the “Hybrid Hyperbola”.

A circle with specific radius r_s centered at the VCP is defined as the Security Region of the wheelchair, as shown in Figure 5.10. A wheelchair is considered to be in danger if any obstacle is detected within the security region. As shown in Figure 5.10, each circle centered at each VCP is a security region. The upper state of the wheelchair is dangerous because the distance between the obstacle and the wheelchair $d < r_s$. An OF F_{ob}, which is along the distance vector, is imposed on the VCP. The lower state of the wheelchair in the figure is in critical safety because the distance $d = r_s$.

Traditional algorithms usually applied the concept of “Histogram Grid” [85] or “Force Reflective Feedback” [79] to calculate the OF. To simplify the algorithm and focus on studies of the principles of feedback, we propose the concept of “Hybrid Hyperbola” to calculate the OF, which is determined by the distance of the nearest obstacle from the CWA.

The OF F_{ob} is a monotonic decreasing function of the distance d. Three kinds of curves are taken into consideration as candidates for the force-distance relationship curve.

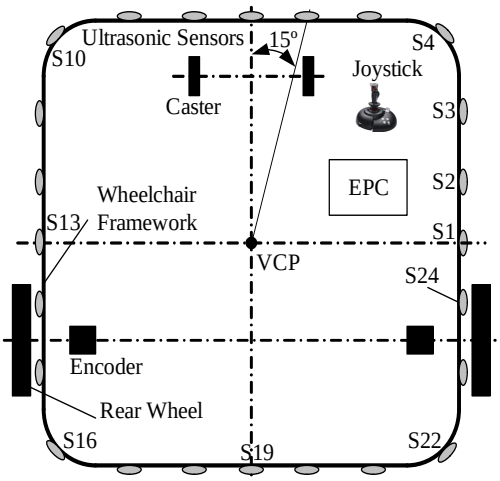

Figure 5.9: Distribution map of ultrasonic sensors around the wheelchair

Linear relationship

The simplest method to determine the relationship between the wheelchair and an obstacle may be by a straight line. As shown in Figure 5.11, the magnitude of F_{ob} is determined by the equation:

$$\|F_{ob}\| = a - bd, \tag{5.1}$$

where a and b are positive constants. a is the nominal value of the largest possible OF when $d = 0$. b is given according to

$$b = \frac{a}{r_s} \tag{5.2}$$

The value of $\|F_{ob}\|$ is a monotonic decreasing function of d that is linear to $-d$. The largest magnitude of the OF is obtained as a when $d = 0$, that is, when the VCP is reached by the obstacle. (This magnitude is not usually applicable since no obstacles

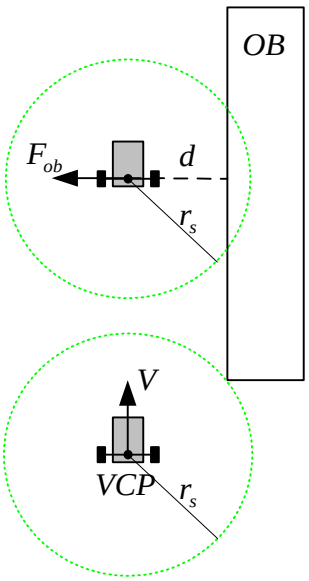

Figure 5.10: Generation of an OF with an obstacle around the wheelchair

would occupy the center of the wheelchair.) The force is of zero value when $d = r_s$, that is, when the obstacle is tangent to the circle outlining the security region. However, this distance may not prevent the wheelchair from colliding with the obstacle because the limited value of OF is not large enough to overcome the inertia of the wheelchair and avoid collision with the obstacle.

Hyperbola with limitation of maximal force

An alternate approach is to employ the hyperbola as the force-distance relationship curve. As shown in Figure 5.12(a), the force-distance relationship is expressed as:

$$d\|F_{ob}\| = a \tag{5.3}$$

The OF is the monotonic decreasing function of d, which approaches infinity when $d \to 0$. However, the large obstacle force exists only when d is very small, which may be impractical because the obstacle cannot be too near to the wheelchair. Thus, the re-

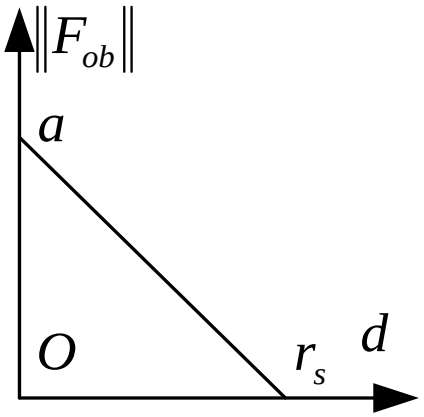

Figure 5.11: Relationship between $\|F_{ob}\|$ and d, expressed as a straight line

lationship curve should be modified, as shown in Figure 5.12(b). The hyperbola moves along the horizontal coordinate by $\|OA\| + \|AC\|$, where $L_w = \|OA\|$ is the effective length of the wheelchair and $C_r = \|AC\|$ is the clearance, the minimally permitted distance between the obstacle and the wheelchair. In addition, the curve should also move along the F_{ob} axis by a value of $-F_0$, where F_0 is the value of OF when $d = r_s$, that is, $(r_s - L_w - C_r)F_0 = a$ in order to avoid the drastic jump at the border of the security region. Moreover, the magnitude of the obstacle cannot exceed its upper limitation F_{max}, because the experiment results indicate that it is very difficult to control the wheelchair when the OF jerks too drastically, as it reaches a very large value with a small variation between the distance and the smallest distance permitted. The modified version of force-distance relationship is given as

$$\begin{cases} F_{ob} = \frac{a}{d - L_w - C_r} - \frac{a}{r_s - L_w - C_r}, H_{min} \leq d \leq r_s \\ F_{ob} = F_{max}, L_w < d \leq H_{min} \end{cases} \tag{5.4}$$

where $H_{min} = \|OD\|$ is the minimum value of distance in the hyperbola.

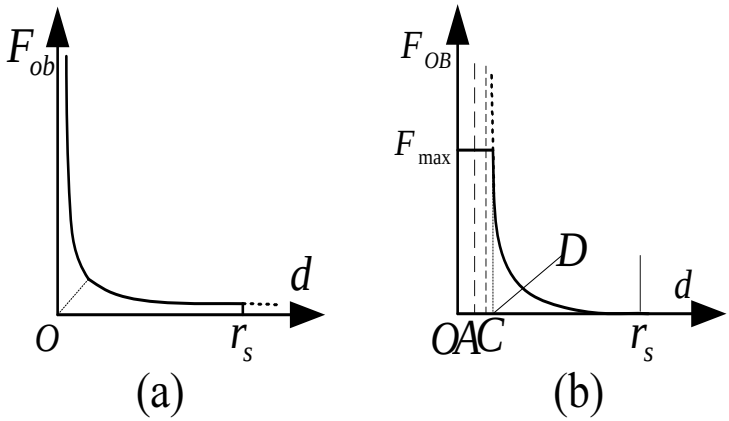

Figure 5.12: Relationship between the OF and the distance expressed as a hyperbola

Hybrid of hyperbola and straight line with limitation of maximal force

Figure 5.12(b) shows that the OF decreases with the increase in distance in the range of $[H_{min}, r_s]$, is unchanged in the range of (L_w, H_{min}), and has zero value when $d > r_s$. The distance is prohibited in the range of $[0, L_w]$, where the obstacle collides with the wheelchair.

However, the wheelchair's motion path easily oscillates in the real time experiments, easily leading to a collision because the user usually has inadequate time to avoid the obstacles after he or she feels the repulsion from the obstacles. This may be because the force and its variation are very small and cannot be felt by the user when the wheelchair is far away from the obstacle, while the force variation is too sharp at the small-distance segment of the hyperbola curve that is near to point C. Therefore, the small OF hardly influences on the driving behavior of the user at the beginning, when the environmental obstacle enters the security region of the wheelchair, but once the user feels the repulsion from the obstacle, it may be too late to get away from the obstacle.

Two possible solutions may address this problem: increase the parameter a so that the user can feel the obstacle repulsion and take measures to counteract it earlier, even when the distance is still relatively large; or incorporate a segment of straight line into the hyperbola curve at the large-distance segment, as shown in Figure 5.13. The curve

segment between D and B is a hyperbola and the one between B and E is a straight line, and the goal of this design is to keep the characteristics of a large slope of the hyperbola in the small-distance segment and to increase the value of slope by substituting a straight line for the hyperbola in the large-distance segment. The primary concern lies in the juncture between these two segments; if the distance at the juncture is too small, the slope of the straight line is very large so the performance improvement is limited; if the distance at the juncture is too large, the slope of the straight line is very small and the modification is meaningless. Thus, the juncture issue should be discussed in detail if this approach is used.

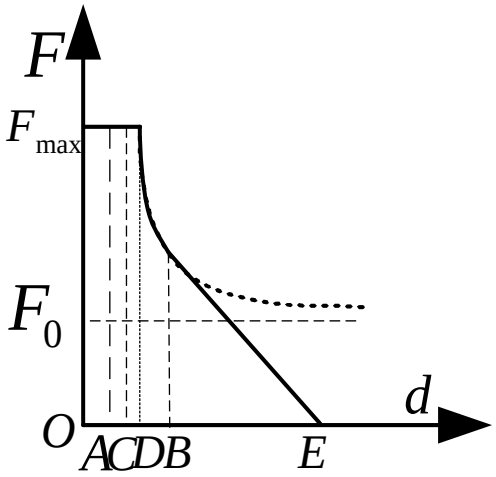

Figure 5.13: Modification of the force-distance relationship using a hybrid curve

If we assume that $H_{max} = \|OB\|$ and $H_{min} = \|OD\|$ is the maximum and minimum values of the distance in the segment of hyperbola, F_0 is the distance that the original hyperbola displaces along the axis of the obstacle force, and k is the slope of the straight line segment with a negative value, the parameters F_{max}, C_r, H_{max} and k are determined by the designer, while a, F_0 and H_{min} are calculated by the constraint condition of the hybrid curve. Since the point B is the juncture of the hyperbola and the straight line, it fits for

expressions of two curves given as:

$$\begin{cases} F_{Hmax} = \frac{a}{H_{max}-L_w-C_r} + F_0 \\ k = \frac{F_{Hmax}-0}{H_{max}-r_s} \end{cases} \tag{5.5}$$

The slopes of the two curves should also be the same to ensure the smoothness and continuality at point H_{max}.

$$\begin{cases} F^{'} = k \\ F^{'} = -\frac{a}{(d-L_w-C_r)^2} \end{cases} \tag{5.6}$$

d in the equation set (5.6) is substituted by H_{max} in (5.5) to work out the value of a: $a = k(H_{max} - L_w - C_r)^2$.

Substituting the value of a into (5.5) gives: $F_0 = k(L_w + C_r - r_s)$. Since point D is also a juncture of the hyperbola and the horizontal line with the maximum value of force, the parameter H_{min} can be obtained by

$$F_{max} = \frac{a}{H_{min} - L_w - C_r} - \frac{a}{r_s - L_w - C_r} \tag{5.7}$$

5.5 Experiments

A series of psychophysical experiments are designed to investigate whether the functionality of feedback can help the users, especially those with serious vision impairment, to improve the performance of obstacle avoidance during the CWA's mobility task, and how it helps the users to achieve this goal. Two cases are considered in this test: per-

pendicular motion toward a wall (Case 1) and obstacle avoidance (Case 2). Six human subjects with no prior experiences with the CWA and without known motor disabilities participated in these experiments. The subjects were first instructed and trained to drive the CWA. Then they were asked to do 5 trials for each of the 4 types of experiments consecutively.

① without vision feedback, without force feedback (Ty1);
② without vision feedback, with force feedback (Ty2);
③ with vision feedback, without force feedback (Ty3);
④ with vision feedback, with force feedback (Ty4).

The GUI and experimental data of each trial were stored in the computer for later analysis. After the subject finished all the experiments, he or she filled out a questionnaire. The whole procedure of experiments took about 130 minutes.

5.5.1 Training and instruction

This step lets the subjects know about the project and makes them familiar with how to drive the CWA.

The subjects were firstly given fundamental knowledge about the project and the related basic concepts such as CWA, EPC, GUI, FM, CM, EM, and force feedback.

Next, the subjects were trained to set the initialization in the GUI and to drive the CWA using the three control modes: FM, CM and EM. The modified GUI for these experiments is shown in Figure 5.14. In the lower central part of this figure are three cases: "0" represents the training stage (Case 0), "1" represents Case 1 and "2" represents Case 2. For Case 0, the subjects can select one of the three control modes in the upper right part of the GUI. For Case 1 and Case 2, however, the control mode has been integrated into the related case. The "Feedback" button is pressed to gain the feedback force in the motion procedure.

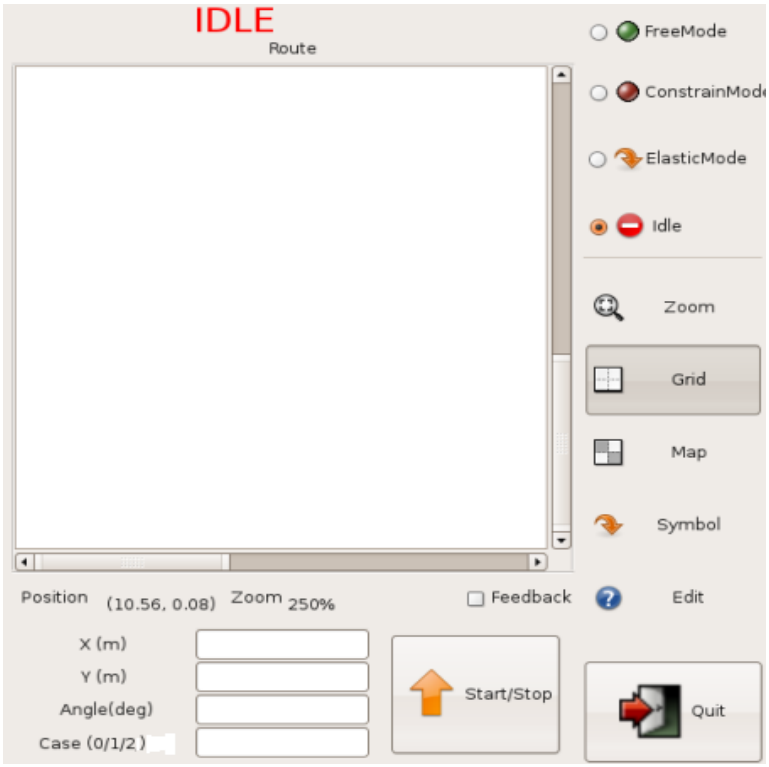

Figure 5.14: GUI for the psychophysical experiments in two typical cases

The subjects exercised the settings of GUI and drove the CWA using the three control modes freely. Then the feedback force was added to the joystick so the subjects could feel the magnitude of feedback force.

After the training and instruction, the subjects were to do a series of experiments about two cases: perpendicular motion toward a wall and avoidance of a circular obstacle. The procedures and results of the experiments are addressed in Section 5.5.2 and 5.5.3.

5.5.2 Perpendicular motion toward a wall

Principle

The aim of this case is to verify that the feedback force through the joystick can assist the user to approach the target without colliding with it. When the wheelchair moves

perpendicularly toward a wall, the joystick will be affected by two feedback forces: the OF F_{OB} and the path error force F_{pe}, as shown in Figure 5.15. If the wheelchair is on the guide path, F_{pe} is zero. F_{OB} is increased when the wheelchair approaches the wall. The human user must overcome these two feedback forces to go toward the wall. Since the user's force is always used to keep balance and counteract the feedback force, the user's force is increased accordingly when the wheelchair is nearer to the wall and decreased when the wheelchair moves in the opposite direction of the wall. The OF disappears when the distance between the wall and the wheelchair is larger than the distance threshold. The user's force or the joystick output F_J is not necessarily related to the OF but is only decided by the position of the joystick.

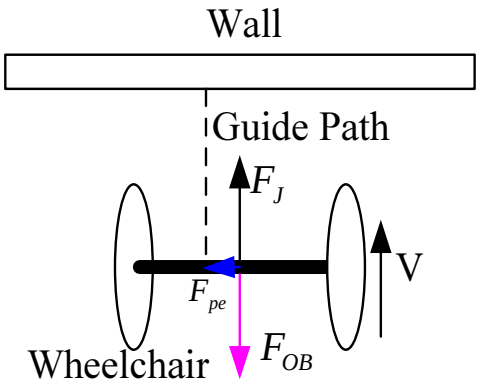

Figure 5.15: The wheelchair moves perpendicularly toward the wall

Procedure

A rectangular cardboard box is put on the ground in the guide path to represent a wall, as shown in Figure 5.16 (a). The corresponding settings of GUI are shown in Figure 5.16 (b), where the purple rectangle represents the wall and the yellow line is the target line of the CWA. The object of the trial is to get the front border of the CWA across the target line without colliding with the "wall". The GUI displays a pink line drawn between the wall and the front of CWA when the trial is successful, and a short red line drawn along the border of the wall when the CWA collides with the wall. Neither the symbol for the wall nor that of the target line are visible in the GUI before the mobility

task terminates. The “wall” is seen by the subjects in the real world during the motion procedure if the “vision” assistant tool is allowed.

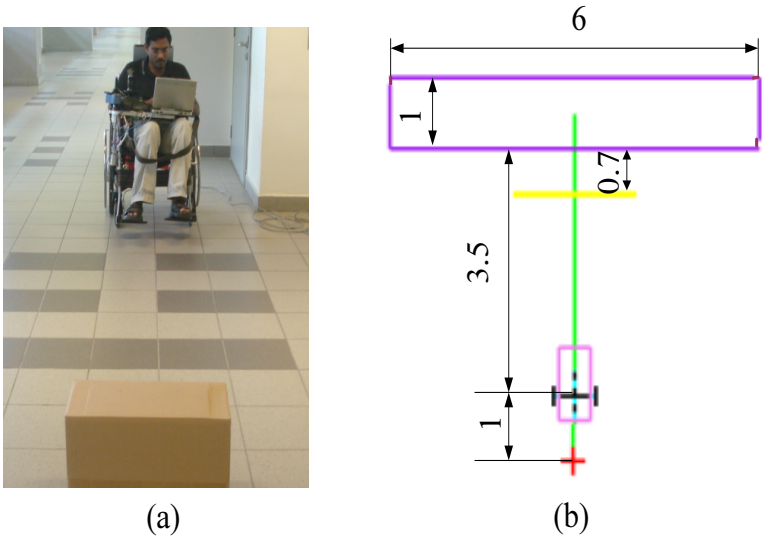

Figure 5.16: Experimental environment and GUI settings for Case 1

Five trials are conducted consecutively by each subject. Only the control mode of CM is conducted for this step in order to reject the disturbance of the CWA’s oscillation. In CM with feedback force, the user can feel the feedback force from the wall, but there is no path error force because the CWA is always in the guide path. The subjects need not select the control mode or set the initialization data because they have already been integrated into the “Case” choosing box.

For the convenience of comparison with the vision assistance, 4 types of experiments are designed and conducted consecutively in this case.

① no vision, no force

The aim of this type of experiments (Ty1) is to be used as a reference for comparison and to show by how much the CWA tends to fail to finish the mobility task without the assistance of vision feedback or force feedback. The subjects are told beforehand the accurate position of a wall in the front of the guide path. They are asked to close their eyes so that they cannot see the environment or the GUI before the CWA moves forward. At the same time, the “Feedback” button in the GUI is not clicked so that the function

of force feedback is disabled. They drive the CWA and stop before the wall according to where they think its position is. The experimental data are recorded and stored in a folder for each of the 5 trials for future analysis.

② no vision, with force

This type of experiments (Ty2) studies the approaching performance of the CWA by way of the force feedback alone. The subjects are required to close their eyes before the CWA moves forward so they cannot see the environmental obstacle or the GUI in the computer before them. However, they can feel and react to the feedback force through the joystick and adjust their motion strategies accordingly. When they feel that the magnitude of the feedback force indicates that the target line has been passed and the wall is near, they can stop the motion of the CWA. Then they open their eyes and click the "Start/Stop" button, record related data and quit the GUI in each trial.

③ with vision, no force

This type of experiments (Ty3) investigates the approaching performance of the CWA by way of vision feedback alone. The subjects can see the symbol of the CWA as well as the guide path in the GUI. At the same time, they can see the cardboard box on the ground in front of them, but they cannot feel the repulsion from the joystick because the feedback functionality is disabled. When the CWA stops before the box, the "Start/Stop" button is clicked and the GUI will display if the experiment is successful, target unreached, or failure. The symbol of the obstacle can also be shown in the GUI for further analysis.

④ with vision, with force

This type of experiments (Ty4) tests if vision can further improve the approaching performance of the CWA with the assistance of force feedback. The subjects can see the symbol of CWA and the virtual guide path in the GUI and the cardboard box on the ground in front of them. At the same tine, they can feel the repulsion from the joystick because the functionality of force "Feedback" is activated. They are required to drive the CWA to move along the guide path toward the wall and they must react to the feedback force by adjusting the joystick position so that the CWA can change its motion speed and direction accordingly. After the CWA stops before the box, the "Start/Stop" button

Table 5.1: Shortest distance between the wall and the CWA

Type	Mean	SD	Min	Max
Ty1	0.6527	0.4385	0.0690	1.5030
Ty2	0.5420	0.1978	0.1870	1.2540
Ty3	0.2359	0.0707	0.1060	0.4000
Ty4	0.3811	0.1358	0.1640	0.6940

is clicked and the experimental data are stored in the computer for future analysis.

Results

The methods used to process the experimental data are:
① For Ty1 experiments, how many hits occur out of all trials.
② For all types, the mean, standard deviation, minimum and maximum of the distance between the wall and the front border of the CWA are calculated.
Some abbreviations are:
Min: minimum value of the shortest distance in one type of experiments;
Max: maximum value of the shortest distance in one type of experiments;
SD: Standard deviation of all the shortest distances in one type of experiments.

1. Numbers of hits on the wall and untouched target lines
The results of all Ty1 trials are shown in Figure 5.17. Each row of the figure includes 5 trials for one subject. In 7 out of the 30 trials, the CWA collides with the wall, and the CWA does not touch the target line in 14 out of the 30 trials. In comparison, only 3 out of 30 trials do not touch the target line and no trial collides with the wall in the Ty2 experiments. This indicates that it is very difficult for the subjects to finish the mobility tasks successfully with neither vision nor force feedback as the assistive tool, and force feedback can improve the mobility performance of the CWA greatly.

2. Shortest distance between the wall and the CWA
The statistical data of the shortest distance between the wall and the CWA are given in Table 5.1.

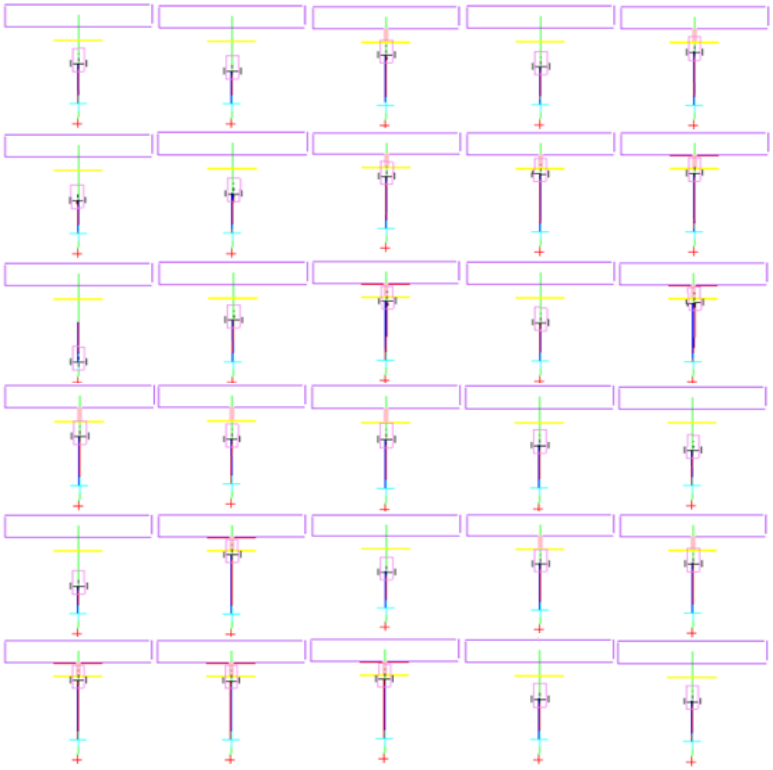

Figure 5.17: Results of all trials in Ty1 for Case 1

The normal probability distribution curve of the shortest distance is drawn in Figure 5.18. The straight line bar represents the border of the wall.

It is seen from Table 5.1 and Figure 5.18 that the SD of the shortest distance in Ty2 (0.1978) is significantly smaller that that in Ty1 (0.4385), which indicates that the force feedback can greatly improve the approaching performance of the CWA to the wall. At the same time, the SD in Ty2 is not much different from that in Ty4 (0.1358), demonstrating that addition of vision on the force feedback does not improve the approaching performance of CWA significantly. It is noted that the SD of Ty3 (0.0707) is much smaller than that in Ty4. The possible reason is that the addition of force feedback to the vision may disturb the user and make it more difficult to approach the wall than the vision alone does.

In conclusion, force feedback is an effective tool to improve the approaching performance of the CWA.

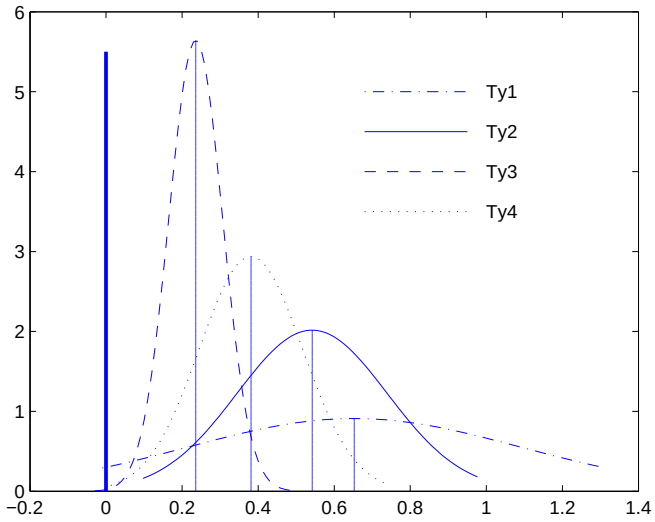

Figure 5.18: Normal probability distribution of the shortest distance between the wall and the CWA

5.5.3 Avoidance of an obstacle

Principle

This experiment is implemented to evaluate the CWA's performance of obstacle avoidance. When the user wants to move towards a round obstacle, he or she must overcome the OF F_{OB}, which is along the extending line of the radius of the obstacle if the center of the circle is taken as the origin of the coordinate system. The distance between the wheelchair and the surface of the obstacle is: $d = \sqrt{x^2 + y^2} - r$, where (x, y) is the position of the wheelchair and r is the radius of the obstacle. When the wheelchair is closer to the obstacle, d is smaller and the OF is larger, so the user must take more effort to overcome the OF to move toward the obstacle. If the user wants to decrease the effect of the OF, he or she must drive the wheelchair to move farther away from the obstacle. When the distance is larger than the threshold, the OF disappears and the user's operation of the wheelchair is no longer influenced by the obstacle. The wheelchair can detour from the obstacle if the guide path of the wheelchair penetrates the obstacle, as shown in Figure 5.19. The dashed line is the guide path, the inner circle is the obstacle,

and the outer circle is the threshold circle within which the wheelchair is subject to a repulsion force that is along the extending line of its radius. The joystick outputs only a parallel joystick force at point A. At point B, there will be a repulsion force from the obstacle. The user must overcome the OF and drive the joystick handle to generate an output that makes the wheelchair turn around to detour from the guide path, as shown in the figure. Later, a restoring force is generated because of the position error at point C and increases because the position error is increased in the motion period. The user should overcome the resulting force of restoring force and OF to drive the wheelchair forward. The actual path of the wheelchair may be like the dashed curve in the figure. The user turns the direction of the wheelchair and continues to follow the guide path at point D.

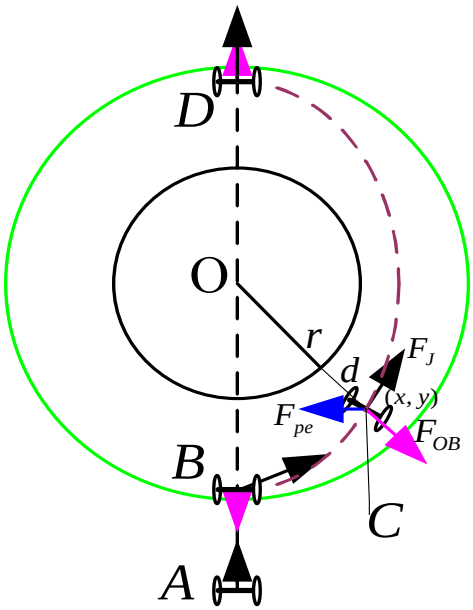

Figure 5.19: The wheelchair detours from an circular obstacle

The effort that the user takes to overcome the feedback force is not necessarily related to the normal force $F_\perp$; the OF plays the role of feedback only so the user can feel the repulsion from the obstacle. The OF is not related to the wheelchair's behaviors and the CWA is still under full control by the users through the joystick output. When the wheelchair is near an obstacle and it is subjected to a large OF, even though the joystick

handle is kept in the central position and the normal force is zero, the user still must make a large effort to maintain this state of balance and drive the wheelchair to move toward the obstacle. The only way to decrease the effect of the obstacle force is to drive the wheelchair to move in the direction opposite to the obstacle.

Procedure

This step is designed to determine whether the force feedback can improve the performance of obstacle avoidance in the mobility task of the CWA. As shown in Figure 5.20, a cylindrical trash bin is placed as an obstacle on the left-hand side of the guide path in front of the subjects. The subjects are required to drive the CWA to avoid the obstacle and then to get through two foam items representing a doorway on the ground on the guide path. During the CWA's motion procedure, the trial is regarded as a failure if the CWA collides with the obstacle. If the CWA reaches the terminal of the guide path but does not pass the "door", the trial is regarded as target-unreached. Only when the CWA passes through the "door" without colliding with the obstacle is the trial regarded as successful. For the comparison with vision assistance, 4 types of experiments are designed and conducted consecutively in this step.

① no vision, no force (Ty1);
② no vision, with force (Ty2);
③ with vision, no force (Ty3);
④ with vision, with force (Ty4).

Before all the experiments, the subjects are told the exact position of an obstacle on the left-hand side of the guide path and a door at the terminal of the guide path, but the obstacle and door cannot be seen by the subjects for the first two types of experiments. In the experiments without vision, the subjects are required to close their eyes before the CWA moves forward. In the experiments with vision, they can see the symbol of the CWA and the virtual guide path in the GUI, and they can also see the real obstacle on the ground on their left side. In the experiments with force feedback, they can feel

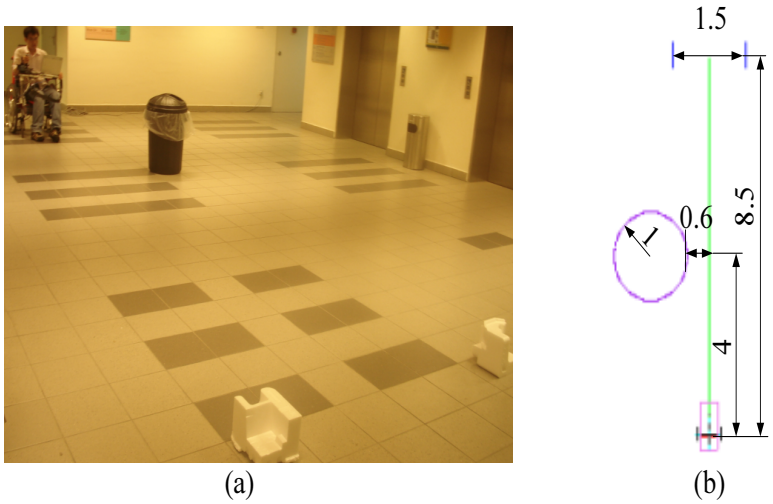

Figure 5.20: Experimental environment and GUI settings for Case 2

the repulsion from the joystick and can react to the effect of feedback force in the left-hand and right-hand side directions, but they should overcome the feedback force in the forward and backward directions so the CWA can keep moving forward until the target is reached.

After each trial is finished, the "Start/Stop" button in the GUI is clicked and the obstacle and door are displayed in the GUI. Then the experimental data are recoded in the computer for future analysis.

Results

The methods used to process the experimental data are:
① For Ty1, the figures of the motion trajectories will be displayed so we know the detailed trajectory of the CWA's motion and the possible reasons for the CWA's collision with the obstacle.
② For other types, we calculate the minimum distance between the obstacle and the CWA for each trial, and calculate the mean, minimum, maximum and standard deviation of that distance.

Table 5.2: Shortest distance between the obstacle and the CWA

Type	Mean	SD	Min	Max
Ty1	0.4408	0.5639	0.0080	2.6200
Ty2	0.5914	0.1995	0.2404	0.9588
Ty3	0.5058	0.1596	0.2521	0.8499
Ty4	0.7329	0.1361	0.4871	1.0385

1. Results of the Ty1 trials

The results of Ty1 for all the 30 trials are shown in Figure 5.21. Each row includes 10 trials for 2 subjects. For the experiments of Ty1, it is seen that 17 out of 30 trials collide with the obstacle. In comparison, no trial of Ty2 experiments collides with the obstacle. This indicates that the feedback force can effectively guide the CWA to avoid the obstacles around the guide path.

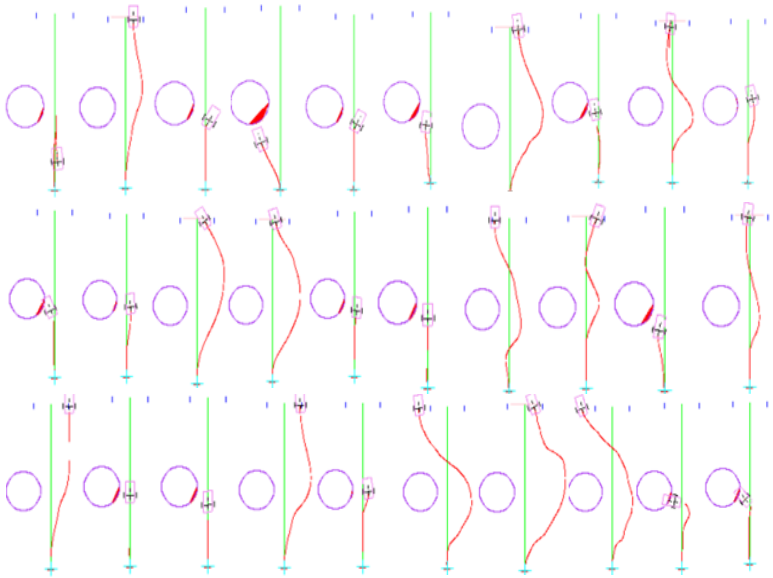

Figure 5.21: Results of all trial in Ty1 for Case 2

2. Shortest distance between the obstacle and the CWA

The statistical data of the shortest distance for all trials are listed in Table 5.2.

The normal probability distribution curve of the shortest distance is drawn in Figure 5.22.

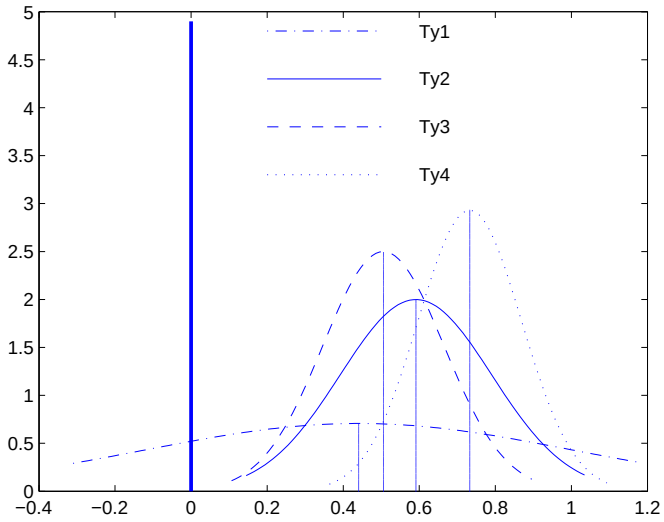

Figure 5.22: Shortest distance between the circular obstacle and the CWA

The SD of the shortest distance in Ty1 (0.5639) is significantly larger than that in Ty2 (0.1995), which shows that the force feedback alone can markedly improve the obstacle avoidance performance of the CWA. The SD of the shortest distance in Ty2 is not clearly different from that in Ty4 (0.1361), which indicates that addition of vision functionality does not improve the performance of the CWA significantly.

The statistical numbers of oscillations for all 6 subjects are shown in Table 5.3. The TTEST2 results of the number of oscillations are given in Table 5.4. Table 5.3 and Table 5.4 show that the mean value of oscillations in Ty2 is not significantly different from that in Ty3 ($p > 0.3275$). Thus, the force feedback alone does not cause more oscillations of the CWA's motion path than vision feedback alone does. In addition, the mean value of the number of oscillations in Ty4 (2.4) is notably smaller than those in Ty2 (3.0) and Ty3 (3.3). This is verified by the TTEST2 results shown in Table 5.4, where the mean value in Ty4 is significantly smaller than that in Ty2 ($p < 0.036$) and Ty3 ($p < 0.0061$). This indicates that the vision feedback combined with force feedback can greatly decrease the oscillations of the CWA's motion path.

Table 5.3: Statistical number of oscillations for all subjects

Type	Mean	SD	Min	Max
Ty2	3.0	1.0828	1	5
Ty3	3.3	1.2635	1	6
Ty4	2.4	1.4288	1	7

Table 5.4: TTEST2 results of the numbers of oscillations

Ty2 = Ty3	Ty4 < Ty2	Ty4 < Ty3
$p > 0.3275$	$p < 0.036$	$p < 0.0061$

5.5.4 Questionnaire

After each subject finished all the experiments, he or she filled out a questionnaire about the functionality of force feedback in comparison with vision feedback as the assistive tool for collision avoidance in the CWA's mobility task. The questionnaire is used to complement the evaluation of the experiments and give a qualitative assessment of the performance of the FFJ. The content of the questionnaire is listed as Appendix B.

The number of subjects selecting a particular answer choice is listed in Table 5.5. The first row lists the question number and the first column lists the choices. The entries in the table give the number of subjects who selected that particular choice for the questions.

Table 5.5: Number of subjects selecting a particular choice

Question No / Choices	2	3	4	5	6
A	3	2	2	0	0
B	3	3	4	1	4
C	0	1	0	4	1
D	0	0	0	0	1
E	0	0	0	1	0

According to Table 5.5, 3 subjects strongly agreed and other 3 agreed that force feedback is an effective tool to avoid obstacles. In comparison, 2 subjects thought the vision is very effective and other 1 thought it average in obstacle avoidance.

The results showed that the force feedback as well as vision feedback is an effective tool to avoid the obstacles.

1 subject felt high effort, 4 felt average effort and 1 felt negligible effort taken by using vision as assistive tool. In comparison, 4 subjects felt high effort, 1 felt average effort and 1 felt low effort taken by using force feedback as assistive tool. This indicated that subjects need to take slightly higher effort to drive the CWA for the obstacle avoidance by force feedback than by vision feedback.

5.6 Conclusion

This chapter introduced and analyzed the functionality of EPC with FFJ as its force input device. By using the FFJ, the users can feel the feedback from the environmental obstacles and the deviation from the guide path, which guides them to avoid the obstacles on the guide path and return to the guide path if no obstacles are on it.

A series of experiments are conducted to test if the force feedback functionality can assist the users with vision impairment in approaching a target and avoiding the environmental obstacles.

The results of experiments show that force feedback greatly improve the approaching performance of the CWA and the addition of vision feedback to the force feedback does not significantly improve the approaching performance of the CWA.

The results also indicate that the force feedback is an effective way to assist in the obstacle avoidance when vision feedback is not available for the CWA users. In addition, force feedback remarkably drops the vibration of the motion path in combination with vision feedback.

Chapter 6

Conclusions and recommendations for future work

The main objectives of this research were to develop a wheelchair system that can cater to the needs of the users. In particular, an EPC that was based on the Brent's path planner which could control the movement in a more stable and more maneuverable way was developed and an FFJ was integrated in the CWA. The results showed that the path following approach that had been used most often in the navigation of collaborative robots could be adapted to the application for human-carrying wheelchairs such as CWA to help disabled users regain their autonomy according to their own control abilities. The main research contributions reported in this thesis are summarized below.

6.1 Contributions

The characteristics of the Brent's path following planner were investigated and the new EPC was developed on the basis of the path planner. Results demonstrated that, with no external normal force, the EPC could implement the task of following the guide path when the wheelchair is on the guide path and asymptotically approaching the guide path

when the wheelchair is not on the guide path. This supports the observation previously reported that the path follower is able to follow or return to the guide path [10].

On the other hand, when obstacles appear in the guide path, the EPC had the capability to drive the wheelchair to deviate from the predesigned guide path with the normal force component. The EPC has these characteristics because it can internally generate a restoring force that pulls the wheelchair back to the guide path when the wheelchair is not on the guide path. When the user exerts a normal force, the normal force will overcome the restoring force and drive the wheelchair to deviate from the guide path.

The singularity issue was also addressed in this thesis. Even though the singularity issue does not often occur during the motion procedures of mobile robots, it may occur at the beginning of motion or when an abrupt change of input is imposed. This singularity issue is due to the fact that the inverse of the control matrix is singular when the front of the wheelchair is perpendicular to the guide path, causing the control input to approach infinity, which causes the motion of the wheelchair to be out of control. Experimental results indicated that the wheelchair moves abruptly far away from the guide path when the heading direction of the wheelchair is perpendicular to that of the guide path, and the wheelchair is unable to return to the guide path even though the normal force is withdrawn afterwards. The occurrence of the singularity issue can pose a serious threat to the stability and safety of the mobile robot. This issue was solved by a pure rotation of the wheelchair which drives the wheelchair out of the singularity region.

A nonlinear EPC was proposed to help the wheelchair avoid large obstacles. The nonlinear EPC was shown to drive the CWA to deviate an unlimited distance from the guide path by means of a limited value of normal force while always keeping the CWA moving stably and smoothly. This result is attributed to the fact that the inverse exponential function included in the nonlinear EPC is a monotonic decreasing function with a limited minimum value. Accordingly, the restoring force including this function is a monotonic increasing function with a limited maximum value. The position error can become large if the normal force is larger than the maximum value of the restoring force. The capacity to avoid obstacles of any sizes conforms to the general criteria for designing an effective

EPC [8].

The FFJ was also integrated into the CWA as an HMI. Experiments indicated that the FFJ as an input device was able to help the users feel the feedback force so they could adjust their input to avoid the obstacles and select a better way to approach the goal position. This functionality is needed in order to cancel out the mis-operation or neglect of the users to the emergent situation in the environment. Experimental results indicate that the force feedback alone is an effective tool to assist in target approaching and obstacle avoidance. Moreover, force feedback can decrease notably the number of oscillations of the motion path when it is combined with the vision feedback.

The newly developed EPC is significant in aiding in the mobility of CWA users with disabilities, as well as in the development and application of path following planners for common mobile robots. The tangent of the guide path instead of the actual path is used as the reference vector for the EPC. The actual tangent is a local reference vector with respect to the wheelchair, which easily leads to instability or a jerk when the input is large or changes abruptly. In contrast, the desired tangent has a global meaning and can be used as a reference vector to eliminate the instability issue.

Secondly, results for the nonlinear EPC are of considerable importance to the mobility task since they suggest that the EPC can be used in more extensive situations with obstacles of any sizes.

Finally, force feedback joystick integrated into the EPC control system helps users to prevent collision and drive the CWA back to the guide path without looking at the real world.

6.2 Future work

Some directions are available as topics for future research on the basis of this thesis.

It is desirable to evaluate the driving performance of the CWA with FFJ by experiments

using disabled users. The CWA with newly developed EPC has been tested by able-bodied subjects. However, the driving performance of the CWA was not evaluated by the disabled users who are actually the end users of the CWA product. For the disabled people as the CWA drivers, the main difficulty lies in the effort that they may take to move the wheelchair. Complexity of the operation is another big challenge to those with mental impairment. Moreover, psychological factors such as sense of security, self-esteem and impatience may also make it difficult to drive the CWA. So it is necessary to design a set of experiment procedure to evaluate if the CWA can cater to different needs of disabled users.

Future work may also study other forms of input as control commands, such as voice recognition [86], movement of eyes [87], and head movements [88] for those users who cannot use the joystick to control the wheelchair. Brain signals can also be used to control the mobility task of the CWA [89]. These forms of commands may be integrated into the present EPC to satisfy the needs of users with varying abilities.

Another research direction is to conduct localization for the CWA. The aim of the localization is to estimate the real-time position of the CWA so the controller can fulfill the mobility tasks more accurately. The encoders mounted on the driving wheels of the CWA can record the position relative to the start position of the CWA. However, the absolute start position is not accurately known in current experiments. Accordingly, the accumulative position errors during the whole experiment procedure may lead to collision of the CWA with the environment. Thus, it is necessary to adopt some devices to detect the absolute positions of the CWA. Barcode scanning approach has gotten satisfactory results for the CWA [90].

Still other possible direction is to do more tests about the selection of adjustment coefficient of the normal force. Equation (3.21) shows that the magnitude of normal force is closely related to the adjustment coefficient β. Larger value of β generates a larger normal force to drive the CWA, which also makes it more difficult to control the driving of the CWA. It is needed to do more trials to select a best value of β for the maneuverability of the CWA.

Bibliography

[1] D. E. Crews and S. Zavotka, "Aging, disability, and frailty: Implications for universal design," *Journal of Physiological Anthropology*, vol. 25, no. 1, pp. 113–118, Jan. 2006.

[2] LaPlante and M. P., "Demographics of wheeled mobility device users," in *Space Requirements for Wheeled Mobility*. Buffalo, New York: Center for Inclusive Design and Environmental Access, 2003, p. 24.

[3] L. H. V. van der Woude, A. J. Dallmeijer, T. W. J. Janssen, and D. Veeger, "Alternative modes of manual wheelchair ambulation: An overview," *Am. J. Phys. Med. Rehabil.*, vol. 80, no. 10, pp. 765–777, Oct. 2001.

[4] S. Kotani, H. Mori, and N. Kinyohiro, "Development of the robotic travel aid 'hitomi'," *Robotics and Autonomous System*, vol. 17, no. 1-2, pp. 119 – 128, 1996.

[5] R. Ceres, J. L. Pons, L. Calderon, A. R. Jimenez, and L. Azevedo, "A robotic vehicle for disabled children," *IEEE Engineering in Medicine and Biology Magazine*, vol. 24, pp. 55 – 63, November - December 2005.

[6] E. S. Boy, C. L.Teo, and E. Burdet, "Collaborative wheelchair assistant," in *IEEE / RSJ International Conference on Robotics and Intelligent Systems*, Lausanne, Switzerland, October 2002, pp. 1511 – 1516.

[7] Q. Zeng, C. L. Teo, B. Rebsamen, and E. Burdet, "A collaborative wheelchair

system," *IEEE Transactions on Neural Systems and Rehabilitation Engineering*, vol. 16, no. 2, pp. 161–170, Apr 2008.

[8] B. Long, "Development of an elastic path controller for collaborative robots," Master's thesis, National University of Sinagpore, 2005.

[9] A. Micaelli and C. Samson, "Trajectory tracking for unicycle - type and two - steering - wheels robots," Inst. National de Recherche en Informatique et en Automatique, Sophia Antipolis, France, Tech. Rep., 1993.

[10] R. B. Gillespie, J. E. Colgate, and M. A. Peshkin, "A general framework for cobot control," *IEEE Transactions on Robotics and Automation*, vol. 17, no. 4, pp. 391 – 401, August 2001.

[11] J. Cao, "A dedicated elastic path controller for unicycle - type cobots," Master's thesis, Imperial College London, September 2005.

[12] H. Ayoub, "Motion controller for a collaborative wheelchair," Imperial College London, Tech. Rep., 2007.

[13] J. C. Latombe, *Robot Motion Planning*. Boston: Kluwer, 1991.

[14] D. Chapman, "Planning for conjunctive goals," *Artificial Intelligence*, vol. 32, no. 3, pp. 333 – 378, July 1987.

[15] D. P. Miller, "Planning by search through simulations," Yale University, Tech. Rep. Technical report YALEU / CSD / RR423, 1984.

[16] N. J. Nilsson, "A mobile automation: an application of artificial intelligence," in *International Joint Conferences on Artificial Intelligence*, 1969.

[17] C. Dunlaing, M. Scharir, and C. K. Yap, "Retraction: A new approach to motion planning," in *the 15th annual ACM symposium on Theory of computing*, 1983, pp. 207 – 220.

[18] S. Rusell and P. Norvig, *Artificial Intelligence: A Modern Approach*. Upper Saddle River, NJ: Prentice - Hall Publishers, 1995.

[19] T. H. Cormen, C. E. Leiserson, R. L. Rivest, and C. Stein, *Introduction to Algorithms*, 2nd ed. MIT Press and McGraw - Hill, 2001.

[20] N. J. Nilsson, *Principles of Artificial Intelligence*. Tioga Publishing Company, January 1980.

[21] J. Pearl, *Heuristics: Intelligent Search Strategies for Computer Problem Solving*. Addison - Wesley, 1984.

[22] J. M. Esposito and V. Kumar, "A method for modifying closed - loop motion plans to satisfy unpredictable dynamic constraints at runtime," in *the 2002 IEEE International Conference on Robotics and Automation*, Washington DC, May 2002, pp. 1691 – 1696.

[23] R. Brooks, "A robust layered control system for a mobile robot," *IEEE Journal of Robotics and Automation*, vol. 2, no. 1, pp. 14 – 23, March 1986.

[24] J. Connell, "A colony architecture for an artificial creature," MIT AI Tech Report 1151, Tech. Rep., 1989.

[25] J. K. Rosenblatt and D. W. Payton, "A fine - grained alternative to the subsumption architecture for mobile robot control," in *the IEEE / INNS International Joint Conference on Neural Networks*, Washington DC, June 1989, pp. 317 – 324.

[26] L. Kaelbling, "An architecture for intelligent reactive systems," SRI International, Tech. Rep., October 1986, sRI Technical Note 400.

[27] D. Payton, "An architecture for reflexive autonomous vehicle control," in *1986 IEEE International Conference on Robotics and Automation*, April 1986, pp. 1838 – 1845.

[28] M. Kadonoff, F. B. Cherif, A. Franklin, J. F. Maddox, L. Muller, and H. Moravec, "Arbitration of multiple control strategies for mobile robots," in *the SPIE - The International Society for Optical Engineering*, 1986, pp. 90 – 98.

[29] R. C. Arkin, "Motor schema based mobile robot navigation," *International Journal of Robotics Research*, vol. 8, no. 4, pp. 92 – 112, August 1989.

[30] R. J. Firby, "Adaptive execution in complex dynamic worlds," Ph.D. dissertation, Yale University, January 1989.

[31] P. Agre and D. Chapman, "Pengi: An implementation of a theory of activity," in *the 6th National Conference on AI (AAAI87)*, 1987, pp. 268 – 272.

[32] O. Brock and O. Khatib, "High - speed navigation using the global dynamic window approach," in *IEEE International Conference on Robotics and Automation*, May 1999, pp. 341 – 346.

[33] S. P. Parikh, V. Grassi, V. Kumar, and J. Okamoto, "Incorporating user inputs in motion planning for a smart wheelchair," in *IEEE International Conference on Robotics and Automation*, April 2004, pp. 2043 – 2048.

[34] T. M. Mitchell, "Becoming increasingly reactive," in *1990 National Conference on AI*, Boston, August 1990, pp. 1051 – 1058.

[35] M. J. Mataric, "Integration of representation into goal - driven behavior - based robots," *IEEE Transactions on Robotics and Automation*, vol. 8, no. 3, pp. 304 – 312, June 1992.

[36] E. Gat, "Robust, task - directed, reactive control of autonomous mobile robots," Ph.D. dissertation, Virginia Polytechnic Institute and State University, 1991.

[37] R. Simmons, "Concurrent planning and execution for a walking robot," in *IEEE International Conference on Robotics and Automation*, Sacramento, CA, April 1991, pp. 300 – 305.

[38] L. Spector, "Supervenience in dynamic - world planning," Ph.D. dissertation, University of Maryland, May 1992.

[39] R. C. Arkin, "Towards cosmopolitan robotics: Intelligent navigation of mobile robot in extended man - made environments," Ph.D. dissertation, University of Massachusetts, 1987.

[40] ——, *Integrating Behavior, Perceptual, and World Knowledge in Reactive Navigation, in Designing Autonomous Agents*, P. Maes, Ed. MIT Press, 1990.

[41] R. C. Arkin and D. Mackenzie, "Planning to behave: A hybrid deliberative/reactive robot architecture for mobile manipulation," in *1994 International Symposium on Robotics and Manufacturing*, Maui, HI, August 1994, pp. 5 – 12.

[42] E. Gat, "Integrating planning and reacting in a heterogeneous asynchronous architecture for controlling real - world mobile robots," in *the 10th National Conference on Artificial Intelligence*, 1992, pp. 809 – 815.

[43] ——, "Low - computation sensor - driven control for task - directed navigation," in *1991 IEEE International Conference on Robotics and Automation*, April 1991, pp. 2484 – 2489.

[44] J. P. Odor, *The CALL Centre Smart Wheelchair*. Call Centre, University of Edinburgh, 1995.

[45] H. H. Kwee, J. J. Duimel, J. A. Woerden, and J. J. Smits, "Development of the manus wheelchair-borne manipulator: A progress report," in *RESNA-Assoc for the Advanced of Rehabilitation Technology*, 1987, pp. 781 – 783.

[46] T. Oderud, J. E. Bastiansen, and S. Tyvand, "Experiences with the manus wheelchair mounted manipulator," in *European Conference on the Advancement of Rehabilitation Technology*, Stockholm, May 1993, p. 29.1.

[47] B. J. F. Driessen, J. A. Woerden, M. W. Nelisse, and G. Overboo, "Mobile robotics and manus: A feasible approach," in *1st MobiNet Syposium: Mobile Robotics Technology for Health Care Services*, Arthens, Greece, May 1997, pp. 115 – 119.

[48] H. Hoyer, R. Hoelper, U. Borgolte, C. Bhler, H. Heck, W. Humann, I. Craig, R. Valleggi, and A. M. Sabatini, "The omni wheelchair with high maneuverability and navigational intelligence," in *the 2nd TIDE Congress: The European Context for Assistive Technology*, April 1995, pp. 285 – 289.

[49] N. I. Katevas, N. M. Sgouros, S. G. Tzafestas, G. Papakonstantinou, P. Beattie, J. M. Bishop, P. Tsanakas, and D. Koutsouris, "The autonomous mobile robot

senario: a sensor aided intelligent navigation system for powered wheelchairs," *IEEE Robotics & Automation Magazine*, vol. 4, no. 4, pp. 60 – 70, December 1997.

[50] T. B. Sheridan, *Telerobotics, Automation, and Human Supervisory Control*. Cambridge, MA: The MIT Press, 1992.

[51] S. P. Levine, D. A. Bell, L. A. Jaros, R. C. Simpson, Y. Koren, and J. Borenstein, "The navchair assistive wheelchair navigation system," *IEEE Transactions on Rehabilitation Engineering*, vol. 7, no. 4, pp. 443 – 451, December 1999.

[52] G. Bourhis, K. Moumen, P. Pino, S. Rohmer, and A. Pruski, "Assisted navigation for a powered wheelchair," in *IEEE International Conference on Systems, Man and Cybernetics*, 1993, pp. 553 – 558.

[53] M. Nuttin, E. Demeester, D. Vanhooydonck, and H. V. Brussel, "Shared autonomy for wheel chair control: Attempts to assess the user's autonomy," in *in Autonome Mobile Systeme*, 2001, pp. 127 – 133.

[54] P. Hoppenot and E. Colle, "Mobile robot command by man - machine cooperation - application to disabled and elderly people assistance," *Journal of Intelligent and Robotic Systems: Theory and Applications*, vol. 34, no. 3, pp. 235 – 252, July 2002.

[55] W. Wannasuphoprasit, R. B. Gillespie, J. E. Colgate, and M. A. Peshkin, "Cobot control," in *IEEE international Conference on Robotics and Automation*, April 1997, pp. 3571 – 3576.

[56] N. H. Beachley and A. A. Frank, "Continuous variable transmissions: Theory and practice," Lawrence Livermore Lab, Tech. Rep. UCRL - 15037, August 1979.

[57] S. Quinlan and O. Khatib, "Elastic bands: connecting path planning and control," in *Proc IEEE International Conference on Robotics and Automation*, Atlanta, GA, 1993, pp. 802–807.

[58] O. Brock and O. Khatib, "Elastic strips: a framework for motion generation in human environments," *International Journal of Robotics Research*, vol. 21, no. 12, pp. 1031–1052, December 2002.

[59] Y. Yang and O. Brock, "Elastic roadmaps: globally task-consistent motion for autonomous mobile manipulation," in *Proc. Robotics: Science and Systems*, Philadelphia, 2006.

[60] J. C. Alexander and J. H. Maddocks, "On the kinematics of wheeled mobile robots," *The International Journal of Robotics Research*, vol. 8, no. 5, pp. 15 – 27, October 1989.

[61] C. A. Moore, M. A. Peshkin, and J. E. Colgate, "Cobot implementation of virtual paths and 3 - d virtual surfaces," *IEEE Trans. Robot. Automat*, vol. 19, no. 2, pp. 347 – 351, April 2003.

[62] M. A. Peshkin, J. E. Colgate, W. Wannasuphoprasit, C. A. Moore, R. B. Gillespie, and P. Akella, "Cobot architecture," *IEEE Transactions on Robotics and Automation*, vol. 17, no. 4, pp. 377 – 390, August 2001.

[63] C. A. Moore, M. A. Peshkin, and J. E. Colgate, "Designing of 3r cobot using continuous variable transmissions," in *IEEE 1999 Int. Conf. Robot. Automat.*, May 1999, pp. 3249 – 3254.

[64] J. E. Colgate and M. A. Peshkin, *Passive Constraint Devices Using Non Holonomic Transmission Elements*, July 1999, u. S. Patent No. 5923139.

[65] W. J. Book, R. Charles, H. Davis, and M. Gome, "Concept and implementation of a passive trajectory enhancing robot," in *ASME Dyn. Sys. Cont. Div. DSC*, 1996, pp. 633 – 638.

[66] L. J. Zhou, C. L. Teo, and E. Burdet, "Development of a novel elastic path controller," in *the 2007 IEEE International Conference on Systems, Man and Cybernetics*, Montreal, QC, Canada, October 2007, pp. 1596 – 1601.

[67] P. Hsu, J. Hauser, and S. Sastry, "Dynamic control of redandent manipulators," in *Proc. IEEE International Conference on Robotics and Automation*, Philadelphia, PA, 1988, pp. 183–187.

[68] K. Chang and O. Khatib, "Manipulator control at kinematic singularities: a dynamically consistent strategy," in *Proc. IEEE International Conference on Intelligent Robots and Systems*, Pittsburgh, PA, 1995, pp. 84–88.

[69] D. Oetomo and H. Ang, "Singularity robust algorithm in serial manipulators," *Robotics and Computer-Integrated Manufacturing*, vol. 25, no. 1, pp. 122–134, February 2009.

[70] S. H. Lee and J. L. Stein, "Robust h2 / h8 state estimation for systems with real parameter uncertainties," in *the American Control Conferences*, Baltimore, Maryland, 1994, pp. 2217 – 2221.

[71] F. Lin and D. Brandt, "An optimal control approach to robust control of robot manipulators," *IEEE Transactions of Robotics and Automation*, vol. 14, no. 1, pp. 69 – 77, 1998.

[72] M. W. Spong, "On the robust control of robot manipulators," *IEEE Trans. Automat. Contr.*, vol. 37, no. 11, pp. 1782 – 1786, 1992.

[73] B. M. Chen and A. Saberi, "Necessary and sufficient conditions under which an h2 - optimal control problem has a unique solution," in *the 31st IEEE Conference on Decision and Control*, Tucson, Arizona, 1992, pp. 1105 – 1110.

[74] A. A. Stoorvogel, "The singular h2 control problem," *Automatica*, vol. 28, no. 3, pp. 627 – 631, May 1992.

[75] K. Zhou, J. Doyle, and K. Glover, *Robust and optimal control*. Upper Saddle River, NJ: Prentice Hall, 1996.

[76] X. Liu, B. M. Chen, and Z. Lin, "Linear systems toolkit in matlab: Structural decompositions and their applications," *Journal of Control Theory & Applications*, vol. 3, no. 3, pp. 287 – 294, August 2005.

[77] R. A. Cooper, D. M. Spaeth, D. K. Jones, M. L. Boninger, S. G. Fitzgerald, and S. Guo, "Comparison of virtual and real electric powered wheelchair driving using a position sensing joystick and an isometric joystick," *Medical Engineering and Physics*, vol. 24, pp. 703 – 708, 2002.

[78] J. B. Park, J. H. Lee, and B. H. Lee, "Rollover - free navigation for a mobile agent in an unstructured environment," *IEEE Transactions on Systems, Man, and Cybernetics, Part B*, vol. 36, no. 4, pp. 835 – 848, August 2006.

[79] R. C. Luo, C. Y. Hu, T. M. Chen, and M. H. Lin, "Force reflective feedback control for intelligent wheelchairs," in *1999 IEEE / RSJ International Conference on Intelligent Robots and Systems*, 1999, pp. 918 – 923.

[80] D. M. Brienza and J. Angelo, "A force feedback joystick and control algorithm for wheelchair obstacle avoidance," *Disability and Rehabilitation*, vol. 18, no. 3, pp. 123 – 129, 1996.

[81] J. L. Protho, E. F. LoPresti, and D. M. Brienza, "An evaluation of an obstacle. avoidance force feedback joystick," in *the 23th Annual RESNA Conference*, 2000, pp. 447 – 449.

[82] J. P. Hong, O. S. Kwon, E. H. Lee, B. S. Kim, and S. H. Hong, "Shared - control and force - reflection joystick algorithm for the door passing of mobile robot or powered wheelchair," in *IEEE, TENCON 99*, 1999, pp. 1577 – 1580.

[83] R. Braden, "Requirements for internet hosts - communication layers," Information Sciences Institute (ISI) at University of Southern California,, Tech. Rep., October 1989.

[84] C. M. Kozierok, "Tcp basic operation: Connection establishment, management and termination," Tech. Rep., 2005.

[85] J. Borenstein and Y. Koren, "The vector field histogram - fast obstacle avoidance for mobile robots," *IEEE Journal of Robotics and Automation*, vol. 7, no. 3, pp. 278 – 288, June 1991.

[86] R. C. Simpson and S. P. Levine, "Adaptive shared control of a smart wheelchair operated by voice control," in *the 1997 IEEE / RSJ International Conference on Intelligent Robots and Systems*, 1997, pp. 622 – 626.

[87] P. Dimattia and J. Gips, *EagleEyes: Technologies for Non - verbal Persons*, K. Thies and J. Travers, Eds. Jones and Bartlett Publishers, July 2005.

[88] G. Pires, R. Araujo, U. Nunes, and A. T. Almeida, "Robchair - a powered wheelchair using a behavior - based navigation," in *AMC'98, 5th International Workshop on Advanced Motion Control*, 1998, pp. 536 – 541.

[89] B. Rebsamen, E. Burdet, C. Guan, Q. Zeng, M. Ang, and C. Laugier, "Hybrid p300 and mu - beta brain computer interface to operate a brain controlled wheelchair," in *IEEE International Conference on Intelligent Robots and Systems*, San Diego, October 2007.

[90] J. W. Yee, *Collaborative Wheelchair Assistant using Barcode Localization*. Bachelor Thesis, National University of Singapore, 2006.

[91] H. Wakaumi, K. Nakamura, and T. Matsumura, "Development of an automated wheelchair guided by a magnetic ferrite marker lane," *J. Rehab. Res. Dev.*, vol. 29, no. 1, pp. 27 – 34, 1992.

[92] P. D. Nisbet, J. Craig, J. P. Odor, and S. Aitken, "Smart wheelchairs for mobility training," *Technol Disabil.*, vol. 5, pp. 49 – 62, 1995.

[93] J. D. Yoder, E. T. Baumgartner, and S. B. Skaar, "Initial results in the development of a guidance system for a powered wheelchair," *IEEE Transactions on Rehabilitation Engineering*, vol. 4, no. 3, pp. 143 – 151, September 1996.

[94] A. C. Balcells and J. Gonzalez, "Tetranauta: A wheelchair controller for users with very severe mobility restrictions," in *3rd European Conf. on Tech. for Inclusive Design and Equality*, Helsinki, Finland, 1998.

[95] R. C. Simpson and S. P. Levine, "Development and evaluation of voice control for a smart wheelchair," in *Annu. RESNA Conf*, Washington DC, 1997, pp. 417 – 419.

[96] J. D. Crisman, M. E. Cleary, and J. C. Rojas, "The deictically controlled wheelchair," *Image and Vision Computing*, vol. 16, no. 4, pp. 235 – 249, April 1998.

[97] N. Nilsson, "Shakey the robot," AI Center, SRI International, 333 Ravenswood Ave., Menlo Park, CA 94025, Tech. Rep. Technical Note 323, April 1984.

[98] H. H. Kwee, J. J. Duimel, J. J. Smits, A. A. Moed, and J. A. van Woerden, "The manus wheelchair - borne manipulator: System review and first results," in *IARP Proceedings of the 2nd Workshop on Medical and Healthcare Robotics*, 1989, pp. 385 – 395.

[99] H. H. Kwee, "Spartacus and manus: Telethesis developments in france and the netherlands," in *Interactive robotic aids - One option for independent living. World Rehabilitation Fund*, R. Foulds, Ed., 1986, pp. 7 – 17.

[100] D. P. Miller and M. G. Slack, "Design and testing of a low - cost robotic wheelchair prototype," *Autonomous Robots*, vol. 2, no. 1, pp. 77 – 88, March 1995.

[101] D. P. Miller and E. Grant, "A robot wheelchair," in *the AAIA / NASA Conference on Intelligent Robots in Field, Factory, Service and Space*, March 1994, pp. 407 – 411.

[102] D. P. Miller and M. G. Slack, "Increasing access with a low - cost robotic wheelchair," in *the IEEE / RSJ International Conference on Intelligent Robots and Systems*, Munich, Germany, 1994, pp. 1663 – 1667.

[103] G. Bourhis and P. Pino, "Mobile robotics and mobility assistance for people with motor impairments: rational justification for the vahm project," *IEEE Transactions on Rehabilitation Engineering*, vol. 4, no. 1, pp. 7 – 12, March 1996.

[104] H. A. Yanco, *Wheelesley: A Robotic Wheelchair System: Indoor Navigation and User Interface*. New York: Springer - Verlag, 1998.

[105] J. Borenstein and Y. Koren, "Error eliminating rapid ultrasonic firing for mobile robot obstacle avoidance," *IEEE Transactions on Robotics and Automation*, vol. 11, no. 1, pp. 132 – 138, February 1995.

[106] T. Gomi and A. Griffith, "Developing intelligent wheelchairs for the handicapped," *Assistive technology and Artificial Intelligence*, vol. 1458, pp. 150 – 178, 1998.

[107] T. Gomi, "New ai and service robots," *Industrial Robot: An International Journal*, vol. 30, no. 2, pp. 123 – 138, 2003.

[108] P. Beattie, "Senario: Sensor aided intelligent wheelchair navigation," in *IEE Colloquium on New Developments in Electric Vehicles for Disabled Persons*, London, UK, March 1995, pp. 2/1 – 2/4.

[109] U. Borgolte, R. Hoelper, H. Hoyer, H. Heck, W. Humann, J. Nedza, I. Craig, R. Valleggi, and A. M. Sabatini, "Intelligent control of a semi-autonomous omnidirectional wheelchair," in *3rd International Symposium on Intelligent Robotic System (SIRS'95)*, 1995, pp. 113 – 120.

[110] U. Borgolte, H. Hoyer, C. Bhler, H. Heck, and R. Hoelper, "Architectural concepts of a semi - autonomous wheelchair," *Journal of Intelligent and Robotic Systems: Theory & Applications*, vol. 22, no. 3 - 4, pp. 133 – 253, July - August 1998.

[111] G. Pires, N. Honorio, C. Lopes, U. Nunes, and A. T. Almeida, "Autonomous wheelchair for disabled people," in *the IEEE International Symposium on Industrial Electronics*, 1997, pp. 797 – 801.

[112] G. Pires, U. Nunes, and A. T. Almeida, "Robchair - a semi - autonomous wheelchair for disabled people," in *3rd Symposium on Intelligent Autonomous Vehicles*, Madrid, 1998, pp. 648 – 652.

[113] K. Schilling, H. Roth, R. Lieb, and H. Stutzle, "Sensor supported driving aids for disabled wheelchair users," in *IFAC Workshop on Intelligent Components for Vehicles*, A. Ollero, Ed., Sevilla, 1998, pp. 267 – 270.

[114] ——, "Sensors to improve the safety for wheelchair users," in *3rd Annual TIDE Congress*, Helsinki, Finland, 1998.

[115] S. J. King and C. F. R. Weiman, "Helpmate autonomous mobile robot navigation system," in *SPIE - The International Society for Optical Engineering*, 1991, pp. 190 – 198.

[116] J. M. Evans, "Helpmate: An autonomous mobile robot courier for hospitals," in *the IEEE / RSJ / GI International Conference on Intelligent Robots and Systems*, September 1994, pp. 1695 – 1700.

[117] T. Skewis, J. Evans, V. Lumelsky, B. Krishnamurthy, and B. Barrows, "Motion planning for a hospital transport robot," in *1991 IEEE International Conference on Robotics and Automation*, April 1991, pp. 58 – 63.

[118] S. Thongchai, S. Suksakulchai, D. M. Wilkes, and N. Sarkar, "Sonar behavior - based fuzzy control for a mobile robot," in *2000 IEEE International Conference on Systems, Man, and Cybernetics*, 2000, pp. 3532 – 3537.

[119] M. Mazo, "An integral system for assisted mobility," *IEEE Robotics & Automation Magazine*, vol. 8, no. 1, pp. 46 – 56, March 2001.

[120] M. Mazo, J. C. Garcia, F. J. Rodriguez, J. Urena, J. L. Lazaro, and F. Espinosa, "Experiences in assisted mobility: the siamo project," in *the 2002 International Conference on Control Applications*, 2002, pp. 766 – 771.

[121] L. M. Bergasa, M. Mazo, A. Gardel, J. C. Garcia, A. Ortuno, and A. E. Mendez, "Guidance of a wheelchair for handicapped people by face tracking," in *the 7th International Conference on Emerging Technologies and Factory Automation*, 1999, pp. 105 – 111.

[122] R. C. Luo and T. Chen, "Target tracking by grey prediction theory and look-ahead fuzzy logic control," in *IEEE International Conference on Robotics and Automation*, May 1999, pp. 1176 – 1181.

[123] R. C. Luo, T. M. Chen, and M. H. Lin, "Automatic guided intelligent wheelchair system using hierarchical grey - fuzzy motion decision - making algorithms," in *1999 IEEE / RSJ International Conference on Intelligent Robots and Systems*, 1999, pp. 900 – 905.

[124] T. M. Chen and R. C. Luo, "Mobile target tracking using hierarchical grey - fuzzy motion decision - making method," in *2000 IEEE International Conference on Robotics and Automation*, 2000, pp. 2118 – 2123.

Appendices

Appendix A. Research progress of robotic wheelchairs

Robotic wheelchairs, or called Wheeled mobile robots (WMRs), are a kind of rehabilitation robots that have emerged over the last two decades because of their ability to assist handicapped people who cannot drive the standard powered wheelchair. In designing a WMR for the handicapped people, the main concerns are adaptability to the needs and abilities of individual users and satisfaction of safety requirements. For these people, it is significant to ensure that the remaining skills of the users can be adequately exploited. As a result, research and industry focus more on semi - autonomous robots than on fully autonomous wheelchairs, even though autonomous robotic wheelchairs are still attractive to the research communities as mobility tool for users with the most severe disabilities [91] [92] [93] [94]. Many autonomous control modes are integrated with other modes [95] [96]. Most research projects that have been done or are underway address safety requirements, versatility of the mechanism, ergonomics, global path planning, local obstacle avoidance, and/or human-machine interface (HMI).

"Shakey" [97], built by Stanford researchers in 1968, was the first mobile robot in the world controlled by artificial intelligence. Shakey was driven by two motors and equipped with sensing devices that included a TV camera, a triangulating range finder, and bump sensors to collect environmental information that was transmitted to a room-sized on-board computer. The computer directed commands to Shakey to move at a speed of about 2 meters per hour. Driven by a problem-solving program called STRIPS, the mobile robot found its path around the halls according to information about its en-

vironment. Shakey's younger cousin, "Flaky", was enhanced with components such as speech recognition and software. Even though it was tremendously bulky and slow, Shakey undoubtedly initiated a new era of robotics and had a substantial influence on modern artificial intelligence and mobile robots.

The CALL (Communication Aids for Language and Learning) [92] [44] Centre smart wheelchair was invented by Edinburgh University mainly for children with severe disabilities to give them a way to communicate, learn, play and gain some independent mobility. The wheelchair is equipped with multiple switches, a scanning direction selector and a communication aid board which can be adapted to the individual habits and skill levels of the users. Many features are used to protect the users as well as the environment: Ultrasonic range finders are able to slow the chair before an obstacle, and collision sensors can stop or turn the chair away when it contacts with the obstacle. The bumpers protect the mobile system from being damaged when a collision occurs, and a track-follower enables the wheelchair to follow some predefined lines on the ground. The CALL wheelchair is simple in structure and functionality and easy to operate an effective tool for training children with disabilities to live independently and to encourage them to regain their confidence and self esteem.

MANUS was a Dutch project to develop a wheelchair-bourn manipulator at the Institute for Rehabilitation Research (IRV) [98]. The MANUS manipulator consists of a 5 DOFs arm built on a rotating base and attached to variety of electric wheelchairs [99]. MANUS uses slip couplings and a watchdog to increase the safety of this manipulator. The MANUS arm has been used to demonstrate the functionality of a proposed wheelchair-based communication standard and was also used in an unstructured domestic environment to show that it significantly improves a user's ability to perform daily tasks more independently [46]. Both the manipulator and the autonomous mobile base provide opportunities for domestic applications of robotics.

The Tin Man [100] project was mainly concerned with the HMI and cost and was dedicated to development of a low-cost wheelchair so that mobility-impaired people could move without collision in many typical environments [101] [102]. Tin Man is built on

the basis of a commercial power wheelchair from the Vector Wheelchair Corporation. Two driving wheels are centered on both sides, and two front casters and one rear caster are linked to the base by springs. Several sensors are distributed around the wheelchair and several pressure switches are mounted on the front bumper. Tin Man can assist in obstacle avoidance, maneuvering through doorways and crowded places and interfacing with a number of input devices.

The VAHM (Autonomous Vehicle for the Disabled) project [52] [103] was aimed at developing a direct way of navigating a powered wheelchair to fulfill the autonomous mobility task as well as to share control between human user and machine based on the user's abilities and the complexity of environment. VAHM used a three-level software architecture on a ROBUTER wheelchair - executive level, control level and intelligent level - which architecture enabled the wheelchair to switch among three control modes: automatic mode, semi-automatic mode and manual mode. However, trajectory errors could appear during navigation because of the inaccuracy of ultrasonic sensors, which made it difficult for the VAHM to pass through some narrow passages, such as doorways and corridors. Moreover, its complicated system made it difficult for the disabled people especially the mentally impaired, to decide how and when to switch among the control modes.

The Wheelsley project [104], developed by MIT AI Lab, was aimed at creating a robot wheelchair for users who cannot drive the powered wheelchairs with standard input devices. The Wheelsley was equipped with 4 sonar sensors and with Hall Effect sensors in the front bumper and is able to navigate safely in an indoor environment using infrared and sonar sensors. One camera and a notebook computer are used as a vision system for collision avoidance and for staying on the sidewalk in outdoor navigation. Wheelsley can also automatically switch between indoor and outdoor navigation modes. In addition, users can communicate with the control system using Graphical User Interface (GUI) running in a Powerbook.

NavChair [51] implements local obstacle avoidance and wall following tasks in a cluttered environment through sonar sensors that detect the environment in the front of the

wheelchair. An Error Eliminating Rapid Ultrasonic Firing (EERUF) method [105] is employed to obtain a highly accurate sonar map by reducing the errors resulting from the bad sonar readings. Navchair also employs a semi-autonomous navigation method, allowing shared control between the human user and the machine, and can choose between multiple task-specific operating modes. The modified version [86] employs the Bayesian networks reasoning mechanism to choose the optimal motion mode for the wheelchair, e.g., wall following or door passage. A voice recognition interface is also installed to enable users who cannot operate the joystick to maneuver the wheelchair.

TAO [106] is a series of robotic wheelchairs developed by Applied Artificial Intelligence Inc. in Canada. TAO-1 (suited to the Canadian market) and TAO-2 (adapted for the Japanese market) both have CCD color cameras as vision systems. Each version was equipped with 12 infrared sensors and several bump sensors for obstacle avoidance and maneuvering in complex environments. Control commands were sent to the wheelchair by the keypad or joystick. Both wheelchairs are mainly used in indoor situations and are able to move in standard office environments, follow walls, avoid obstacles and crowded situations, pass through the narrow doorways, and so on. The TAO series has now been upgraded up to TAO-7 [107] and provides an autonomous mobile base using behavior-based AI (new AI) techniques. It can also use a voice recognition device to control its behavior and can run using the conventional position control method by optional encoders.

SENARIO (SENsor Aided intelligent wheelchaiR navigatIOn) [49] is an autonomous wheelchair that provides with high-level navigation assistance to users with severe disabilities. This wheelchair system includes 5 subsystems: sensor, user control, power control, localization and risk avoidance. The center is the risk avoidance subsystem, which processes the environmental information from the sensor, localization and control subsystems, and sends commands to the power control subsystem to drive the wheelchair [108]. SENARIO can operate in two modes: Semi-autonomous mode and Autonomous mode. In semi-autonomous mode, the controller accepts commands from the user to move forward while avoiding obstacles according to environmental infor-

mation from the on-board sensors. The user can override the system to execute some special actions, such as approaching closer to a wall than the automatic system permits so the control task is shared between the user and system. In fully-autonomous mode, the system can locate itself and fulfill the mobility task using only the instructions of the goal position. The system can plan a path according to the environment map and avoid all the obstacles on the way to the goal. During the motion procedure, the user can intervene with the system, as in the semi-autonomous mode.

OMNI (Office wheelchair with high Maneuverability and Navigational Intelligence) is a European project developed in Germany [109] [48] [110]. The OMNI system can move the wheelchair independently in all directions as well as in cramped office rooms or bathrooms. The ultrasonic and infra-red sensors can automatically detect obstacles and support the obstacle avoidance functionality. Alternate operating devices, such as head or foot buttons, enable users who cannot maneuver the joystick to control the mobility tasks. Users can also remotely control the devices using the environmental control module

Robchair [111] [112] was developed by a research group from Portugal to assist people with physical or mental disabilities to steer powered wheelchairs. Robchair is built on the basis of a conventional powered wheelchair and equipped with a detecting system, including 12 infrared sensors, 4 ultrasonic sensors, one tactile bumper and two optical encoders. It provides several levels of functionality, including autonomous and assistive modes, to suit users with different abilities. The potential field method and reactive path planning approach are used for local obstacle avoidance,along with safety and improvement of mobility. Robchair implements remote communication through Graphics User Interface (GUI) and an Ethernet network to fulfill remote control tasks for disabled users [88]. It can also be controlled through a standard joystick or a voice HMI as command input device for those with serious impairment.

INRO, developed in Germany, is a wheelchair system with capabilities of indoor and outdoor navigation. It uses the related sensor technique to assist handicapped users of electrical wheelchairs with respect to navigation and obstacle detection [113]. It pro-

vides functionality in hospital environments for convoying the multi-wheelchair driving and autonomous driving on preset courses by sensor fusion of a differential GPS system, an ultrasonic range sensor system, active laser markers and encoders [114]. A notebook PC is used for data processing and control, a joystick is employed as input device, a display is used as output device, and a radio modem is used to communicate with the central control station for safe reaction in case of emergencies.

HelpMate is an intelligent material transportation mobile robot used to transport items in a hospital environment. It provides autonomous navigation along the passages of a hospital, crossing interconnecting corridors and communicating with the outside by radio. By using sensory data, it can follow straight paths to reach its goal position and it is also able to sense obstacles on the path and modify the path to avoid them [115]. Ultrasonic ranging sensors are mounted around HelpMate to locate the robot and measure the environment, such as the location of walls and obstacles, through a structured light vision system that detects the obstacles accurately. Contact bumpers and dead-reckoning navigation in reference to the ceiling lights are also used to complete the sensing and navigation tasks [116]. Sensor-based motion planning algorithms are also used to handle the problem of navigation in unknown and unstructured environments and to handle unmodeled factors such as sensory inaccuracies, position estimation errors and moving obstacles [117]. A behavior-based fuzzy control approach combines the data from all the sonar sensors to fulfill the tasks of wall-following, goal-seeking, obstacle avoidance, emergency-handling, and so on [118].

SIAMO (Integral System for Assisted Mobility) was developed in Spain. The main objective of the project was to design a versatile modular electronic system on the basis of a conventional powered wheelchair to fit the different needs of potential users [119]. The system architecture of the SIAMO prototype is composed of four functional blocks: Power and motion controller, HMI, environmental perception and integration, and navigation and sensory integration. Each functional block includes several optional modules to suit the individual needs of each user, and the modules are connected by LonWorks Serial Bus for communications. The HMI incorporates special command input forms,

such as breath expulsion, head movement, and voice [120]. A face-tracking system is also employed to compute the head movements of the user, and some commands are given to control the wheelchair accordingly. The system can learn the face features for people of different races, and it is adaptive to light and background variations in indoor environments [121].

LUOSON-III, which was developed in Taiwan [79], provided an assistant control mode especially developed for the blind wheelchair users. 16 ultrasonic range sensors are distributed around the wheelchair to detect obstacles in the environment. A force feedback joystick is applied to transmit the user's command to the wheelchair and to reflect the environmental information to the users by simulating the effect of a wall or other objects. At the same time, gray theory was used to predict the target position, and look-ahead fuzzy logic was used for the motion control of the tracking robot in an unknown environment [122]. In order to solve the multiple data fusion problem, which limits the application and performance of the controller, the Hierarchical Grey-Fuzzy Motion Decision-making (HGFMD) algorithm was used to fuse the multiple sequential data and prediction results for decision-making [123] [124].

Appendix B. Questionnaire about the Assistive Obstacle Avoidance of the CWA

Name:_____

Age:____ years____months

Gender: M/F

1. Do you have experiences of driving the wheelchairs? A. Yes B. No

2. Do you think that the force feedback function is an effective tool for obstacle avoidance of the wheelchair?

A. Strongly agree B. Agree C. Not available D. Disagree E. Strongly disagree

3. How do you evaluate the function of vision in the obstacle avoidance without force feedback?

A. Very effective B. Effective C. Average D. Ineffective E. Very ineffective

4. How do you evaluate the function of vision in the obstacle avoidance with force feedback?

A. Very effective B. Effective C. Average D. Ineffective E. Very ineffective

5. What do you think about the effort that the user takes assisted by vision?

A. Very high B. High C. Average D. Low E. Negligible

6. What do you think about the effort that the user takes assisted by force feedback?

A. Very high B. High C. Average D. Low E. Negligible

Signature:_____

Date:_____

Publications

1. L. J. Zhou, C. L. Teo, and E. Burdet, "An elastic path controller for a collaborative wheelchair assistant," in *Proceedings of the 1st international Convention on Rehabilitation Engineering & Assistive Technology: in Conjunction with 1st Tan Tock Seng Hospital Neurorehabilitation Meeting (i-CREATe07)*, Singapore, Apr 23-26, 2007, ACM, New York, NY, pp. 73-76.

2. L. J. Zhou, C. L. Teo, and E. Burdet, "Development of a Novel Elastic Path Controller," in *Proceedings of 2007 IEEE International Conference on Systems, Man and Cybernetics (SMC07)*, Montreal, QC, Canada, Oct 7-10, 2007, pp. 1596-1601.

3. L. J. Zhou, C. L. Teo, and E. Burdet, "Analysis and Parameter Optimization of an Elastic Path Controller," in *Proceedings of IEEE/RSJ International Conference on Intelligent Robots and Systems (IROS07)*, San Diego, CA, Oct 29-Nov 2, 2007, pp. 789-794.

4. L. J. Zhou, C. L. Teo, and E. Burdet, "A Nonlinear Elastic Path Controller for a Robotic Wheelchair," in *the 3rd IEEE Conference on Industrial Electronics and Applications (ICIEA08)*, Singapore, June 3-5, 2008, pp. 142-147.